CELLULAR AND PROTEOLYTIC STUDIES OF ALZHEIMER'S DISEASE AMYLOID BETA PEPTIDE WITH MICROGLIA, STEM CELLS AND MMP9

By

EMALICK GOREE NJIE

A DISSERTATION PRESENTED TO THE GRADUATE SCHOOL
OF THE UNIVERSITY OF FLORIDA IN PARTIAL FULFILLMENT
OF THE REQUIREMENTS FOR THE DEGREE OF
DOCTOR OF PHILOSOPHY

UNIVERSITY OF FLORIDA

2010

I dedicate this to the half that’s never been told.

ACKNOWLEDGMENTS

I thank Dr. Borchelt and Dr. Streit for giving me this opportunity to develop my mind. I would like to extend my gratitude to members of the Streit and Borchelt labs for their support and smiles. I would like to thank my committee for ideas and inspiration and to my collaborators Svetlana Kantorovich, Dr. Boelen, Dr. Zheng, Dr. Steindler, and Dr. Rowland. Most of all, I thank my sister, my mother and my extended family. They have supported me with the strength of a strong village with one son.

TABLE OF CONTENTS

page

LIST OF FIGURES

LIST OF ABBREVIATIONS

1,10 PNTL	1, 10 Phenanthroline
AD	Alzheimer’s disease
Aβ	Amyloid beta
AMPA	*p*-aminophenylmercuric acetate
AU	Arbitrary unit
CMV	Cytomegalovirus
CNS	Central nervous system
EDTA	Ethylenediaminetetraacetic acid
EF1	Elongation factor 1
FACS	Fluorescence activated cell sorting
GFP	Green fluorescent protein
GSH	Glutathione
IL-6	Interleukin 6
LPS	Lippopolysaccharide
mRNA	messenger ribonucleic acid
MGC	Mixed glial culture
MMP9	metalloprotease 9
NSC	mouse neuronal stem cell
PBS	Phosphate buffered saline
PLR	Path of least resistance
ROS	Reactive oxygen species
SDS	Sodium dodecyl sulfate
SEZ	Subependymal zone
SGV	Subgranular zone

TNF-α	Tumor necrosis factor-α

Abstract of Dissertation Presented to the Graduate School
of the University of Florida in Partial Fulfillment of the
Requirements for the Degree of Doctor of Philosophy

CELLULAR AND PROTEOLYTIC STUDIES OF ALZHEIMER'S DISEASE AMYLOID BETA PEPTIDE WITH MICROGLIA, STEM CELLS AND MMP9

By

eMalick Goree Njie

August 2010

Chair: Wolfgang J. Streit
Major: Medical Sciences-Neuroscience

Alzheimer's disease (AD) is a common neurodegenerative disease that primarily affects the elderly. In the brains of Alzheimer's patients, neurons progressively die and synapses withdraw. Behaviorally, Alzheimer's patients typically present with emotional instability and a marked depreciation in memory. In the spaces in between the cells of AD patients, one finds large aggregates of proteins. The amyloid beta (Aβ) peptide is the primary molecule within these aggregates and thus forms a hallmark pathology in AD. Genetic data from a rare set of families and from those with Down syndrome indicate that producing more Aβ leads to AD. However, the role of these aggregates in the majority of AD patients is largely unknown due to our lack of understanding of how the Aβ molecule is catabolized by the brain. We examined microglia to shed light on one of the brain's mechanisms for regulating Aβ. We also explored mouse neuronal stem cells (NSCs) as a possible therapeutic intervention to treat Aβ pathology. Microglial cells are typically associated with the removal of extraneous materials from the brain. We find that they do not degrade Aβ. Instead, microglia appear to continually recycle Aβ, perhaps to minimize the pool of Aβ that can form aggregates. Importantly, we find that this recycling of Aβ deteriorates significantly with age. To truly determine

whether Aβ is causative of AD, previously existing Aβ must be removed and a clinical improvement observed. Drug treatment regiments to remove Aβ have by and large failed. This is partly because blood vessels block most drugs from entering the brain. Drugs that are directly injected into the brain are typically broken down rapidly. One possible way to circumvent these issues is to transplant cells that continually produce drugs directly within the brain. The neuronal stem cell can live outside the brain for months before being transplanted. We demonstrate that transplants of neuronal stem cells typically settle in predefined regions within the hippocampus and are associated with reductions in Aβ aggregates. We also find that neuronal stem cells can be genetically manipulated to overexpress MMP9, a molecule that may further reduce Aβ aggregates in the brain or protect cells from Aβ toxicity. In mice modeling Alzheimer's disease, neuronal stem cells formed larger transplants after we genetically manipulated them to express human MMP9. Together, our findings further our understanding of Alzheimer's disease by demonstrating that microglia are less able to process Aβ with age and that neuronal stem cells may prove useful for treating Aβ pathology in Alzheimer's patients.

CHAPTER 1
INTRODUCTION

Alzheimer's Disease and Aβ Pathology

Alzheimer's disease is a neurodegenerative disease that affects more people than all other neurodegenerative diseases (Association, 2007). Half of all persons reaching the age of 85 will be diagnosed with AD (Association, 2007). Temporally, every 72 seconds someone within the U.S is diagnosed with AD. The mean life span of patients following diagnosis ranges from 3 years to 9 years (Brookmeyer, et al., 2002). The 150 billion dollars spent annually in healthcare costs for these individuals will only grow as our population's overall life expectancy increases (Association, 2007). Patients with this disease have noticeably enlarged ventricles and severe memory deficits as a result of progressive neuronal cell death. Patients inevitably deteriorate over a period of years to the point where they require constant assistance to manage even the most mundane of life's activities. Although currently available therapies can slow the progression of AD by as much as 5 years, they do not remedy the underlying cause of neurodegeneration (Auld, et al., 2002, Parsons, et al., 2007, Terry and Buccafusco, 2003, Zandi, et al., 2004).

The Amyloid Cascade Hypothesis

In the aged and AD brain, levels of Aβ peptide have been shown to increase (Armstrong, et al., 1996). It has been postulated that this increase in extracellular Aβ, ranging from 50x to 1500x above normal (Farris, et al., 2007), is neurotoxic and sets the stage for the neurodegeneration found in AD (Lewis, et al., 2001, Walsh, et al., 2002). This belief is based on the amyloid cascade theory. The theory states that the presence of high amyloid burden (amyloidosis), in the form of extracellular Aβ plaques or

oligomers initiates a cascade that leads to the disruption of cytoskeletal tau protein (Tanzi and Bertram, 2005). Aβ and tau are among a class of fibril forming proteins whose β-spines naturally interdigitate to form highly stable dry 'steric zippers' (Sawaya, et al., 2007). Two other notable proteins that multimerize via a dry steric zipper mechanism are the prion protein of Bovine Spongiform Encephalitis (Mad Cow Disease) and α-synuclein of Parkinson's disease (Sawaya, et al., 2007). Family linked mutations that cause AD create more total Aβ or create more aggregation prone forms of Aβ (Goate, et al., 1991, Kumar-Singh, et al., 2006, Motte and Williams, 1989, Rovelet-Lecrux, et al., 2006). This supports the position of Aβ as the initiator of a neurotoxic cascade. Secondarily, murine models that are genetically engineered to overexpress Aβ have memory and learning impairments similar to that which occurs in humans (Higgins and Jacobsen, 2003, Hsiao, et al., 1996, Savonenko, et al., 2005, Westerman, et al., 2002, Wong, et al., 2002).

Mouse Models of Alzheimer's Disease

Given the limitations associated with post-mortem studies on human brains, since the mid-nineties several transgenic mouse lines have been created to model Alzheimer's disease. These mouse models emulate with great success the deposition of Aβ in the neocortex and the hippocampus, but not necessarily neurodegenerative changes, such as neurofibrillary tangles. Transgenic mice typically overexpress the amyloid precursor protein (APP) with familial AD mutations under the control of various promoters, and although there are more than a dozen strains available, most studies are done on the PDAPP, Tg2576, APP23 and most recently, the mo/hu APPswe/PS1dE9 mice (Borchelt, et al., 2002, Games, et al., 1995, Hsiao, et al., 1996, Sturchler-Pierrat, et al., 1997). The mutations carried in the hAPP transgene introduced

into these mice originated from genetic studies done on families with early onset AD. In general, the transcription of these genes causes dense Aß plaque to be deposited in the neocortex and the hippocampus usually between six and twelve months of age. The hAPP transgene in the PDAPP model has the V717F mutation (Indiana family origin) (Games, et al., 1995). The dual point mutations in Tg2576, APP23 mice are at K670N/M671L (Swedish family origin). In addition to the Swedish mutation, mo/hu APPswe/PS1dE9 co-expresses Presenilin 1 with a familial AD mutation (accelerates Aß42 deposition) together with the humanized form of mouse APP. Eponymous PDAPP mice have hAPP under the control of platelet derived growth factor promoter (PD). In the Tg2576 and mo/hu APPswe/PS1dE9 models, the APP gene is driven by the prion protein promoter, while the APP23 model has hAPP driven by the neuron specific Thy-1 promoter. These animals constitutively over express the APP transgene. Recently, a inducible Tet-off mo/huAPPswe/ind transgenic mouse model was generated using a tetracycline responsive promoter (Jankowsky, et al., 2005).

The various mouse models have demonstrable impairment in learning and memory that typically manifest at around the same time Aβ plaques deposits become prevalent in the limbic structures of these animals (Higgins and Jacobsen, 2003, Hsiao, et al., 1996, Westerman, et al., 2002). Mice exhibit loss of dendritic spines and loss of synapses in subcortical cholinergic projections, Aβ plaque associated gliosis, and cerebrovascular abnormalities (Beckmann, et al., 2003, German, et al., 2003, Moolman, et al., 2004, Stalder, et al., 1999, Wegiel, et al., 2004). APP23 mice exhibit neurodegeneration (Sturchler-Pierrat, et al., 1997) while the Aβ plaques in Tet-off/APPswe/ind mice persist for the lifetime the mouse even when APP transgene

production is halted early on (Jankowsky, et al., 2005). However, the lifespan of the Tet-off/APPswe/ind mouse is not significantly shortened by the presence of these Aβ plaque deposits. This highlights an inherent shortcoming of modeling AD in animals whose normal lifespan is less than 5% that of a normal human. Mouse models also do not have hyperphosphorylated tau neurofibrillar tangles or the same level of complement system activation found in AD (Higgins and Jacobsen, 2003, Schwab, et al., 2004, Xu, et al., 2002). Rat models of AD have not gained widespread popularity because rat brains are more resistant to the formation of dense Aß plaques and AD-like learning & memory deficits (Ruiz-Opazo, et al., 2004).

The transgenic mice listed above have been mated to other mice deficient or containing mutant proteins that are informative for AD studies. For instance, hybrid mice were created by mating Tg2576 mice to mice deficient in expression of the immune cell chemotaxis receptor CCR2 (El Khoury, et al., 2007). As described in the following, these mice proved instrumental in further understanding microglial contribution to the central nervous system (CNS) challenged with amyloidosis.

Extracellular Trafficking and Internalization of Aß

Though not a complete replicate of Alzheimer's disease, transgenic mouse models are nonetheless useful in understanding the genetics and biochemical cascades that lead to learning and memory deficits found in humans. As mentioned, the amyloid Aβ plaques in these models attract glia (Stalder, et al., 1999). As the brain's endogenous immunocompetent cells microglia are among the first cells recruited to the Aβ plaques (El Khoury, et al., 2007, Frautschy, et al., 1998, Stalder, et al., 1999). The Aβ-protein from these plaques has been found inside microglial lysosomes indicating that these cells actively phagocytose portions of Aβ plaques (Cole, et al., 1999,

Frautschy, et al., 1998). The process of internalizing Aß is mediated by several cells surface receptors. In the brain parenchyma, macrophage scavenger receptor Type A (MSR-A) is only expressed by microglia. Studies by Chung and coworkers, and others have shown that MSR-A is responsible for uptake of up to 60% of internalized fibrillar Aß (non-opsonized) in the brain (Chung, et al., 2001, El Khoury, et al., 1996). Interestingly, MSR-A knock-out animals expressing hAPP with Indiana and Swedish mutations under PD control have similar amounts of Aβ plaque burden when compared to their littermates with normal MSR-A expression (Huang, et al., 1999). Other receptors, such as MSR-B, and receptor for advanced glycation end products (RAGE) are capable of internalizing Aβ, and it is likely that these compensate for the loss of MSR-A (Huang, et al., 1999, Rogers, et al., 2002, Yan, et al., 1996).

Another way in which Aβ can be internalized is as a non-covalent conjugate to complement factors or antibodies (opsonization). Microglia have an assortment of receptors such as Cd11b and Fc gamma receptors which can mediate the phagocytosis of opsonized Aβ (Chung, et al., 2001, Lue and Walker, 2002). A recent study showed that APP is transported to cholesterol rich lipid rafts in neurons by low density lipoprotein receptors like protein (LRP) (Yoon, et al., 2007), however, its Aβ cleavage product can be carried by high density lipoprotein like protein (HDL) in the extracellular space and then internalized by microglial LRP (Fagan, et al., 1996). Apolipoproteins E (ApoE) and J (ApoJ) in complex with HDL-Aβ reduce the eventual degradation of Aβ in microglia (Cole, et al., 1999).

Allelic differences in ApoE, along with mutations in APP and PS1/2 are among the most well defined genetic risk factors for familial AD, and it is interesting that

microglia & astrocytes are the major contributors of extracellular ApoE in the brain (Xu, et al., 2000). Release of ApoE into the extracellular space is dependent on protein prenylation and is sensitive to statin treatment (Naidu, et al., 2002). Micromolar concentrations of Aβ can induce the secretion of ApoE from microglia *in vitro* (Bales, et al., 2000). Conversely, the fibrillization of Aβ is thought to be promoted by ApoE since the ApoE can bind to Aβ (Carter, et al., 2001, Xu, et al., 2000) and mice with the Indiana or Swedish mutations that have ApoE knocked out no longer have dense Aβ plaques or have delayed deposition of Aβ plaques, respectively (Fryer, et al., 2005, Irizarry, et al., 2000).

Lysosomal and Non-lysosomal Degradation of Aβ

Frautschy et al. quantified up to five-fold increases in microglial density surrounding Aβ plaques in mice with the Swedish mutation under the prion promoter (Frautschy, et al., 1998). El Khoury et al. demonstrated that elimination of CCR2 dependent microglial chemotaxis results in earlier appearance of amyloidosis, twice as much Aβ42 and ~36% greater mortality in mice co-expressing the prion promoter Swedish mutation (El Khoury, et al., 2007). A plethora of reports have provided evidence of mouse and human microglial degradation of Aβ via the endosomal-lysosomal pathway (Frautschy, et al., 1998, Qiu, et al., 1998, Rogers, et al., 2002). However the rate and quantity of this degradation is a subject of great concern as the kinetics of degradation (in relation to Aβ deposition) has direct physiological relevance to Alzheimer's disease progression. Several articles from Maxfield's group have shown that microglial cells from neonatal mice degrade Aβ at much slower rates compared to blood macrophages (Majumdar, et al., 2007a, Paresce, et al., 1997). In an elegant series of experiments, they showed that in the course of three days, neonatal microglia

in vitro degrade only 20% of the fibrillar Aβ they are exposed to while peritoneal macrophages degrade close to 80%. While microglia and macrophages are able to make similar cleavages at the N-terminus of the fibrillar Aβ, the macrophages were able to make far more thorough cuts along the Aβ molecule. Neither cell type was able to cut the C-terminal portion of the molecule. Perhaps the localization of Aβ's highly stable twisted beta pleated sheet at the C-terminus confers this resistance to degradation. This pleated sheet is the fundamental secondary structural element underlying multimers of Aβ (Sawaya, et al., 2007). The authors proposed that microglia are hindered in their capacity to degrade Aβ, relative to their macrophage counterparts, due to an incomplete set of lysosomal enzymes (Majumdar, et al., 2007a). This is indirectly supported by the observation that microglial degradation of Aβ *in vitro* is enhanced when global endocytosis of lysosomal enzymes is enhanced (Majumdar, et al., 2007a). It is worth mentioning that a recent study focusing on macrophages from the blood of AD patients concluded that these cells are impaired in their ability to phagocytose Aβ when compared to non-diseased subjects (Fiala, et al., 2005).

TGF-β1 is a cytokine that attracts and activates microglia. Bigenic mice overexpressing hAPP with Swedish and Indiana mutations under PD promoter in addition to TGF-β1 (cSJL x B6D2 background) have a 50% reduction in brain parenchymal Aβ plaque burden compared to their non- TGF-β1 overexpressing littermates (Wyss-Coray, et al., 2001). Since microglia exposed to TGF-β1 *in vitro* display enhanced degradation of Aβ, it is postulated that the marked *in vivo* reduction of Aβ plaque burden in these TGF-ß1 transgenic mice is due to microglial action. TGF-β1 and similar factors that stimulate microglia most likely cause degradation of Aβ through

either intracellular lysosomal degradation at the N-terminus, as already described, or through extracellular degradation via cell surface enzymes.

Neprilysin, a zinc dependant endopeptidase and insulin degrading enzyme (IDE), a zinc dependant metalloproteinase, are two well defined brain proteases. It is thought that microglia express these proteases on the cell surface and also release them into the extracellular space (Qiu, et al., 1998, Takaki, et al., 2000). A series of reports have a built a compelling case for neprilysin being the major soluble Aβ catabolic enzyme in AD animal models, in AD patients and in non-diseased humans (Iwata, et al., 2001, Leissring, et al., 2003). Of note are reports quantifying 50% reductions in neprilysin mRNA in hippocampal regions classically susceptible to amyloidosis (Yasojima, et al., 2001) and ~48% less mouse brain neprilysin mRNA in Tg2576 mice deficient in microglial recruitment to Aβ plaques due to CCR2 knockout (El Khoury, et al., 2007). As mentioned previously, these CCR2 knockout mice have twice as much Aβ42. Even though neprilysin is found in neurons, its major degradative function in the brain parenchyma appears to be microglial based. On the other hand, recent studies show that neprilysin cannot degrade the fibrillar Aβ commonly found in dense plaques (Yan, et al., 2006) or especially neurotoxic oligomeric Aβ (El-Amouri, et al., 2007). Thus, neprilysin activity can modulate normal Aβ catabolism *in vivo* (Marr, et al., 2003) and prevent the onset or progression of AD, however, its specificity for less multimeric forms of Aβ will likely prevent its use as a therapy for reversing the course of symptomatic AD.

The CCR2 knockout mice mentioned (El Khoury, et al., 2007) have normal IDE mRNA levels. This suggests that neurons and astrocytes are able to supply basal levels of IDE when microglial function is perturbed (El Khoury, et al., 2007). IDE is

present in the cytosol where it degrades the cytoplasmic portion of APP (Edbauer, et al., 2002), however cell surface IDE and secreted IDE are more likely the species of this protein responsible for extracellular Aβ clearance (Qiu, et al., 1998). In three month-old mice lacking IDE (and not expressing APP transgenes), a 64% increase in cerebral endogenous Aβ40 has been found (Farris, et al., 2003). However in 16-month-old mice with the Swedish mutation under the prion promoter, astrocytes proximal to Aβ plaques display a two-fold increase in IDE immunoreactivity at the same time point diffuse Aβ condenses into plaques (Leal, et al., 2006). Surprisingly, there was no reported reduction in Aβ plaque deposition (Leal, et al., 2006). In these studies, microglia surrounding the Aβ plaques do not produce IDE at levels detectable by immunohistochemistry.

IDE is one of the leading drug candidates for AD therapy. A recent study suggested that chemical modifications in its active site for the purpose of keeping the enzyme in a constitutively open state should be pursued (Shen, et al., 2006). This could result in a forty fold increase in catalytic activity and hence a therapeutic increase in Aß degradation. One must be prudent however as insulin is a major substrate for IDE degradation. Unlike other tissues, the brain does not maintain energy reserves so perturbations in sugar homeostasis caused by constitutively active IDE could result in severe side effects. This is less of an issue with neprilysin as a therapy since its other proteolytic substrates lie mostly outside the CNS compartment.

Consequences of Aβ Immunization and Inflammation

The field of AD research has experienced a significant disappointment following the termination of the Aβ42 immunization (AN-1792) clinical trial due to life threatening inflammatory side effects (Patton, et al., 2006). In contemplating the cause of

meningoencephalitis which afflicted 6% of the study's subjects, one must consider the role of microglial interaction with Aβ as a possible activating agent (Floden, et al., 2005, Tan, et al., 1999). This is thought to be mediated via the binding of complement factor C1 conjugated with Aβ to complement receptors CR3 & CR4 on the microglial cell surface (Heneka and O'Banion, 2007) inducing a highly cytotoxic complement cascade. It is worth noting that 20% of the subjects in the trial had the desired antibody response to Aβ immunization. However, in this subgroup, 22% suffered from meningoencephalitis. This suggests that the pathogenic inflammation that halted the study likely involved antibody-induced inflammation. Perhaps the antibody response changed the Aβ to a species that is more inflammatory?

In vitro studies have shown that Aβ can induce synthesis of inflammatory cytokines via a NfκB dependant pathway (Heneka and O'Banion, 2007). Floden and colleagues reported that there are age related differences in the ability of different forms of Aβ to induce inflammatory responses (Floden and Combs, 2006). Microglia isolated from neonatal and adult mice (C57BL/6 non-transgenics) are able to induce the secretion of TNFα when exposed to oligomeric Aβ while fibrillar Aβ can only induce TNFα production when exposed to neonatal microglia. If this finding holds true in humans, it could perhaps lend greater understanding to the AN-1792 trial - in the gray and white matter of AD patients with an antibody response to the Aβ42 immunization, post-mortem analyses intriguingly found dramatic increases in soluble Aβ as a result of antibody-dependent plaque disassembly. In fact, the quantity of soluble Aβ increased fifteen-fold in one subject. This antibody-dependent disassembly of fibrillar Aβ into soluble Aβ caused an unintended increase in oligomeric species of Aβ. The

investigators found Aβ plaque-derived dimers, trimers, tetramers and higher order oligomeric structures of up to 30kDa in the brains of these patients. As described by Floden et al., oligomeric but not fibrillar species of Aβ can selectively induce adult microglial production of proinflammatory TNFα (Floden and Combs, 2006) and directly cause neuronal death (Floden, et al., 2005, Tan, et al., 1999).

Novel Approaches for Study of Aβ Regulation and Therapy

As described above, studies on the catabolism of Aβ have shed light on the brain's mechanisms of regulating extracellular Aβ. Studies from neuroimmunology labs have demonstrated that microglia, the primary immune cell of the CNS (Giulian, 1987), have a considerable role in Aβ regulation in the AD brain (Chung, et al., 2001, El Khoury, et al., 2007, Frautschy, et al., 1998, Rogers, et al., 2002). However, clinical trials aimed at emulating microglial-like functions (anti-oxidant trials) or curtailing microglial functions (anti-inflammatory trials) have largely failed at treating AD. Interestingly, these trials, which targeted a disease of the elderly, were conspicuously carried out on knowledge primarily from studies on *in vitro* neonatal mouse models. Nevertheless, it is generally accepted that glia play a role in the regulation of the extracellular space including the metabolism of extracellular Aβ.

The emerging field of stem cell research has demonstrated that the neuronal stem cell of the subependymal zone (SEZ) is a very glial-like immature cell that may provide a window for novel approaches to treat AD pathology (Kukekov, et al., 1997, Laywell, et al., 2000, Raponi, et al., 2007). Our goal was to bring together the knowledge base of neuroimmunology and stem cell biology in order to answer two questions:1) is there a loss of microglial Aβ catabolic functionality in the aged brain and 2) can stem cells be used as a therapeutic approach to lessen Aβ burden in brains where Aβ homeostasis is

perturbed? Our hypotheses was that 1) there is a depreciation of Aβ degradation in the aged and AD brain and 2) the biology of stem cells uniquely positions them as a platform to counter Aβ burden. These hypotheses were founded on the following observations. First, in both the aged and AD brain, there are greater levels of Aβ (Armstrong, et al., 1996). This increase in Aβ cannot be fully explained by currently known genetic risk factors since these factors confer increased AD susceptibility by affecting Aβ anabolism. Because most AD cases are 'late onset' without any known genetic causes, the possibility of dysregulation of Aβ catabolism in AD remains (Association, 2007). Second, histological evidence from human and rodent autopsy brain sections show that microglia appear dystrophic with similar morphological features in both the aged and AD brains (Flanary, et al., 2007). Thus, lose of microglial function could contribute to increased Aβ burden with age and AD. Third, cell replacement therapy using stem cells is a promising approach because of the physiological flexibility inherent to stem cells. These cells naturally undergo self renewal *in vivo* and *in vitro* and are capable of being transplanted after being expanded *ex vivo* (Marshall, et al., 2006, Walton, et al., 2006a). This unique property allows for genetic introduction of candidate anti-Aβ molecules in culture for delivery *in vivo*.

In the following, I shall detail our experimental findings in quantifying glial aged-related biology as well as determining the Aβ disrupting ability of 1) transplanted stem cells and 2) stem cells used to deliver the candidate anti-Aβ therapeutic, MMP9. Our studies have implications in understanding catabolic pathways that contribute to Alzheimer's disease pathology and clinical approaches to treating said pathology.

CHAPTER 2
EX VIVO CULTURES OF MICROGLIA FROM YOUNG AND AGED RODENT BRAIN REVEAL AGE-RELATED CHANGES IN MICROGLIAL FUNCTION

Introduction

A multitude of studies have implicated microglia as important players in the etiology of a number of age-related neurodegenerative diseases, including Alzheimer's disease, Parkinson's disease and amyotrophic lateral sclerosis (Boillee, et al., 2006, Chung, et al., 2001, El Khoury, et al., 2007, Frautschy, et al., 1998, Rogers, et al., 2002). To understand how microglial cell function may change with aging, various protocols have been developed to isolate microglia from the young and aged central nervous system (CNS). While histological studies are essential in providing clues regarding the cells' involvement, they are limited in terms of evaluating the functions of living cells. In the past decade, protocols to isolate living microglia from postnatal animals have become available (Carson, et al., 1998, de Haas, et al., 2007, Frank, et al., 2006, Hickman, et al., 2008, Ponomarev, et al., 2005). These protocols either trap microglia using antibodies to cell-specific antigens (Hickman, et al., 2008, Tham, et al., 2003) or separate microglia using density centrifugation (de Haas, et al., 2007, Frank, et al., 2006). In both cases, the rapid isolation of microglia enables *ex vivo* experimentation of endogenous microglia in a controlled setting largely devoid of neurons, oligodendrocytes and astrocytes.

Protocols utilizing density centrifugation are advantageous to those utilizing antigen traps in terms of yield per brain (de Haas, et al., 2007). They also avoid artificial cellular reactions caused by antigen cross linking, a risk carried with the use of antibodies in trapping protocols. However, in our hands, significant amounts of non-microglial, debris contaminate current density centrifugation derived cultures. In the

present study, we sought to modify density centrifugation methodology to eliminate debris fields present in such cultures. With these modifications, microglial yields were preserved or slightly increased.

These improvements allowed us to study microglial function with regard to alterations during normal aging. We found that microglia from aged mice constitutively secrete greater amounts of interleukin-6 (IL-6) and tumor necrosis factor-α (TNF-α) relative to microglia from younger mice and are less responsive to stimulation. Also, microglia from aged mice have reduced glutathione levels and internalize less Aβ while microglia from mice of all ages do not retain the Aβ peptide for a significant length of time. These studies offer further support for the idea that microglial cell function changes with aging. They suggest that microglial Aβ phagocytosis results in Aβ redistribution rather than biophysical degradation *in vivo* and thereby provide mechanistic insight to the lack of amyloid burden elimination by parenchymal microglia in aged adults and those suffering from Alzheimer's disease.

Methods

Solutions

Dispase II (Roche, Mannheim, Germany) was reconstituted at 2U/mL in dispase buffer (0.9% HEPES, 50mM NaCl, pH 7.4) according to manufacturer's instructions. Percoll (GE Healthcare, St. Giles, UK) was diluted 1:10 with 10x phosphate-buffered saline (PBS) to create an isotonic solution. 1x PBS was added to isotonic percoll to create working solutions ranging from 75% to 25% percoll.

Animals

Debris reduction experiments were performed with non-transgenic C57BL/6 mice and mice expressing GFP under the fractalkine-receptor promoter (Jung, et al., 2000).

Experiments were performed using young (1-2 month old) and aged (14-16 month old) male C57BL/6 mice. The mice were housed at 22˚C in a controlled 12hr light/dark cycle and provided food and water ad libitum. Animals were euthanized by exsanguination using transcardiac perfusion with PBS under deep anesthesia with sodium pentobarbital (50mg/kg body weight). This method of euthanasia is consistent with the recommendations of the Panel of Euthanasia of the American Veterinary Medical Association. After perfusion, the brain (telencephalon, cerebellum and midbrain) was rapidly removed.

Reduction of Debris Produced by Brain Homogenization

Each brain was washed in cold 1x PBS, then minced using a small scissors. Brain tissue was gently dissociated by immersion into 10mLs (per brain) of dispase II solution (2U/mL), trypsin solution (0.05%) or by grinding within a tissue homogenizer (glass Potter, Braun, Melsungen, Germany). Dissociated brain tissue was placed within a 50mL conical tube and laid horizontally in an orbital shaker set to shake for 1hr, 37°C at 150rpm. Remnant tissue chunks were further homogenized by rapidly triturating with a 10mL pipette (BD Biosciences, Boston, MA) with a wide bore to prevent cell shearing. This was carried out with a fully charged pipette aid (Drummond). Enzyme activity was halted by diluting the resultant homogenate 1:1 with cold 10% FBS in 1x PBS. Meninges and clumped cells were removed with 70um filtration (BD Biosciences, Boston, MA) to obtain a suspension of single cells.

Preparation of Discontinuous Percoll Gradients

The homogenate was spun 1000 x g for 10min at 4°C. The supernatant was discarded and the pellet of an individual brain was resuspended in 6mLs of 75% isotonic percoll (high percoll) (GE Healthcare, Buckinghamshire, U.K). Three mLs of this

mixture was then aliquoted into a 15mL polystyrene tube. Five mLs of 35% isotonic percoll (low percoll) was layered atop the high concentration percoll at a rate of 150ul/sec to create a distinct interface between the percoll layers. To replicate gradients described in the literature, 25% percoll was utilized for low percoll. 1x PBS was layered atop the low concentration percoll. The resultant discontinuous gradient was then allowed to settle on ice for 15 minutes allowing most of the homogenate to naturally rise towards its isopycnic position. The gradient was then centrifuged at 800 x g for 45min in a HS-4 swinging bucket rotor (Thermo Fisher Scientific, Waltham, MA) set to 4°C. We did not notice changes in microglial yields with high acceleration or the application of the brake. However, yields were significantly diminished if the gradients are not processed immediately following centrifugation. To process the gradients, the volume of the PBS layer and the low concentration percoll layer were rapidly aspirated. A band of microglia (usually 0.5-1.5mL), captured between the low concentration and high concentration percoll layers was then collected and diluted in 50mL of 1x PBS. This was centrifuged at 1000 x g for 10min at full acceleration and brake. The supernatant was quickly decanted and the cell pellet resuspended in DMEM culture media containing 10% FBS. We also added 0.15ug/mL granulocyte monocyte colony stimulating factor (GM-CSF, R & D Systems, Minneapolis, MN), authouth this is not required for the culturing of microglia.

Immunochemistry

Isolated cells were grown in culture media overnight. Cells were then washed, fixed in 4% paraformaldehyde and processed for immunofluorescence of microglial antigen Iba1 (1:500, Wako, Richmond, VA), microglial antigen Cd11b (1:1000, Serotec, Raleigh, NC), astrocyte antigen GFAP (1:1000, Dako Corporation, Carpinteria, CA), and

neuronal antigen NeuN (1:500, Millipore, Bellirica, MA). Cells were rinsed and incubated with goat anti-rabbit Alexa 488 (Invitrogen, Carlsbard, CA) and goat anti-mouse Alexa 568 (Invitrogen, Carlsbard, CA). Cells were photographed with an Olympus DP71 camera mounted on an Olympus BX60 microscope.

Cell Viability

Microglial mitochondrial respiratory activity, a measure of cell viability, was determined using a colorimetric MTT (methylthiazolyldiphenyl-tetrazolium bromide) assay (Bioassay Systems, Hayward, CA). This was compared to a reference value of HEK-293 cells, a highly viable immortal cell line, and dying cultures treated with 1% Triton X-100, a toxic reagent.

Microglial Stimulation

In order to compare the inflammatory reaction of microglia in young and aged brains, cells were isolated from 2 and 14 months old mice, as described above, and seeded in 96-well tissue culture plates (Corning Incorporated, Corning, NY) at a density of 3×10^5 cells/well. The cultures were incubated overnight at 37°C with 5% CO_2 and saturated humidity. The next day, cells were stimulated by replacing the original culture media with media containing 2% FBS and inflammatory agents in different concentrations. Two highly potent inflammatory stimuli were selected, i.e. lipopolysaccharide (LPS), (*Escherichia coli* 055:B5) (Sigma, St. Louis, MO), a toll-like receptor 4 (TLR4) agonist and PamCSK3 (Invitrogen, Carlsbard, CA), a TLR2 agonist. LPS and PamCSK3 were added at a concentration of 10-100ng/mL (LPS) or 0.1-1ug/mL (PamCSK3). Control conditions were included, containing no stimuli. After 24hrs of incubation, the media of stimulated microglia were collected and centrifugated

for 10min at 20°C and 1200rpm. The supernatants were used for IL-6 and TNF-α enzyme-linked immunosorbent assays (ELISA). For every condition, cytokine levels were calculated in three different wells, while each experiment was performed fourfold.

IL-6 ELISA

Mouse IL-6 secreted protein levels were determined with a general sandwich ELISA protocol. Briefly, an enhanced protein binding ELISA plate (Nunc, Rochester, NY) was incubated overnight at 4°C with the capture antibody, rat anti-mouse IL-6 (BD Bioscience Erembodegem, Belgium). After blocking the non-specific binding for 2hrs, standards (BD Bioscience Erembodegem, Belgium) and samples were added for 2hrs at room temperature. Subsequently, biotinylated rat anti-mouse IL-6 (BD Bioscience Erembodegem, Belgium) was used as a detection antibody. Following incubation with a Streptavidin-**Horseradish Peroxidase** conjugate (Dako Cytomation, Heverlee, Belgium), a TMB substrate (BD Bioscience Erembodegem, Belgium) was applied to the plate. Finally, optical densities (OD) were read between 450-570nm, using a spectrophotometer (Powerwave X Select) and concentrations were calculated. The detection limit of the assay was 10pg/mL.

TNF-α ELISA

Mouse TNF-α secreted protein levels were measured using a commercially available ELISA kit (eBioscience, San Diego, CA), according to the manufacturer's instructions. Concentrations were determined according to the OD values, measured using a spectrophotometer (Powerwave X Select) at a wavelength between 450-570nm. The detection limit of the assay was 8pg/mL.

Glutathione Measurements

Total glutathione (reduced and oxidized) was measured in microglia using a glutathione reductase enzymatic recycling assay (Cayman Chemical, Ann Arbor, MI) that is based on the colorimetric conversion of nitrobenzoic acid to 5-thio-2-nitrobenzoic acid (Tietze, 1969). Briefly, microglia from the brains of young or aged mice were lysed immediately following isolation and prepared for glutathione measurements according to manufacturer's instructions. Glutathione levels within the range of standards were attained by combining microglia from four brains. Therefore to attain three repetitions, 12 mice per age group were assayed. All samples were normalized to total protein using bicinchonic acid (BCA) colorimetric assay (Pierce, Rockford, IL).

Aβ42 Fate Analysis

Aβ42 lyophilized protein with and without a FITC conjugate (rPeptide, Bogard, GA) was resuspended to 1mg/mL in 1% NH_4OH and stored at -20°C according to manufacturer's directions. To visualize internalized Aβ in living cells, Aβ42-FITC was diluted to 4ug/mL in DMEM and added to microglia for 3hrs. The cells were then stained with DAPI nuclear counterstain (1:1000) for 5min. and then imaged. For enhanced subcellular resolution of internalized Aβ, cells (exposed to non-conjugated Aβ42) were fixed as described above for immunocytochemistry using antibodies against Aβ (6E10, 1:2000, Signet Laboratories, Dedham, MA) and the lysosomal associated protein, Lamp 1 (1:2, gift from Dr. Notterpek, University of Florida). To determine the aggregation state of Aβ42 in stock solutions used in internalization and fate experiments, samples were diluted in Laemmli sample buffer containing 2% sodium dodecyl sulfate (SDS) and loaded in 4-20% TG-SDS gels (Invitrogen, Carlsbad, CA) for standard SDS-PAGE. Immunoblots were probed with 6E10 at a dilution of 1:5000.

6E10 has affinity to individual Aβ42 peptides and therefore monomers, oligomers and higher order conformers of Aβ42 are distinguishable by size difference. Gel blots were photographed using a Fugi imaging system (Fugifilm Life Science, Stamford, CT).

RS chambers (Nunc, Roskilde, Denmark) that contain a hybrid of glass and polystyrene surfaces have reduced non-specific interaction with Aβ and were therefore chosen for fate analysis experimentation. To further reduce non-specific Aβ42 absorption, these chambers were blocked with 10% milk for 1hr. Microglial cells were then isolated from 1 month old mice, 15 months old mice and mixed glial cultures (MGC) were seeded on RS chambers at approximately 3 x 10^5 cells/chamber. The cultures were incubated overnight at 37°C with 5% CO_2 and saturated humidity. The next day, cultures were rinsed and given Aβ42 diluted in DMEM at 4ug/mL. The cells were allowed to internalize Aβ42 from the media for 3hrs in 37˚C. The cells were then rinsed and incubated at 37˚C with 1.5mLs of culture media lacking Aβ42. This media and that of cells lysed immediately following rinsing were collected, as were the conditioned media and lysate from wells incubated for 3hrs and 16hrs. The lysis buffer consisted of NP40 (Invitrogen, Carlsbard, CA) supplemented with protease inhibitor cocktail (1x, Sigma, St. Louis, MO) and PMSF (1mM). For each age group, lysate and media representing 3-6 adult mice or 14 neonatal pups (2 (MGCs) were collected. To determine the fate of Aβ42, we employed a sandwich-style ELISA (Invitrogen, Carlsbard, CA), configured with two capture antibodies (recognizing epitopes on the N terminus and C terminus of human Aβ42) to first capture the N terminus of Aβ42 and then the C terminus (Schmidt, et al., 2005). Microglial degradative activity on Aβ42 causes N terminal truncations (Majumdar, et al., 2007b), thus ELISA reactivity is limited

to non-degraded Aβ42. We were therefore able to 1) follow the loss of Aβ42 and 2) the expulsion of Aβ42 from microglia. The ELISA was processed with duplicates of each sample and absorbance read at 450nm using a spectrophotometer (Bio-Tek, Winooski, VT). Data was normalized to mock treated wells that were treated as described above but contained no cells. The detection limit of the assay was 10pg/mL.

Statistical Analysis

Average cytokine data are presented as mean ± SEM. Statistical analysis was carried out using SPSS ver. 14.0 for Windows (SPSS, Chicago, IL). To analyse differences between groups, we used unpaired, two-tailed Student's t-test or ANOVA with a post hoc Bonferonni's test when appropriate. A p-value of <0.05 was considered statistically significant. Average Aβ data are presented as mean ± SEM. For statistical comparison of Aβ internalization between age groups, we used unpaired, two-tailed Student's t-test. For statistical comparison of Aβ fate, paired, two-tailed Student's t-test was used to compare Aβ levels immediately following internalization and 16hrs later. A p-value of <0.05 was considered statistically significant.

Results

As reported previously (de Haas, et al., 2007, Frank, et al., 2006), centrifugation of dissociated whole brain within discontinuous percoll gradients can separate microglia from other brain cells. In our hands, the techniques described in the literature yielded insufficiently pure cultures for the pulse-chase experiments we performed (Fig. 2-1B-C). Specifically, we observed that debris fields, which could possibly sequester Aβ peptide (Li, et al., 2005). To address this, we utilized dispase II, an enzyme that has been described as particularly gentle, yet capable of tissue dissociation (Borchelt, et al., 1992, Gao, et al., 2004, McDermott, et al., 2003). Furthermore, we increased the

density of percoll by 16% from that described in the literature (de Haas, et al., 2007). We observed that brains treated with this methodology 1) had greater separation of dissociated microglia from tissue chunks (Fig. 2-1A-B), 2) yielded numerous adherent microglia and 3) were largely devoid of debris (Fig. 2-1C-D).

Altogether, the combination of these techniques resulted in the extraction of up to 3×10^6 microglia per brain. On average, 8.5×10^5 microglia per brain were extracted from young and aged mice (Fig. 2-2B). 94% of DAPI counterstained cells were reactive to Iba1 (Fig. 2-2A) as determined by 3 observers. The cells had a characteristic amoeboid, phase bright morphology similar to previous reports of adult microglia isolated with different methodology (Tham, et al., 2003). To further confirm that our isolated cells were indeed microglia, we isolated cells from transgenic mice where GFP expression is under the fractalkine receptor promoter. These mice are reported to have microglia as the only brain cell type to express GFP (Jung, et al., 2000). Upon isolation of cells, our cultures were reactive to antibodies specific to GFP (Fig. 2-3A). Ex vivo cultures of adult microglia that were allowed to adhere overnight were comparable to the HEK 293 cell line in viability (Fig. 2-2C). Recent studies have raised the possibility that GM-CSF could push cultured microglia towards a dendritic cell fate (Esen and Kielian, 2007). In our cultures, microglia grown in 0.15ug/ml GM-CSF or in GM-CSF free conditions both maintained a rounded morphology (Fig. 2-3B) and had no immunoreactivity to the dendritic cell antigen, Cd11c (data not shown). Interestingly, neonatal microglia derived from mixed glial cultures lacking GM-CSF exhibited a ramified phenotype when cultured overnight in GM-CSF containing media (Fig. 2-4). This morphology is similar to that observed in mixed glial cultures with prolonged

exposure to GM-CSF (Esen and Kielian, 2007). It is possible that the conditions within mixed glial cultures prime microglia to adopt a dendritic-like morphological phenotype upon exposure to GM-CSF.

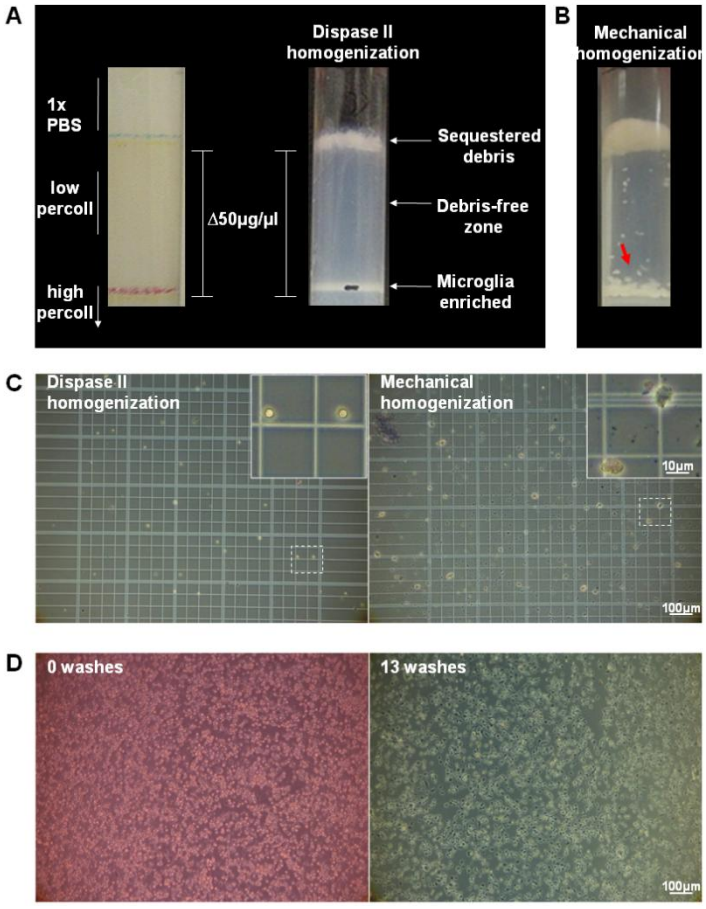

Figure 2-1. Dispase II density centrifugation methodology. (A) Brain hemispheres that were homogenized with dispase II and loaded onto discontinuous gradients composed of 35% 'low' percoll and 75% 'high' percoll sequestered microglia to an isopynic density of 1.077mg/ul as determined by beads with known densities. This configuration spatially separated unwanted brain matter to a density 50ug/ul more buoyant. (B) Density centrifugation methodology as described in the literature involved mechanical homogenization and reduced percoll densities. In our hands, such methodology failed to channel unwanted brain matter (tissue chunks, red arrowhead) to an isopynic position distal to the microglia enriched band. (C) Phase contrast images of freshly prepared cells under a hemacytometer demonstrate viable phase-bright cells (resistant to trypan blue) as well as reduced particulate matter from dispase II homogenized brains. Following 24hrs of culture, these cells remain adherent after multiple washes (D) and are thus compatible with experiments that involve media exchanges.

Previously, histological findings of dystrophic microglia in the aged and diseased brain have led our laboratory to suggest microglial function may deteriorate with normal aging. Therefore, we sought to study elements of pathology that are mainly conferred by microglia *in vivo* and are known to change with aging and disease (Bolmont, et al., 2008, El Khoury, et al., 2007, Meyer-Luehmann, et al., 2008, Streit, et al., 2004, Ye and Johnson, 1999). Recent studies have shown that mRNA copies of inflammatory cytokines are increased in microglia from aged brains (Sierra, et al., 2007, Ye and Johnson, 1999). However, mRNA transcripts may not necessarily translate to secreted protein levels (Munger, et al., 1995, Storm van's Gravesande, et al., 2002), a more ultimate measure of functional change. To determine if microglia vary their secretion of cytokines with age, we obtained microglia from young and aged mice and measured their cytokine levels with and without exogenous immune stimulation.

The most striking observation in this respect was the dramatic increase in IL-6 release under basal conditions (young: 211.8±31.7 pg/ml vs. aged: 3735.9±1000.2 pg/ml, $p<0.001$). In both young and aged microglia, a significant dose-effect relation following either LPS or PAMCSK3 stimulation was observed (Fig. 2-5A). Moreover, maximal release of IL-6 was significantly enhanced in aged microglial cells following LPS (100ng/ml) or PAMCSK3 (1ug/ml) stimulation (Fig. 2-6).

As with IL-6, the amount of TNF-□□produced by aged microglial cells was significantly higher under basal conditions when compared to young microglia. While microglia derived from young mice produced no TNF-□ under basal conditions, the amount was significantly increased to 917.2 ± 91.9 pg/ml in supernatants of aged microglia cultured for 24h without any exogenous stimuli ($p<0.001$). This striking

difference confirms age-related higher basal levels of cytokine production previously observed with mRNA transcript analysis (Sierra, et al., 2007) and indicates that aged microglia are hyperactive when compared to microglia from young mice. This high release under basal conditions may explain the lack of a significant dose-effect relation in TNF-□ production following either LPS or PAMCSK3 stimulation (Fig. 2-5B). In contrast, in young microglia a significant dose-effect relation was observed. Moreover, although the maximal amount of TNF-□ released by aged microglia in response to 1□g/ml PAMCSK3 was slightly though significantly increased, responses to 100ng/ml LPS were not different between aged or young microglia (Fig. 2-6B).

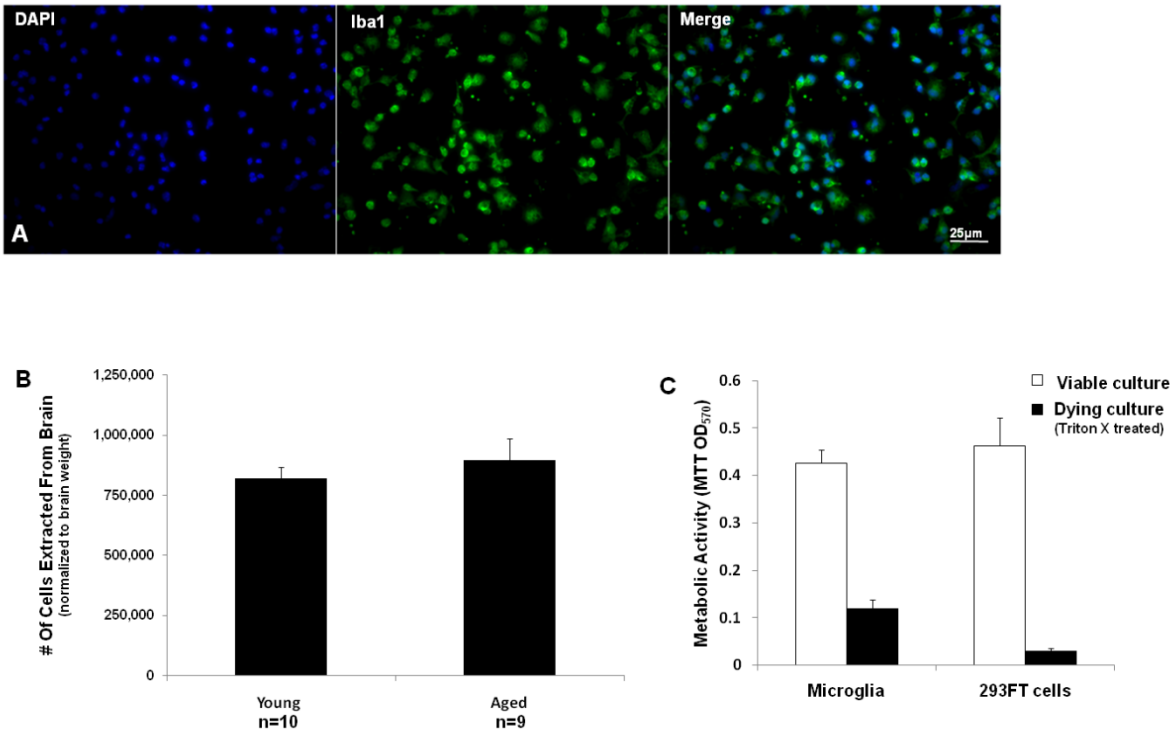

Figure 2-2. Purity, yield and viability of microglia. (A) Microglia isolated with dispase II density centrifugation methodology express Iba1, a marker commonly used to identify *in vivo* microglia. (B) Yields of microglia from 1 month and 15 month old mice typically obtained using dispase II based density centrifugation methodology show little variability with age. (C) Measurement of mitochondrial respiratory activity indicated that isolated microglia form cultures comparable in viability to HEK 293 cells, an immortal cell line.

In addition to quantifying microglial cytokine production as a function of age, we were interested in whether the ability of microglia to serve as an oxidative sink and to internalize Aβ changes with age. Glutathione acts as antioxidant by neutralizing free radicals and peroxides and microglia are reported to be the primary glutathione containing cells in the brain (Hirrlinger, et al., 2000, Lindenau, et al., 1998). We found a trend indicating that microglia in aged brains have 21% less total glutathione (oxidized and reduced) compared to microglia from young brains (Fig. 2-7). This result suggests the reactive oxygen species (ROS) insult that can be caused by Aβ internalization (Milton, et al., 2008) maybe more injurious to microglia in aged brains.

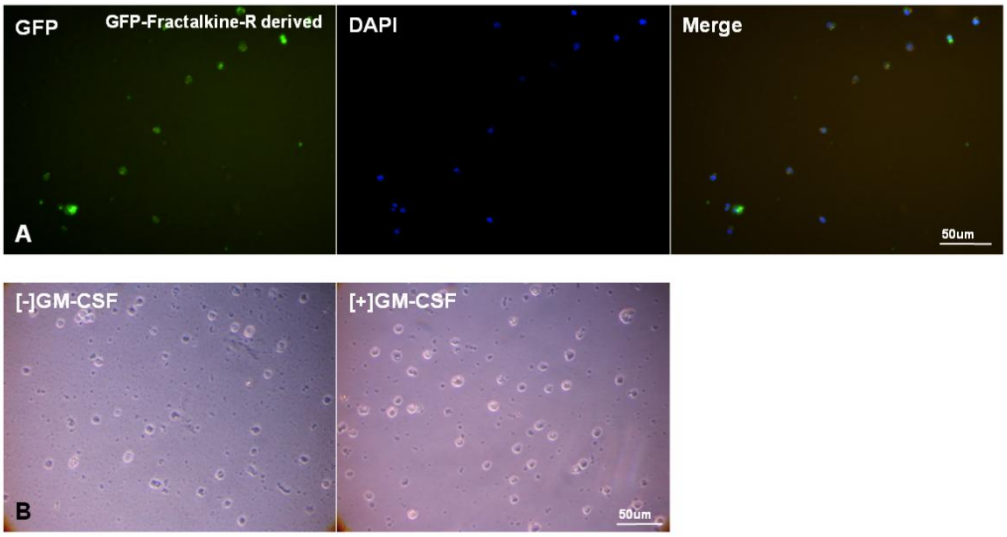

Figure 2-3. Adult microglial morphology. (A) GFP-Fractalkine-Receptor transgenic mice, where microglia are the only *in vivo* GFP expressing neuronal cells yielded cultures composed of GFP positive cells. This provided independent confirmation that our isolation methodology extracted *in vivo* microglia. (B) Adult microglial cells remained rounded and did not adopt a dendritic morphology when cultured for 24hrs with media containing GM-CSF (n=2 mice).

Aβ accumulation is a well recognized feature of AD, however extensive amyloid deposits may be found in many aged, non-demented individuals (Bouras, et al., 1994). This pathology may result from AD-independent deterioration of clearance processes. Microglial scavenger activity on Aβ is proposed as a clearance process that contributes in maintaining Aβ at physiological levels by counterbalancing constitutive Aβ secretion by neurons. Our laboratory and others have published accounts of microglial degeneration that is associated with age (Flanary, et al., 2007, Simmons, et al., 2007, Streit, et al., 2008, Streit, et al., 2004). If microglia represent a major Aβ clearance mechanism, their degeneration would result in progressively increasing Aβ levels with age and therefore would have significant implications to the occurrence of amyloidosis in AD and some aged individuals. We currently lack the means to isolate degenerating microglia for experimentation. However *ex vivo* assessment of microglia acutely isolated from young and aged mice likely emulates *in vivo* processing of Aβ more so than neonatal and 'microglial like' cell lines and may give insight to the degeneration of microglia with age. *Ex vivo* cultures of microglia were given media with 4ug/mL of Aβ42-FITC conjugate or non-conjugated Aβ42. Western blot analysis indicated that non-conjugated Aβ42 preparations contained Aβ42 monomers, oligomers and SDS resistant species larger than 220kDa that are likely fibrils thus reflecting *in vivo* amyloid burden (Fig. 2-8A). Internalization of Aβ42 by living microglia was visually confirmed with cell-associated FITC fluorescence (Fig. 2-8B). Aβ42 observed in fixed cells was colocalized with lysosomes (Fig. 2-8C). To quantify internalization, microglial lysates were measured using an Aβ42 sensitive ELISA. Our results indicate that microglia from aged mice internalize 53% less Aβ42 relative to microglia from young mice (Fig. 2-9A).

We next wanted to determine if Aβ42 phagocytosis by neonatal microglia (derived from mixed glial cultures) is reflective of microglia from adult mice. To our surprise, neonatal microglia internalized significantly more Aβ42 than microglia derived from young mice. This suggests that microglia from mixed glial cultures may not necessarily model microglial Aβ42 clearance activity in the postnatal brain. Internalization of Aβ42 is a prerequisite step for intracellular clearance; however it is by no means a surrogate marker for biophysical Aβ42 degradation. To more comprehensively determine the fate of phagocytosed Aβ42, we bathed cells in fresh media and measured the levels of Aβ42 in this media and within cells over 16hrs. We observed that internalized Aβ42 is invariably expelled by microglial cells in an age-independent manner within 3hrs (Fig. 2-9B). This result concurs with previous reports of lackluster microglial anti-Aβ activity *in vivo* (Simard, et al., 2006) that may stem from impaired lysosomal activity (Majumdar, et al., 2007b).

Discussion

Improvements on Microglial Isolation

In this study, we aimed to reduce debris contamination which is a feature of microglial cultures derived from gradient centrifugation based methodology. The brains of mice that are designated by the National Institute on Aging as an aging model were treated successively to steps that significantly increased the purity of *ex vivo* microglial cultures. Analysis of such cultures, derived from mice of various aging categories, revealed that microglia from aged brains have markedly increased basal levels of IL-6 and TNF-α secretion, have reduced glutathione levels and have a limited capacity to ingest Aβ42. In contrast, microglia from younger mice are able to temporarily contain

Aβ42. Together, these *ex vivo* findings provide evidence that microglia are subject to age-associated changes in biology.

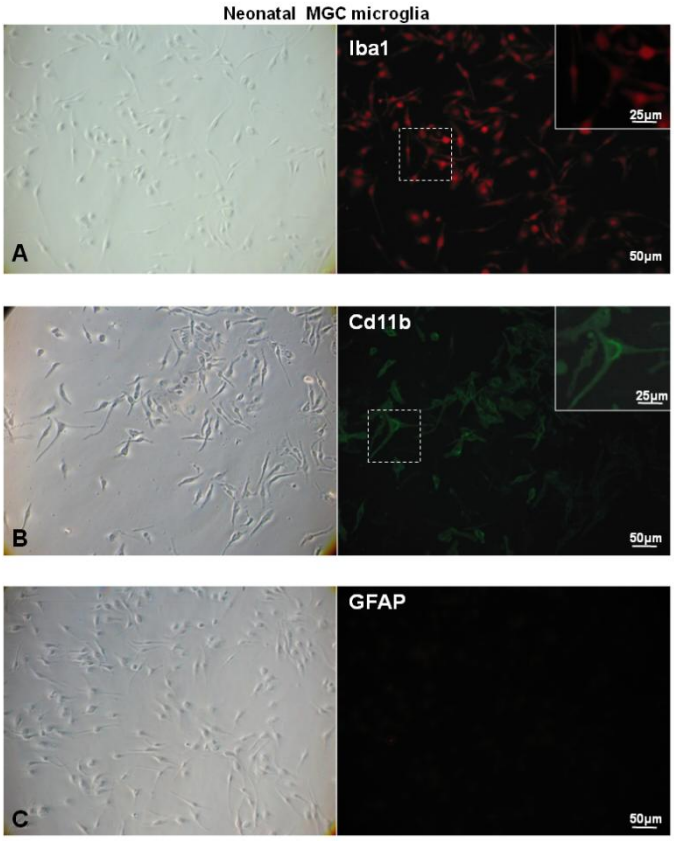

Figure 2-4. Neonatal microglial morphology. Neonatal microglia express Iba1 (A), however they are distinguished from adult microglia (young and aged) by ramified cytoplasmic processes visible under phase contrast microscopy and Cd11b immunoreactivity (B). Purity of neonatal microglial cultures was confirmed by lack of GFAP immunoreactivity, a marker for astrocytes and immature neurons.

Age-related Changes in Microglial Cytokine Release

Prior reports from our laboratory have shown that microglia have IL-6 and TNF-α mRNA (Streit, et al., 2000) and more recently, others have found age-related changes in microglial IL-6 and TNF-α mRNA (Sierra, et al., 2007). We extend on these results by measuring secreted IL-6 and TNF-α proteins (experiments performed by Ellen Boelen). Our results indicate significantly more pronounced changes in basal cytokine production

and responsiveness. It is difficult to make direct comparisons of mRNA and secreted protein measurements. However, it is of note that the margin of change we observe in the basal production of IL-6 between microglia from young and aged mice is approximately 4-fold higher than that observed by mRNA analysis (∆17.6x vs. ∆5x respectively). We also did not observe detectable levels of basal TNF-α by microglia from young animals in our studies. These differences can perhaps be explained by varying sensitivities of the employed detection methodologies or by post-transcriptional effects. The half-life of mRNA can often be rate-limiting in translation (Ross, 1995). Secondarily, secretory pathway modulation of newly produced cytokines may also modulate the concentration of cytokines in the extracellular milieu independent of DNA transcription. As microRNAs are involved in regulation of gene expression at the post-transcriptional level, possible changes in this machinery can also be mentioned to explain the discrepancy between protein and mRNA levels. Our results, though in agreement with previous reports, indicate that microglia from brains of various aging groups have much greater differences in cytokine production, and responsiveness to immune stimulation than was previously thought.

Implications of Age-related Changes in Microglial Cytokine Release

What are the possible implications of age-related changes in microglial cytokine production? A number of authors commonly describe IL-6 and TNF-α as neurotoxic molecules involved in AD pathogenesis (Bruunsgaard, et al., 1999, Collins, et al., 2000, Culpan, et al., 2003, He, et al., 2002, Li, et al., 2007, Licastro, et al., 2000, McGeer and McGeer, 2001). However, experiments presenting alternative viewpoints have been published (Brunello, et al., 2000, Loddick, et al., 1998, Marz, et al., 1998, Streit, et al., 2000, Tarkowski, et al., 1999, Thier, et al., 1999, Wei, et al., 1992). IL-6 may have a

role in regeneration of injured tissue in the brain (Loddick, et al., 1998, Streit, et al., 2000, Tarkowski, et al., 1999), has known anti-apoptotic properties (Wei, et al., 2001) and in mice that overexpress both IL-6 and its receptor, IL-6Rα, there is no evidence of neurotoxicity (Brunello, et al., 2000). Inflammation is a component of wound healing in the CNS (Klein, et al., 1997, Streit, et al., 2000). Recently, it has been reported that lesions typically ascribed to cause AD dementia, are present in 20-40% of non-diseased, aged adults (Price, et al., 2009) and both TNF-α and IL-6 increase with age (Bruunsgaard, et al., 1999, Wei, et al., 1992). Thus the aging brain appears to exist in a constant state of injury. Inflammatory processes, such as microglial secretion of IL-6, maybe needed for persistent regeneration or neuroprotection. The viewpoints that cytokine release is exclusively neurotoxic or neuroprotective could be equally considered speculative. Further studies which consider region-specific and age-specific differences in cytokine response are needed, amongst others, to shed light onto the role of cytokines released by microglia on the nervous system.

Age-related Changes in Microglial Glutathione Levels

Microglial surveillance of the parenchyma involves scavenging of potentially hazardous materials. Proteins such as LPS and Aβ induce ROS and it is thought that the increased levels of antioxidant molecules such as glutathione found in microglia relative to other brain cells (Hirrlinger, et al., 2000, Lindenau, et al., 1998) protect microglia from ROS burden associated with scavenging activity (Dringen, 2005, Milton, et al., 2008, Qin, et al., 2004, Tchaikovskaya, et al., 2005). Our findings of reduced glutathione levels in microglia immediately analyzed after brain extraction maybe indicative of broader microglial loss of function with age.

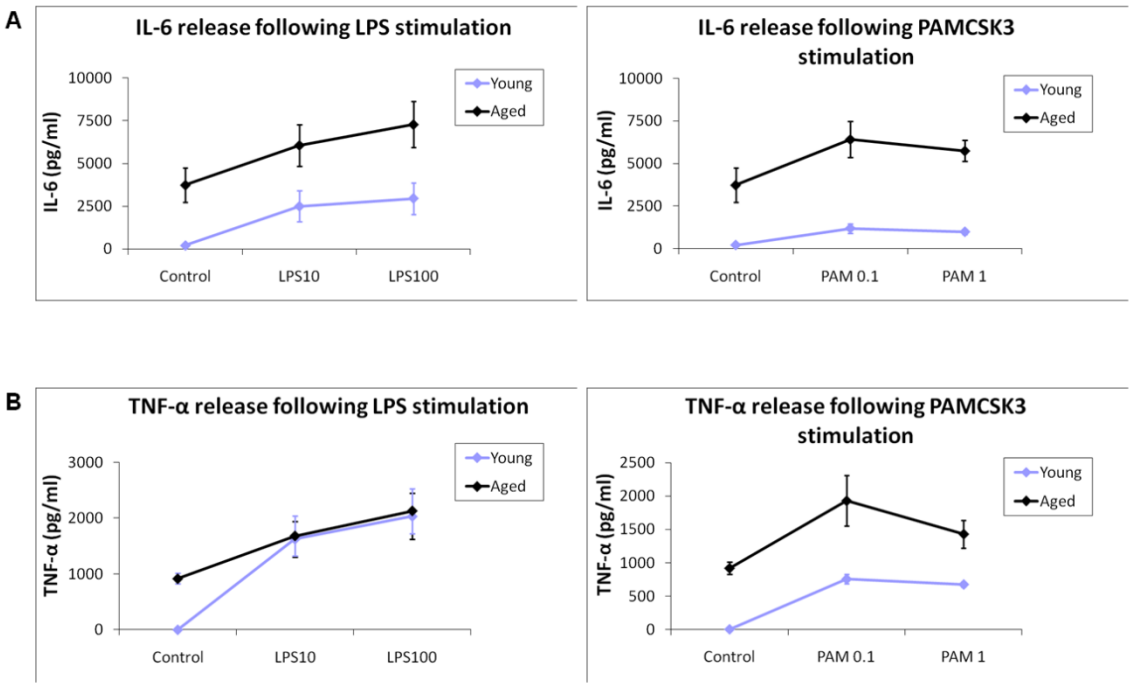

Figure 2-5. Microglial reaction to immunostimulation. Dose dependent increases in either IL-6 (A) or TNF-□ (B) release following different concentrations of LPS (10-100ng/ml) or PAMCSK3 (0.1 – 1ug/ml). Under all conditions, except for the TNF-□ secretion by aged microglia following either LPS or PAMCSK3 stimulation, a significant effect of concentration was observed. No significant age-dose interaction was observed under all conditions. Moreover, all figures show the marked increase in cytokine release by aged microglia under basal condition (Cytokine experiments performed by Ellen Boelen).

Age-related Changes in Microglial Processing of Aβ

Microglia are thought to participate in Aβ plaque burden regulation by sequestering and processing of Aβ. Our purpose in performing Aβ metabolism experiments with *ex vivo* cultures of microglia was to further understand the relationship between microglia and Aβ42 homeostasis. Individual microglia surrounding Aβ plaques become enlarged as plaques become smaller with time (Bolmont, et al., 2008). Despite this correlative evidence of microglial participation in Aβ plaque reduction, natural processes do not appear to reverse amyloidosis (Jankowsky, et al., 2005). Previously, we have suggested that microglial function may deteriorate with time. This was mainly inspired

by histological findings, demonstrating the appearance of a dystrophic microglia phenotype with normal aging and around Aβ plaque deposits in AD brains (Miller and Streit, 2007). The finding that microglia from young brains internalize Aβ42 while microglia from aged brains do not, likely reflects a more global change in microglial functionality with age as we do not observe dystrophic microglia in aged mice.

Interpretation of Aβ Expulsion by Younger Microglia

In younger mice, the temporary sequestration of Aβ42 suggests that microglia are not directly involved in degradation. However there is clear potential for microglia, which are highly motile (Bolmont, et al., 2008), to be involved in the movement of Aβ in the nervous system. The cycling of Aβ42 through microglial endocytosis and exocytosis could result in redistribution that modulates peptide availability for amyloid formation. Our observations indicate that microglia remove Aβ peptide out of the extracellular miliu at ng/ml quantities, possibly creating a dynamic cellular compartment *in vivo*. A 2 to 4-fold age-related decrease in microglial Aβ internalization as observed in our experiments could result in less transfer of Aβ from the extracellular space --thereby making available more Aβ for plaque formation. Amyloidosis occurs in a significant amount of non-diseased aged adults (Price, et al., 2009). Therefore, it is plausible that the dynamic redistribution of Aβ, a protein that is particularly aggregation prone, is needed for homeostatic maintenance. Perturbation of this process due to age-related changes of microglial function such as that described here could contribute to unhinged accumulation of Aβ to toxic concentrations in the extracellular space.

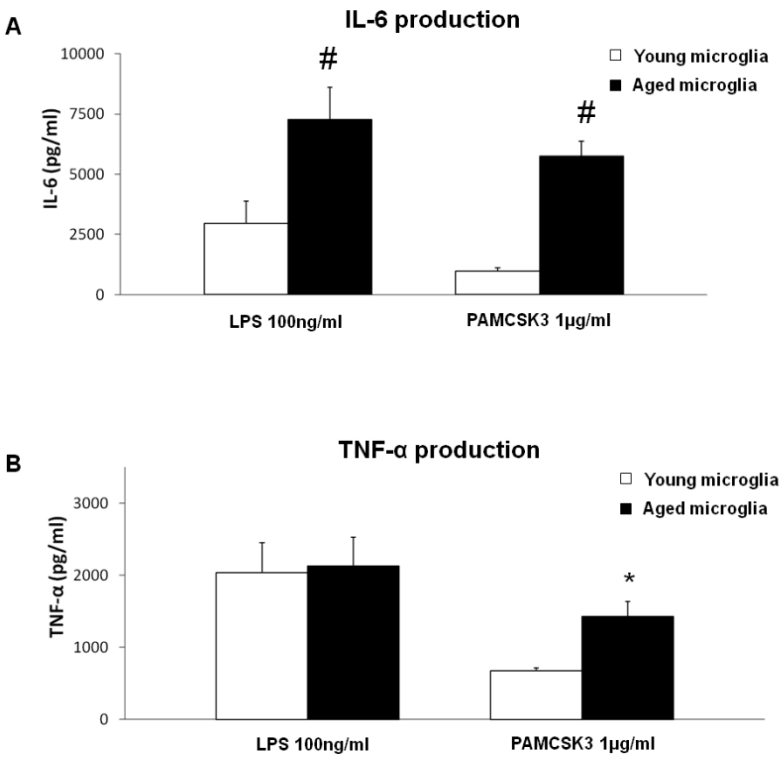

Figure 2-6. Cytokine secretion of young and aged microglia. (A) Upon stimulation with the biological inflammatory reagent LPS (100ng/ml) or Pam3CSK4, a synthetic agonist of toll-like receptor 2 (1ug/ml), IL-6 production by aged microglia was markedly increased when compared to young microglia. (B) LPS (100ng/ml) stimulated similar TNF-□ production between microglia derived from young and aged mice. Yet, TNF-□ production was significantly increased in aged microglia following Pam3CSK4 (1ug/ml) exposure. *, $p<0.05$; #, $p<0.001$.

Concluding Comments

Together, our *ex vivo* quantification of microglial functions of cytokine production, glutathione levels and Aβ42 scavenging activity paint a complex picture of endogenous activity. Microglia from young mice produce less cytokines, while microglia derived from aged mice have higher basal levels of cytokine secretion than was previously thought and have reduced glutathione levels. Microglia derived from aged mice lack comparable Aβ42 internalization capacity compared to less aged microglia while microglia from young mice and mixed glial neonatal cultures do not seem to retain

internalized Aβ42. These direct assessments of microglial function in *ex vivo* experiments, free of confounding contributions of other brain cells and debris, demonstrate a nuanced view of microglial function and suggest that microglial biology may change with aging.

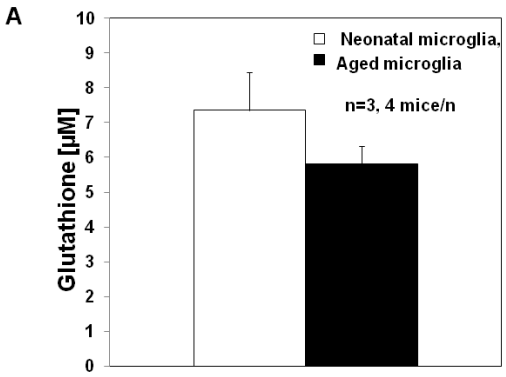

Figure 2-7. Microglial glutathione content. Microglia from aged mice have a 21% reduction of glutathione antioxidant. Data is normalized to total protein and represents oxidized and reduced forms of glutathione detected in microglia analyzed immediately following brain extraction. p=0.27.

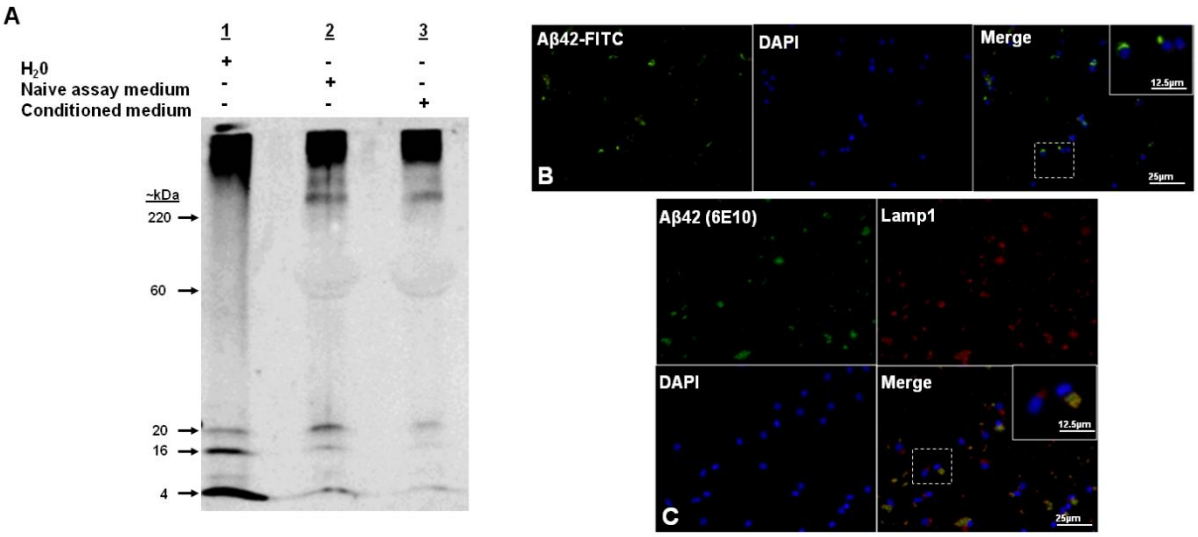

Figure 2-8. Species of Aβ42 used for microglial experiments. (A) Western blot analysis using 6E10, an antibody specific to the first 16 amino acids of Aβ42, indicates monomeric (4kDa), oligomeric (16kDa, 20kDa) and higher-order conformations larger than 220kDa in stock preparations as well as preparations that have been exposed to microglia. Higher-order conformations larger than 220kDa persist following the exposure of samples to buffer containing 2% SDS suggesting the presence of fibrillar species. 10% serum in media overloads gel at 60kDa and may block visibility of some Aβ42 species. 75ng Aβ42/well. (B) Internalization of Aβ42 by microglia from adult mice was directly observed in living microglia with FITC conjugated Aβ42 peptide and with 6E10 immunocytochemistry. In both cases, Aβ42 had a peri-nuclear localization. Lamp1 colocalization with 6E10 immunoreactivity suggests that some Aβ42 reached microglial lysosomal compartments (C).

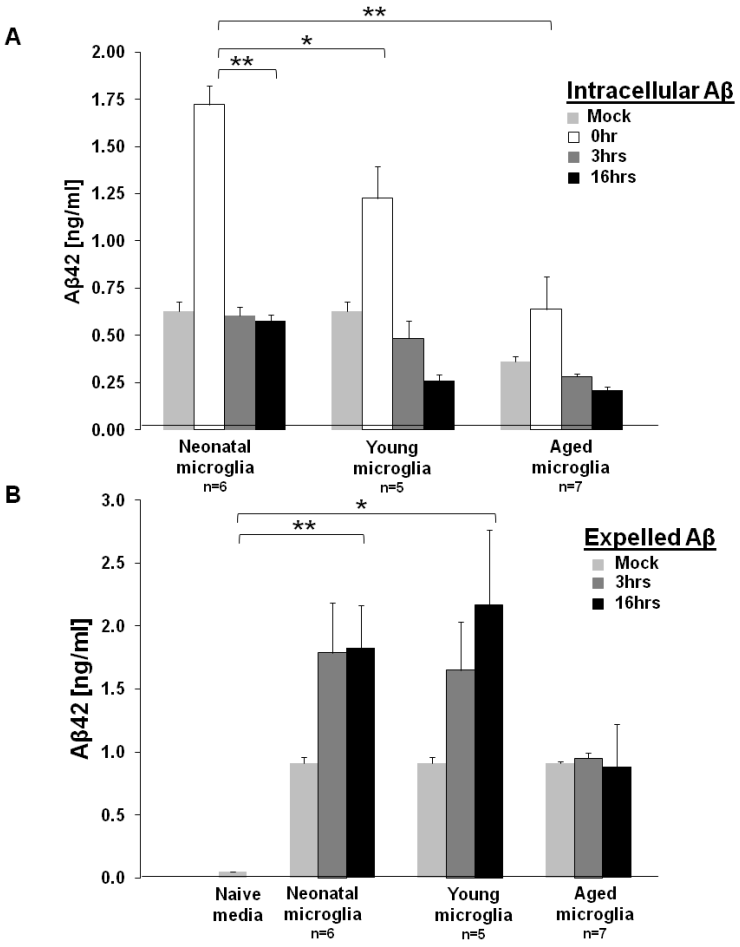

Figure 2-9. Fate of Aβ internalized by microglia. Microglia extracted from mice of various ages were exposed to Aβ42 preparations containing monomeric, oligomeric and SDS-resistant fibrillar species (reflecting in vivo amyloid diversity) in pulse-chase experiments. (A) Neonatal and young microglia respectively internalized 74% and 53% more Aβ42 relative to aged microglia. (B) Invariably, internalized Aβ42 was expelled by neonatal and young microglia within 3hrs of ingestion, suggesting disengagement from biophysical degradation following phagocytosis. Mock data (gray) represents experiments without the presence of cells to control for non-specific adherence of Aβ to culture wells. Detection of Aβ42 requires the presence of both NH2 and COOH terminals of Aβ42, thus only intact Aβ42 peptides are quantified in the above experiments. *, $p<0.05$; **, $p<0.01$.

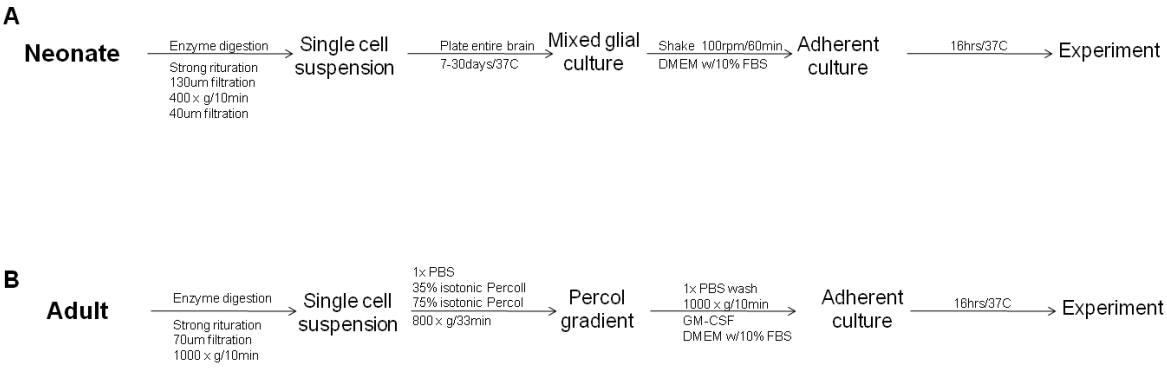

Figure 2-10. Overview of mixed glial culture (MGC) and density centrifugation methodologies utilized to obtain microglia. MGC derived microglia were harvested after 1 to 4 weeks of growing atop a multi-cell feeder layer comprised mostly of astrocytes. Homogenized brains of neonatal origin form MGCs while adult brains do not, thus MGC microglia are of neonatal origin. Density centrifugation based isolation offered the advantages of immediate culture creation from young and aged brains. This was important because microglia from brains of aging models were accessible and *ex vivo* analysis utilized cells temporally proximate to *in vivo* microglia.

CHAPTER 3
ENGRAFTMENT PATTERNS OF NSCS TRANSPLANTED INTO MOUSE MODELS OF ALZHEIMER'S DISEASE

Introduction

The brains of AD patients are characterized by Aβ pathology as well as neuronal cell death. This has led to interest in the use of neuronal stem cells (NSCs) for cell replacement or delivery of therapeutic molecules such as proteases that reduce Aβ pathology. Before such studies can be carried out on humans, several fundamental questions must first be addressed. First, do NSCs survive in brains with the pathologies of AD? Second, how does the complex architecture of the brain effect the engraftment of transplanted NSCs? Third, does the region of engraftment affect integration and migration within the parenchyma? And finally, does transgene expression in genetically modified NSCs effect engraftment?

The question of NSC survival in AD or models of AD has been explored in *in vitro* and in *in vivo* (non-transplant) settings. Unfortunately, these studies present contradictory data on how NSCs are affected by Aβ pathology. Specifically, *in vitro* and post mortem studies yield data contradictory to studies performed on mouse models of AD. Lopez et al., and Calafiore et al., report that Aβ oligomers induce isolated subependymal zone (SEZ) and subgranular zone (SGZ) mouse NSCs to differentiate into neurons. They also report that Aβ concentrations that are toxic to neurons do not induce apoptosis in SGZ and SEZ stem cells or hinder their proliferation (Calafiore, et al., 2006, Lopez-Toledano and Shelanski, 2004). These observations are consistent with research which quantified increases in neurogenesis in humans with AD (Jin, et al., 2004, Ziabreva, et al., 2006). Conversely, multiple publications report evidence of decreased and abnormal neurogenesis in the hippocampus of several mouse models of

AD (Dong, et al., 2004, Donovan, et al., 2006, Wang, et al., 2004). Our lab recently reported that the amount of Aβ deposition in AD mice reflects negatively on the survival of new born SGZ neurons as they reach functional maturity.

Because the current literature fails to explicate how Aβ burden affects endogenous NSCs, how transplanted NSCs will behave in AD patients remains an open question. To shed light on this topic, we performed NSC transplant studies in mice modeling AD Aβ pathology. Our specific aim was to define engraftment patterns in the hippocampus. The pathology in the hippocampus is linked to dementia (Braak and Braak, 1995, Braak, et al., 1996). Therefore, the hippocampus is a region of great clinical interest for cell restoration and drug delivery therapies. Our primary findings in this study demonstrate that physical forces relating to hippocampal anisotropic architecture dictate the distribution of NSCs more so than cell migration. We also find that genetic overexpression of MMP9 is associated with significant enhancement of NSC graft size.

Methods

Isolation of NSCs

The protocols for isolating NSCs are contained in the literature (Marshall, et al., 2006, Zheng, et al., 2006). In brief, a rectangular forebrain block containing the subependymal zone was isolated from neonatal (P4-P9) green fluorescence protein transgenic mice (003116, The Jackson Laboratory, Bar Harbor, MI) or from non transgenic B6 mice (bred in house). This was done by removing the OB, cerebellum, hippocampus, lateral portions of the striatum, and lateral and dorsal cerebral cortex. This block was minced with a razor blade, incubated in 0.25% trypsin/EDTA (Atlanta Biologicals, Lawrenceville, GA) and dissociated into a single cell suspension by triturating through a diametrically descending series of glass pipettes. Cells were then

pelleted and washed several times before plating in NSC media (DMEM/F12 with 5% FBS, penicillin (100U/ml), streptomycin (100ug/ml), Bovine Pituitary Extract (35ug/ml), Fungizone (250ng/ml). NSC monolayer's were kept in an immature state within tissue culture flasks by supplementing the media with 20ng EGF and 20ng FGF every two to three days (Walton, et al., 2006a, Zheng, et al., 2006).

Transplantation into Amyloid Beta AD Mice

The Line 85 and the Line 107xtTa mouse models, which constitutively overexpress and selectively express human Aβ, respectively, have been previously described to model the Aβ physiology that is a hallmark AD pathology. Host and donor mice are immune-matched due to their shared B6 background. Mice were induced to a state of deep anesthesia with 1-5% isoflurane. The hair on their scalps was shaved and the surgical area sterilized with betadine antiseptic and 70% ethanol. The mice were securely mounted with ear bars and a nose bar to a stereotaxic apparatus. The anesthesia mixture was delivered through an inlet within the nose bar enclosure for the duration of the surgery. A sterile scalpel was used to make a small incision into the skin above the skull. The skin was reflected in order to expose Bregma. A Hamilton 10ul syringe with a 33 gauge needle (Hamilton Company, Reno, NV) was then loaded with NSCs prepared at 1×10^5 cells/ul for lateral ventricle injections and $\sim 5 \times 10^4$ cells/ul in 1x dPBS for multi-deposit hippocampal injections. The cells were derived from a trypsinized and pelleted monolayer of NSCs, washed with 200ul 1x dPBS and diluted to the appropriate volume using a reference cell count done on a hemacytometer. The following coordinates relative to Bregma were used to target the lateral ventricle: anterior/posterior (AP): -0.2mm, medial/lateral (ML): +/-1.2mm, dorsal/ventral (DV):-2.5mm from the dura. Occasionally, needle tracks using these coordinates were found

in the base of the hippocampus where it meets the thalamus. This border region is not termed in modern atlases (Paxinos Atlas and Allen Online Atlas) and vaguely referred to in a study by Nagaraja and colleagues (Nagaraja, et al., 2005). Cerebrospinal fluid research 2005). There may be cerebrospinal fluid in this border in the posterior brain (midbrain). However, this is not the case in the rest of the brain. Therefore, we refer to this region here as the 'hippothalamic' fissure rather than the 'hippothalamic' cistern. To target the corpus callosum, we used: AP: +1.2mm, ML: +/-0.5mm, DV: - 2.5mm from the dura. We used multiple depth coordinates in an attempt to maximally disperse cells in the hippocampus. The regions targeted were the ventral hippocampus (dentate gyrus, SGZ region), the medial hippocampus (molecular cell layer, hippocampal fissure region) and the dorsal hippocampus (CA3). The coordinates used were: AP: +2mm, ML: +/-2mm's, DV: -2.0mm, -2.3mm, -2.5mm from the skull surface. 1.25×10^5 cells were deposited at -2.0mm and -2.3mm, while 2.5×10^5 cells were deposited at -2.5mm. In all injections, 4ul-8ul total volume was deposited at the rate of 0.25ul per 15 seconds (dependant on cell concentration). Subsequently, the needle was left alone for 5 minutes to allow for the diffusion of cells from the injection tract. It was then retracted slowly to minimize damage along the injection tract. The incision was closed with a staple and the mouse placed in a warm, dark recovery area. To avoid or minimize the discomfort, distress and pain associated with this procedure, 0.1mg/kg of buprenophine was administered as the animals recovered on the day of surgery and the subsequent day. The mice were checked for signs of abnormal recovery during the survival periods. At the end of the survival periods, the mice were deeply anesthetized in an isoflurane induction chamber, euthanized by Beuthanasia administration and then perfused with

cold 1x PBS. Whole brains were quickly dissected out and placed in cold 4% paraformaldyhyde fixative overnight. The brains were immersed in 30% sucrose before sectioning within a cryostat. 20um sections were stored in anti-freeze media at -20C until further processing.

Immunochemistry

4% paraformaldehyde fixed cells or tissue sections processed for immunofluorescence in solutions containing 0.1% Triton-X, 10% goat serum in 1x PBS. Primary antibodies used in this study include copGFP (1:2000, Evrogen, Moscow, Russia), anti human MMP9 Clone 56-2A4 (Abcam, Cambridge, MA), anti-Aβ 6E10 (1:2000, Signet, Dedham, MA), microglial antigen Iba1 (1:1000, Wako, Richmond, VA), astrocyte antigen GFAP (1:1000, Dako Corporation, Carpinteria, CA), and neuronal antigen NeuN (1:500, Millipore, Bellirica, MA), neuronal antigen BIII Tubulin (1:500, Covance, Princeston, NJ). Cells were rinsed and incubated with goat secondary antibodies Alexa 488, 568 (Invitrogen, Carlsbard, CA). Cells were photographed with an Olympus DP71 camera mounted on an Olympus BX60 microscope.

Modeling Paths Of Least Resistance (PLR)

To simulate PLR's that may occur within the hippocampal formation, 3ml's of 1% agarose (w/v) in PBS was allowed to solidify in a clear 15ml polystyrene tube. Addition of 100ul of H_2O atop this solidified block formed a layer ~1mm to 3mm in height. 3ml's of warm 1% agarose was then added. As the two layers of agarose fused, a region of weakness developed due to an abrupt decrease in agarose density at the H_2O layer. 5-10ul of crysyl violet solution was then injected at various regions in the agarose block.

Results

NSCs robustly propagate *in vitro* (Reynolds and Weiss, 1992, Walton, et al., 2006a). In our hands, cells from the brains of two neonatal mice have been passaged >10x for a duration of six months producing a conservative estimate of approximately one hundred million cells. NSCs formed monolayers of elongated cells (Fig. 3-1A, C) similar to that of human NSCs (Walton, et al., 2006a). NSCs were also similar to human NSCs in their immunoreactivity for the neuronal progenitor markers GFAP and βIII Tub (Fig. 3-2A-B). Iba1 reactivity was observed in some cells in NSC cultures (Fig. 3-2C), indicating the presence of microglia. However, these cells were much larger than adult *ex vivo* microglia (compare Fig. 3-1B-C & 3-2C) and had a morphology similar to neonatal microglia from mixed glial cultures (Fig. 2 .4, see Chapter 2). It has been suggested that microglia derived soluble factors maintain the self-renewal capacity of NSCs *in vitro* (Walton, et al., 2006b).

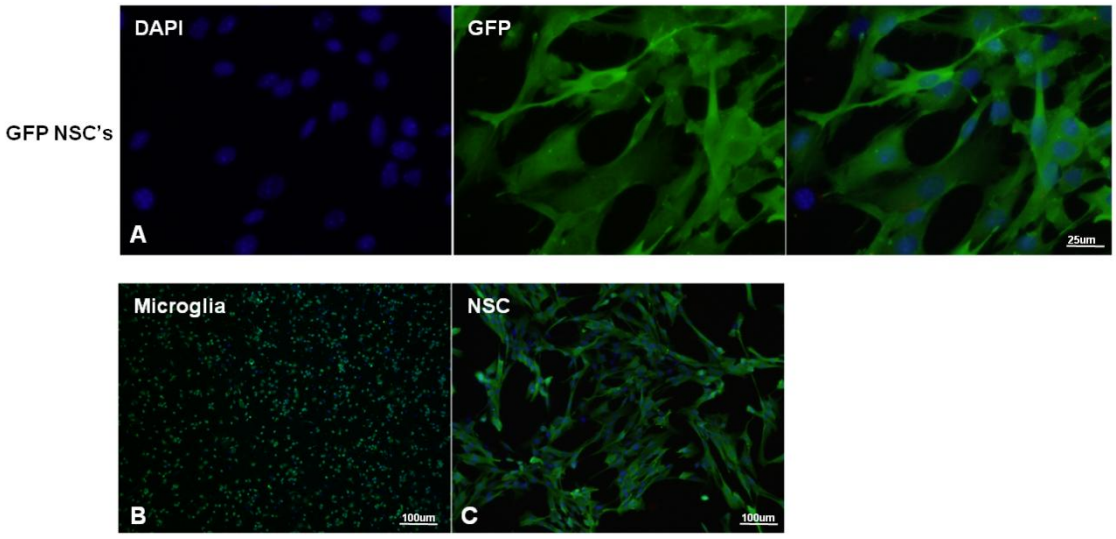

Figure 3-1. Morphology of *in vitro* NSCs. NSCs form monolayers of elongated cells (A) and are significantly larger than microglia acutely isolated from adult mice (B).

We initially transplanted NSCs from GFP transgenic mice into the lateral ventricle (LV) in order to recapitulate previous reports of rostral migration into the olfactory bulb (Marshall, et al., 2006, Zheng, et al., 2006). In our AD models, this is a region of high Aβ plaque burden and in humans, the loss of smell is purportedly amongst the first signs of AD (Fusetti, et al.). Therefore, the migratory potential of NSCs suggests the possibility of wide-spread dispersion of candidate therapeutics to relevant regions of the brain. We performed transplants of GFP cells on non transgenic mice and transgenic mice symptomatic for Aβ pathology using previously published stereotactic coordinates (Zheng, et al., 2006). Similar to previous studies with SEZ NSCs (Walton, et al., 2006a, Zheng, et al., 2006), mice were sacrificed 4-8 weeks later. In transplants where the needle track was confirmed to have entered the lateral ventricle, we did not observe ventricular wall colonization or extravasation towards the olfactory bulb (non transgenic; n=3, TG=4), (data not shown). This result was not due to the inability of NSCs to form grafts as some surviving cells were observed alongside needle tracks that had entered the lateral ventricle.

These results motivated us to modify stereotactic coordinates to directly target the hippocampus. Our goal was to achieve maximal cell dispersion within the hippocampus. We therefore chose 3-point depth coordinates for simultaneous injection into the dorsal hippocampus (proximal to CA3), the medial hippocampus (hippocampal fissure, molecular cell layer and lateral arm of the dentate gyrus) and the ventral hippocampus (subgranular zone of the dentate gyrus). The accuracy of these coordinates was verified with injections of the tracer crysl violet (n=4/depth coordinate, data not shown) on freshly deceased mice. A total of 5×10^5 cells were injected, a

value corresponding with previous animal work (Parl et al., Exp Neurol 2006) and proportional to human NSC clinical trials (Stem Cells Inc; American Association of Neurological Surgeons Annual Meeting 2010).

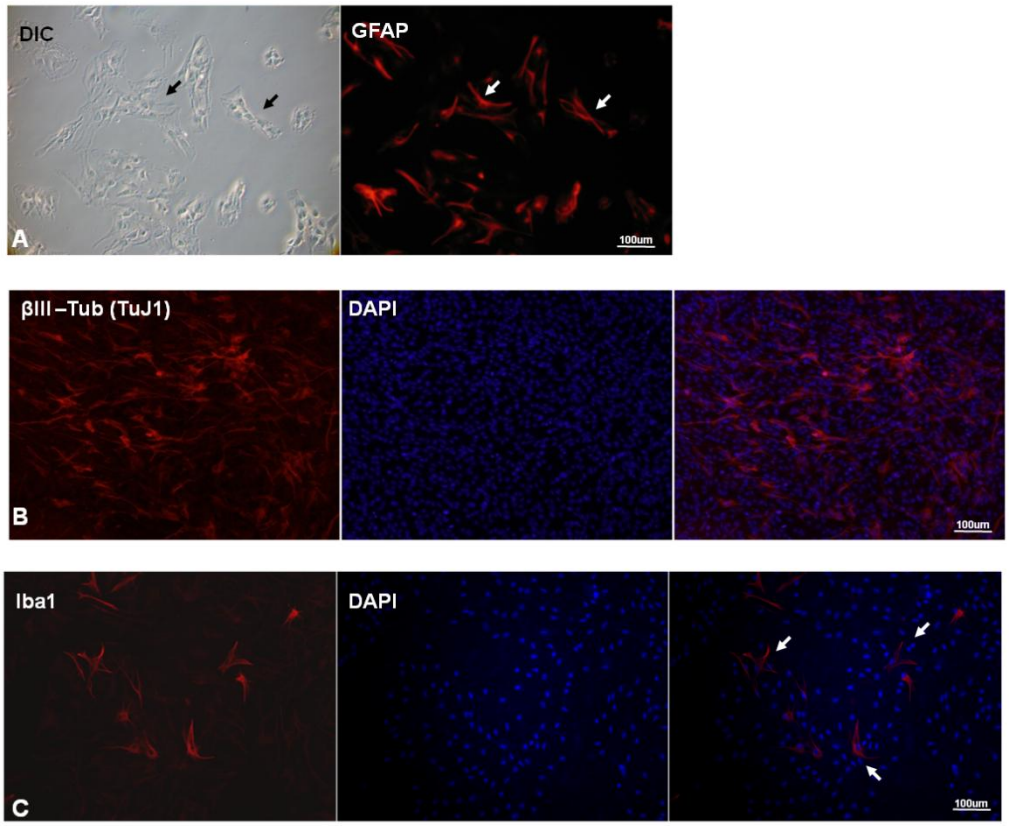

Figure 3-2. *In vitro* characteristics of NSCs. NSC cultures were characterized by GFAP (A) and BIII Tubulin immunoreactivity (B). Some cells were immunoreactive for the microglial marker, Iba1 (C). n=4 cultures per immunostain.

We then injected NSCs with lentiviral directed expression of 1) MMP9 and GFP or 2) GFP only. The GFP used here is from the plankton copepod. It is similar in size to EGFP (26kDA), but has more fluorescence output (Shagin, et al., 2004). GFP NSCs and MMP9 NSCs had equal fluorescence output of A.U>10^3 as determined by fluorescence activated cell sorting (FACS) (see Chapter 4).

After a month of survival, brains were confirmed to have hippocampal needle track penetration in several mice. MMP9 NSCs formed graft cores that were 82.4%

larger than GFP NSCs (n=4; GFP NSC, n=5; MMP9 NSC, Fig. 3-3A-C). Interestingly, the effect of MMP9 on survival is diminished with increasing amounts of proximal Aβ plaques (R^2=0.701), (Fig. 3-3D). This data suggests that Aβ amyloidosis is toxic to NSCs and that MMP9 genetic modification partly rescues cell survival. No other differences were observed between GFP NSCs and MMP9 NSCs. The engraftment patterns described below apply to both cell types.

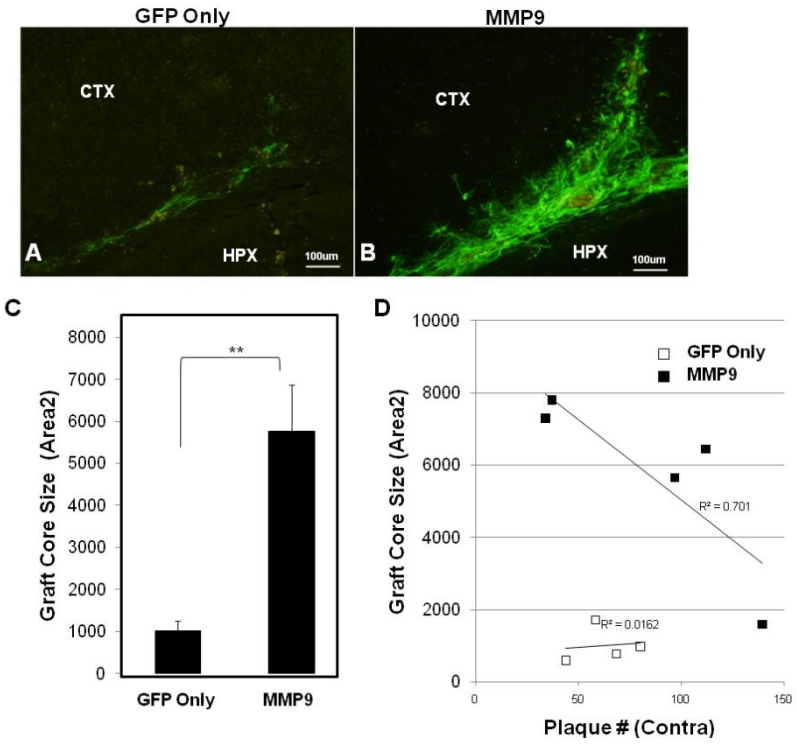

Figure 3-3. MMP9 associated changes in engraftment. MMP9 NSC grafts (n=5) were 82.4% larger than GFP NSC grafts (n=4) (A-C). The fluorescence intensity of both cell types were matched with FACS analysis (A.U>10^3). The size of MMP9 GFP grafts was negatively correlated with the amount of nearby Aβ plaques (R^2=0.701) (D). As seen here, the horizontal distribution of GFP NSCs and MMP9 NSCs appears similar. **, p<0.001

Both GFP NSCs and MMP9 NSCs formed grafts in subcortical and corpus callosum white matter tracks despite injection within the interior of the hippocampus (Fig. 3-3A-B, Fig. 3-4A,C). This distribution was observed in all mice (n=9). NSCs

formed a smaller, secondary graft within the hippocampal fissure in 33% of mice (Fig. 3-3-4B). This distribution pattern was confirmed in a separate cohort of mice that survived two months following surgery (n=7), (Fig. 3-9A). NSC engraftments in the white matter and the hippocampal fissure had a consistent disc-shaped morphology that extended horizontally; ~1mm on the anterior/posterior plane and ~1mm on the medial/lateral plane in needle track containing sections and adjacent sections.

NSCs injected directly into the corpus callosum and allowed to graft for 3 days in non transgenic mice (n=2) resulted in engraftment that was strikingly similar to the distribution found in Aβ transgenic mice (compare Fig. 3-4A & D). Furthermore, NSCs that were engrafted for 1 year in the fimbria white matter of non transgenic mice were similarly distributed horizontally at the hippothalamic fissure (n=3), Fig. 3-4E-F).

Recently, several investigators have suggested directional migration of NSCs as an explanation of why cellular transplantation into the hippocampal gray matter paradoxically results in engraftment of cells in the white matter (Blurton-Jones, et al., 2009, Pihlaja, et al., 2008, Radojevic and Kapfhammer, 2009, Raedt, et al., 2009, Tang, et al., 2008). As described above, our transplant studies were characterized by 1) white matter grafts in Aβ transgenic mice receiving NSCs in the hippocampus and 2) white matter grafts in non transgenic mice receiving NSCs in the white matter of the fimbria and corpus callosum. With the exception of NSCs closely associated with the hippocampal fissure, transplanted cells did not form graft cores in gray matter. If cell migration were a major factor determining the distribution of transplanted NSCs, one would expect a range of hippocampal distribution reflecting NSCs in transit. However, our long and short term survival studies resulted in a predictable distribution of NSCs

along horizontal fissures of the hippocampus and surrounding white matter. Consequently, we hypothesized that the distribution of transplanted cells was largely determined by PLR's that exist between anisotropic regions of fissures, white matter and densely packed layers of neurons.

To provide support for this hypothesis, we decided to simulate a region of horizontal weakness using 1% agarose. We placed a thin layer of water (~1 to 3mm) on top of already solidified agarose. This created a non-uniform (anisotropic) region of agarose density when a new layer of agarose was added. Crysl violet tracer that was injected above or below this region resulted in a vertical distribution of tracer (n=5), (Fig. 3-5A-B). However, a horizontal distribution was observed upon injecting into the region of weakness (n=3), (Fig. 3-5C). These results demonstrate a change in agarose density creates anisotropic forces that direct movement of infusate along a horizontal path. Such forces may occur in the hippocampus. If this is the case, anisotropic forces that distribute NSCs during surgery may explain why transplantation of NSCs into hippocampal gray matter results in distal white matter engraftment.

To gain insight on this question, we injected GFP NSCs proximal to the corpus callosum, hippocampal fissure, the dentate, the hippothalamic fissure and sacrificed mice immediately following surgery. As a control, we also injected GFP NSCs into regions of the brain we suspected to have a more uniform (isotropic) distribution of tissue. These included the cortex, the hippocampus and the striatum. We found that injection of NSCs into the hippocampus at various dorsoventral depths resulted in immediate NSC distribution along the horizontal features of fissures and white matter (Fig. 3-6). Specifically, NSCs that were injected into the dorsal aspect of the

hippocampus yielded distributions throughout the subcortical white matter tracks above the hippocampus (corpus callosum, cingulum bundle, alveus) and to a lesser extent, CA1 (n=8), (Fig. 3-6A). NSCs targeted to the ventral aspect of the hippocampus distributed mediolaterally at the base of the hippocampus (i.e., hippothalamic fissure) (n=8), (Fig. 3-6B). The horizontal distribution of the NSCs extended hundreds of micrometers; from the 3rd ventricle to lateral regions such as above the dorsal lateral geniculate nucleus. NSCs targeted to the dorsoventral center of the hippocampus (hippocampal fissure coordinates) distributed within the corpus callosum, the hippocampal fissure and the base of the hippocampus (n=6), (Fig 3-6C).

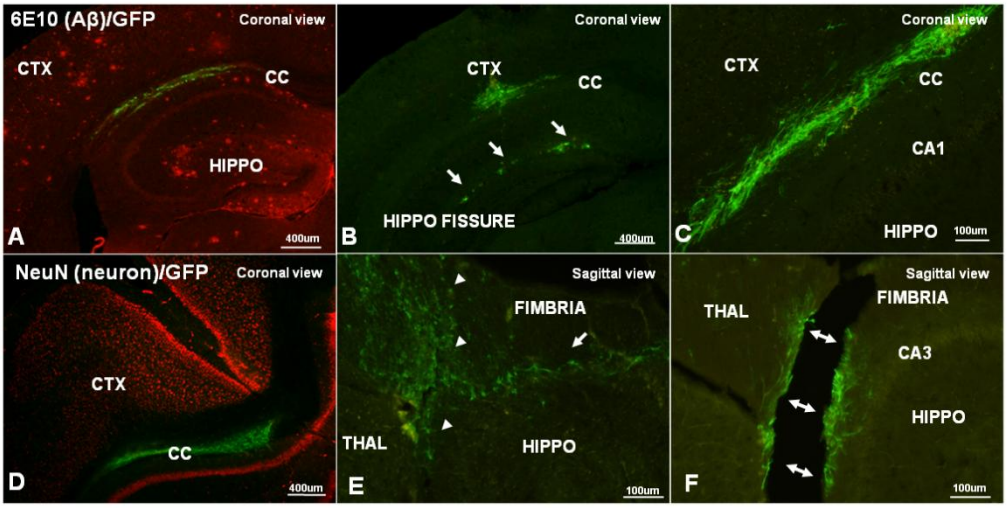

Figure 3-4. Survival and distribution of transplanted NSCs. Deposition of NSCs into hippocampal gray matter of Aβ transgenic mice resulted in horizontal engraftments within subcortical and corpus callosum white matter (n=9) (A,C). In 33% of mice, secondary engraftments were observed in the hippocampal fissure (B, arrows). Deposition of NSCs into the corpus callosum (n=2) or fimbria (n=3) of non transgenic animals resulted in PLR engraftments with similar horizontal distributions (D-E, arrows indicate needle track, arrowheads indicate hippocampal fissure). The separation of tissue observed in panel F (double arrows) provides evidence of a fissure with natural weakness into which NSCs selectively distributed into. Aβ transgenic mice were sacrificed a month following NSC transplantation (D-F). Non transgenic mice were sacrificed 3 days (A) and 1 year (B,C) following NSC transplantation.

This result agrees with previous studies investigating the influence of hippocampal structure on infusate distribution patterns (Astary, et al., 2010). As noted in Astary et al, distribution profile and shape of our infusions were also dependent on neuroanatomical and cytoarchitectonic structure. Therefore, in contrast to NSCs injected into anisotropic white matter or cell-free CSF-filled regions, NSCs that were injected into the thalamus (n=6) (Fig. 3-6D), cortex (n=2, data not shown) or striatum (n=6), (Fig 3-6E) had circular or vertical distributions. Notably, NSC striatal distribution bifurcated along the gray matter and radiating fibers of white matter (Fig. 3-6E).

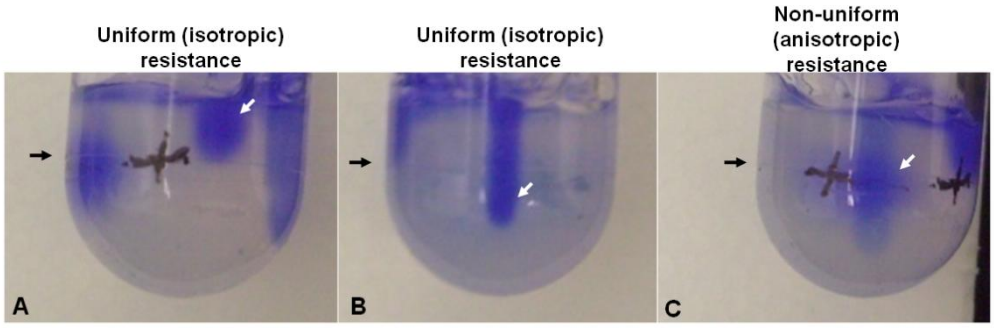

Figure 3-5. Modeling paths of least resistance. A 1% agarose block, with structural weakness in the region denoted by arrows and crosses was injected with the tracer, crysl violet. Deposition above (n=5) (A) or below (n=5) (B) the arrow resulted in a vertical distribution of the tracer. Deposition at the area of structural weakness resulted in a horizontal distribution of the tracer (n=3) (C).

This data together with our long term survival experiments suggests that the initial distribution of transplanted NSCs is the main determinant of engraftment pattern. Our long term survival experiments also demonstrated that transplanted NSCs are not characterized by wide-spread penetration into the hippocampal parenchyma. However we have encouraging results that suggest an alternate route may be used to attain such a result. Extensive intra-hippocampal grafts occurred in transplants that deposited NSCs in the point of the hippothalamic fissure that is proximal to the dentate, (Fig. 3-7).

Similar to transplants that result in subcortical white matter engraftment, NSCs distributed horizontally at the hippothalamic fissure. However, engraftment in this region uniquely resulted in significant representation of cells around and within the dentate. In Aβ transgenic mice, these cells extended processes into the surrounding gray matter at two weeks (Fig 3-7A) and appear to be migratory at two months (Fig. 3-7B). In a non transgenic animal that survived five months, NSC grafts were found within the dentate of the ipsilateral hippocampus (Fig. 3-7C). However, in the contralateral hippocampus, NSCs were found in the hippothalamic fissure (Fig 3-7C, 2nd and 3rd panels). This suggests cells were deposited at this PLR. In both hemispheres, cells appear to be migrating dorsally from the graft core (Fig. 3-7C). We did not find cells in the thalamus in these animals. This suggests vertical directional migration away from the thalamus possibly due to factors associated with the endogenous NSC niche that exists in the SGZ. The robustness of these engraftments prompted us to perform further transplants to repeat these results. These studies are ongoing.

Previous work from our lab has shown that the survival of newborn neurons (NSC progeny) is negatively correlated with the presence of Aβ pathology (Verret, et al., 2007). However, the survival of astrocytes, which were more than 50% of the newborn population, was not affected. The differentiation of transplanted NSCs has been well characterized in multiple studies. In general, 30-90% of endogeneous and transplanted NSCs express glial markers in multiple studies using various NSCs in different disease models (Hattiangady, et al., 2007, Lundberg, et al., 1997, Shetty, et al., 2008, Svendsen, et al., 1996, Tang, et al., 2008, Verret, et al., 2007). A minority of transplanted NSCs become neurons (Shetty, et al., 2008). However, a few studies

describe neurons as the major phenotype transplanted NSCs differentiate into (Bennett, et al., 2010, Lu, et al., 2007, Park, et al., 2002). Due to this ambiguity, we were interested in determining the differentiation state of NSCs we transplanted in Aβ transgenic mice. As mentioned above, these cells are immunoreactive for GFAP and βIII Tubulin (Tuj1) *in vitro.* A subpopulation of cells in NSC cultures express Iba1. We stained Aβ transgenic mice tissue sections containing NSC white matter engraftments with antibodies against these markers and NeuN, a marker for post-mitotic neurons. We did not observe βIII-Tubilin or NeuN immunoreactivity in any sections (n=2 mice, 4x20um sections), (data not shown). However, there was strong graft associated immunoreactivity for Iba1 and GFAP (n=3), (Fig. 3-8, 3-9). The elongated morphology of Iba1 and GFAP positive NSCs *in vitro* matches that of transplanted cells *in vivo* (compare Fig. 3-2 to 3-8 & 3-9, arrows). This morphology contrasts that of endogenous quiescent glia or glia reacting to nearby Aβ plaques (Fig. 3-8, 3-9, arrowheads).

As described above, transplant cells largely remained within a graft core. Amyloid beta plaques proximal to graft cores (<50um or ~3 cell lengths) did not attract NSCs (Fig. 3-4A, 3-8B, 3-9) thus confirming prior reports (Burton-Jones, PNAS 2009). It is possible that white matter tracks support a unique NSC niche that is defined by a glial-like phenotype. However, transplanted cells in this niche do not respond to or do not have access to the cues that direct chemotaxis of endogenous glia towards Aβ plaques.

Discussion

Newly discovered properties of NSCs, namely long-term *in vitro* expansion and engraftment potential (Walton, et al., 2006a, Zheng, et al., 2006), have generated significant interest for application towards novel therapies such as cell replacement and

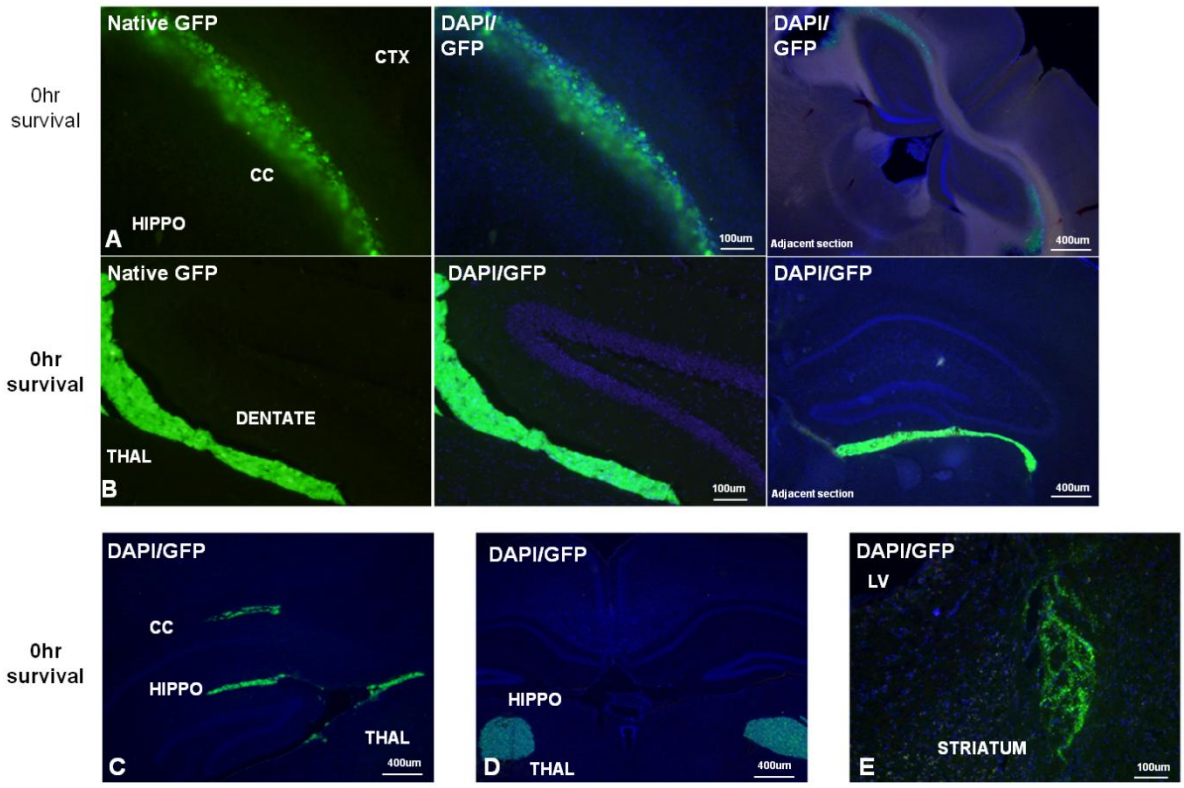

Figure 3-6. Immediate distribution of NSCs in paths of least resistance. 5 x 10^5 NSCs were injected into various regions and analyzed immediately following surgery. Deposition of NSCs in the hippocampus which has variably dense layers of tissue resulted in horizontal distribution along anisotropic paths of least resistance (A-C). These included the corpus callosum (n=8) (A), the hippothalamic fissure (n=8) (B), the dentate (n=6) (not shown) and the hippocampal fissure (n=6) (C). Interestingly, NSCs whose target was the hippocampal fissure were found hundreds of microns away from the site of injection (C). Because directional migration occurs in the order of hours to days, this distribution can only be explained by anisotropic forces directing cell distribution. In contrast to anisotropic horizontal distribution observed in A-C, a vertical or circular distribution was observed with NSCs injected into isotropic regions such as the thalamus (n=6) (D), the cortex (n=2) (data not shown) and the striatum (n=6) (E). In the striatum, NSCs distributed in a radial pattern that likely reflects white matter that is striated within gray matter.

drug delivery. However, a series of clinical questions regarding how NSC grafts behave in diseased brains motivated us to study transplanted NSCs in mouse models of AD. In this study, we aimed to determine the engraftment patterns of NSCs in mouse brains with Aβ pathology. Our studies indicate that NSCs can survive in an environment with

Aβ pathology, however these cells do not migrate towards Aβ plaques. The localization of cell engraftment is largely dependent on previously uncharacterized paths of least resistance. These paths distribute cells in a horizontal pattern along both lateral/medial and anterior/posterior planes. Process extension and migration appear most robust in NSCs deposited proximal to the hippothalamic fissure and dentate. Graft size is significantly enhanced by overexpression of MMP9. Because MMP9 NSC graft size is inversely correlated to Aβ plaque number, MMP9 may be a novel factor for protecting NSCs in pathologic amyloid environments.

Paths of Least Resistance versus migration

Our observations of the pattern of NSC engraftment are also observed in studies that focuse on a myriad of pathologies including ischemia, epilepsy and Alzheimer's disease (Blurton-Jones, et al., 2009, Olstorn, et al., 2007, Pihlaja, et al., 2008, Prajerova, et al., Radojevic and Kapfhammer, 2009, Raedt, et al., 2009, Tang, et al., 2008, Watson, et al., 2006). In these studies, NSCs (including those from humans) (Olstorn, et al., 2007), formed graft cores at sites distal to where they were targeted. To explain this paradox, several authors suggest transplanted cells directionally migrate (Blurton-Jones, et al., 2009, Pihlaja, et al., 2008, Raedt, et al., 2009, Tang, et al., 2008).

If migration is the primary force determining why transplanted NSCs are frequently found in white matter, one would expect a trail of in transit cells orienting away from the site of deposition. We not observe NSCs in the hippocampal fissure migrating dorsally towards the white matter or ventrally towards the hippothalamic fissure. Migration undoubtedly occurs *in vivo*, especially towards lesions. However as observed in Olstorn et al., migration to a site of infarct is secondary to a PLR distribution (Olstorn, et al., 2007). In this study, transplant human NSCs in a non injured brain distributed hundreds

of micrometers in the corpus callosum white matter. These NSCs then migrated tens of micrometers to the infarct zone in CA1. Within the infarct zone, a PLR-like distribution was maintained. This suggests a pre-existing PLR distribution was a significant factor in determining the final distribution of migrating cells.

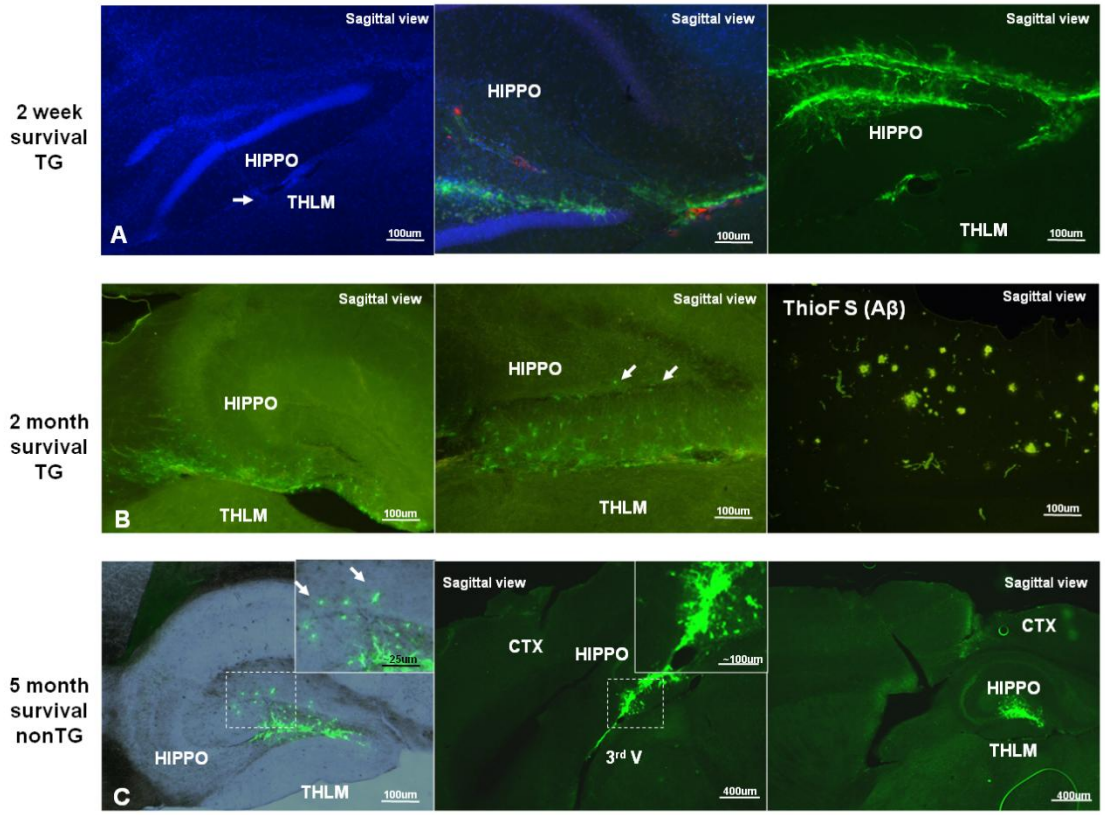

Figure 3-7. Engraftment patterns of NSCs deposited at the ventral border of the hippocampus. Needle tracks (A, arrow, left panel) which deposited NSCs proximal to the hippothalamic fissure resulted in NSC distribution along this horizontal border and the dentate (A-C). Process extension and directional migration from the point of cell deposition was observed in Aβ transgenic animals (n=2) (A,B) and in a non transgenic animal (n=1) (C). Unilateral injection resulted in bilateral distribution of NSCs along the hippothalamic fissure (C, middle, right panels). No cells were found in the thalamus in these studies.

Our experiments on mice sacrificed immediately after surgery provide definitive proof that NSCs distribute hundreds of micrometers along horizontal PLR's. Depending on which region of the hippocampus was targeted, NSCs distributed horizontally in 1)

the subcortical and corpus callosum white matter, 2) the hippocampal fissure or 3) the hippothalamic fissure or in all three. Horizontal distribution along PLR's was also seen in MRI studies of tracers infused into the hippocampus (Astary, et al.). Our observation of NSCs horizontally spread in graft cores hundreds of micrometers apart within minutes of being injected in the hippocampal parenchyma provides a mechanistic demonstration of engraftment patterns observed in multiple studies (Blurton-Jones, et al., 2009, Olstorn, et al., 2007, Pihlaja, et al., 2008, Prajerova, et al., Radojevic and Kapfhammer, 2009, Raedt, et al., 2009, Tang, et al., 2008).

In studies were less than 1 x 10^5 NSCs were transplanted, PLR distribution is infrequently found (Hattiangady, et al., 2007, Ryu, et al., 2009). PLR distribution is also not found in studies where NSCs are compacted into neurospheres (Shetty, et al., 2008) or restricted in distribution by nature of being enclosed in a capsule (Imitola, et al., 2004, Park, et al., 2002). An exception to this observation is a neurosphere study by Radojevic and colleagues (Radojevic and Kapfhammer, 2009). The amount of NSCs injected in many rodent studies equals or exceeds 1 x 10^5 cells. In our study, we chose to inject 5 x 10^5 NSCs because this amount is proportional by weight to the amount of NSCs injected in the first and currently only FDA-approved clinical trial for transplanting human stem cells into humans (Stem Cells Inc). In these studies, 1 to 2 billion NSCs were injected into children suffering from Batten's disease. This amount recently passed phase 1 safety trials (American Association of Neurological Surgeons Annual Meeting 2010). Another reason to inject greater than 1 x 10^5 NSCs is that brain transplants in rodents and humans are generally characterized by 40-97% loss of transplanted cells (Bjorklund, et al., 2003, Lundberg, et al., 1997, Olstorn, et al., 2007,

Raedt, et al., 2009, Tang, et al., 2008). Therefore, the amount of NSCs to be injected in future studies that explore stem cell potential in mice and humans will likely yield PLR distributions. The importance of PLR's in these future studies is further underscored by the persistence of PLR distributions in two month engraftments within mice modeling Alzheimer's disease and in one year engraftments within non diseased mice.

Research and Clinical Relevance of Paths of Least Resistance

The PLR's described here inherently restrict cell distribution. This presents is a possible pitfall in the exploration of NSCs for use in cell replacement or drug delivery. For instance, studies by Prajerovaet et al., resulted in corpus colossal PLR distribution despite transplantation with cortical coordinates. Alternatively, one can view PLR's as an opportunity to attain consistent engraftment patterns in the course of multiple transplants. The horizontal nature of hippocampal PLR's favor precision by buffering against stereotaxic error. In our experience, deposition across a range of hundreds of micrometers in the medial/lateral and anterior/posterior plane yielded similar hippocampal engraftments.

We envision targeting of various PLR's for unique research and clinical aims. The PLR of the hippothalamic fissure appears to support dorsal directionality of cell migration. The extensive process extension by cells in this region suggests integration into the dentate architecture.

On the other hand, cells in the white matter PLR appear stationary for at least two months in AD mice. Genetically modified NSCs stationed in this PLR have access to both the cortex and hippocampus for long-term infusion of therapeutic molecules. However the dense layer of CA1/CA3 neurons may restrict movement of infusate. More

studies are needed to understand the effect of dense cell layers on the distribution of candidate therapeutic molecules.

To further understand the movement of cells injected into the hippocampus, MRI technology may be used to visualize quantum dot labeled NSCs (T. Zheng, personal communication). This technology can possibly reveal coordinates for bilateral engraftment with unilateral cell injection. Our observation in one mouse provides evidence for a pathway, perhaps through the 3rd ventricle, for contralateral colonization. This pathway may allow for less invasive brain surgery on humans without sacrificing therapeutic distribution.

MMP9 Associated Changes in Graft Size

We find larger NSC graft sizes are associated with overexpression of MMP9. This result demonstrates that *ex vivo* genetic modification of NSCs can result in changes in engraftment pattern. To our knowledge, this finding is novel and may be an important observation to consider in future studies that aim to deliver other candidate therapeutics through NSC overexpression and transplantation. It is possible that MMP9 is making the graft site more survivable by degrading toxic molecules such as Aβ. The negative correlation of graft size to surrounding Aβ plaques suggests this. However, it may be that MMP9 is modifying the ECM in a manner that enhances cell survival. Studies of MMP9 have largely concentrated on its association with cancer (Chambers and Matrisian, 1997, Lubbe, et al., 2006, Moll, et al., 1990). However, a growing body of work demonstrates the function of MMP9 in important biological functions. Of particular relevance to this study is recent work demonstrating the need for MMP9 in the migration of endogenous NSCs *in vitro* (Wang, et al., 2006) and to sites of ischemia (Kang, et al.,

2008). It is likely that there exists a spectrum of MMP9 physiology. At one end of this spectrum, MMP9 enables metastasis of cancer cells (Chambers and Matrisian, 1997, Lubbe, et al., 2006, Moll, et al., 1990). At the other end, MMP9 facilitates endogenous NSC function in stroke (Kang, et al., 2008), modulates Aβ (Yin, et al., 2006), and is associated with larger NSC grafts in a pathological environment, as demonstrated here. As mentioned above, multiple laboratories report 40% to 97% loss of NSCs following transplantation in animals and humans (Bjorklund, et al., 2003, Lundberg, et al., 1997, Olstorn, et al., 2007, Raedt, et al., 2009, Tang, et al., 2008). MMP9 overexpression may be a novel method to address cell loss.

We aim to perform further studies to determine whether MMP9 associated changes in engraftment occur in non transgenic mice. A positive result would mean that the effect of MMP9 on NSC survival is more associated with tissue remodeling than mitigating Aβ pathology.

Concluding Comments

In summary, the data presented here provides evidence for consistent NSC engraftment in three regions within the hippocampus. These regions are characterized by a change in neural density and therefore provide paths of least resistance for the flow of cells at the moment of injection. The tightly, bound and layered nature of the hippocampus is not unique within the brain; the olfactory bulb and cerebellum also share similar structural organization. Therefore further studies aimed at characterizing putative PLR's may yield more specific targeting of NSCs for cell restoration or drug delivery throughout the brain. We find that MMP9 is associated with significant increases in the size of transplanted NSCs. This data suggests that MMP9 may be used to enhance the robustness of grafts for cell restoration and drug delivery studies.

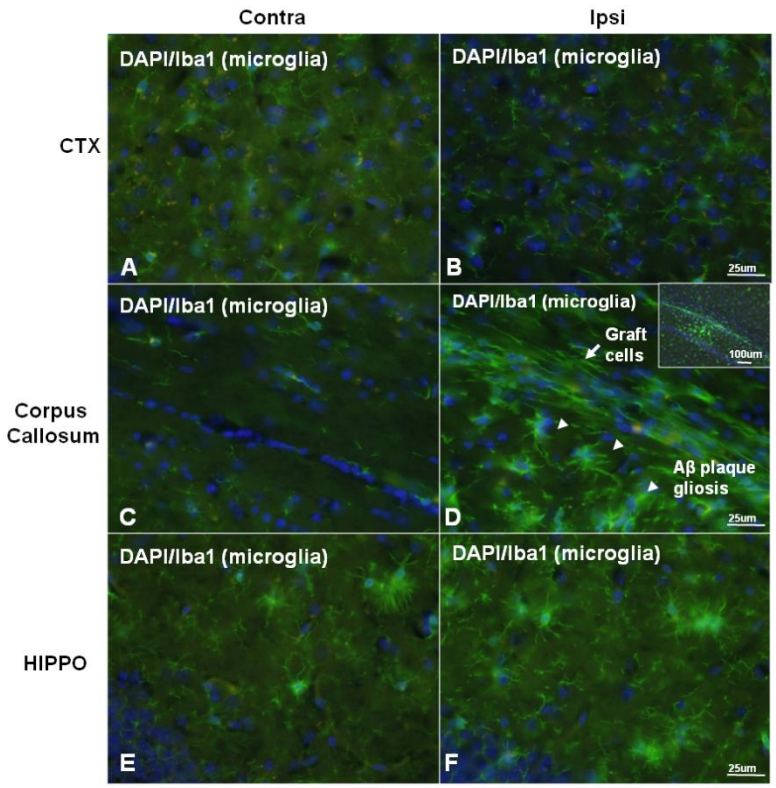

Figure 3-8. Iba1 expression and lack of Aβ migration by engrafted NSCs. Representative images of microglia on both hemispheres indicate increased Iba1 reactivity in the region of GFP NSC engraftment (n=3) (D, arrow). Cells have an elongated phenotype that is similar to GFP immunostained cells (Fig 3-3F). This morphology is distinct from that of ramified, quiescent microglia dorsal to the graft site (B) or Aβ reactive glia (D, arrowheads, E, F). We did not observe clustering of NSCs around Aβ plaques such as the one located less than 20um from this engraftment (D, arrowheads). Control images of adjacent sections stained with only 2º antibody indicated that native GFP was not a source of significant green fluorescence background (data not shown).

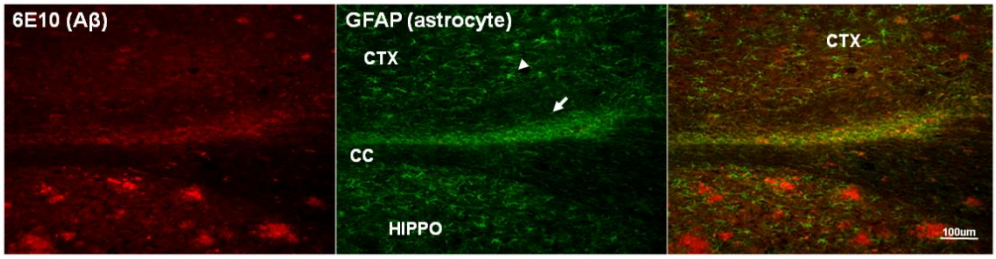

Figure 3-9. GFAP expression by engrafted NSCs. GFAP immunoreactivity is colocalized with NSC engraftment (n=3). Cells have an elongated morphology similar to that seen with Iba1 immunoreactivity (Fig 3-8D). NSCs did not migrate to nearby Aβ plaques. Aβ transgenic mice shown here were sacrificed two months following NSC transplantation. New Aβ production was genetically halted in these mice during the survival period. Control images of adjacent sections stained with only 2º antibody indicated that native GFP was not a source of significant green fluorescence background (data not shown).

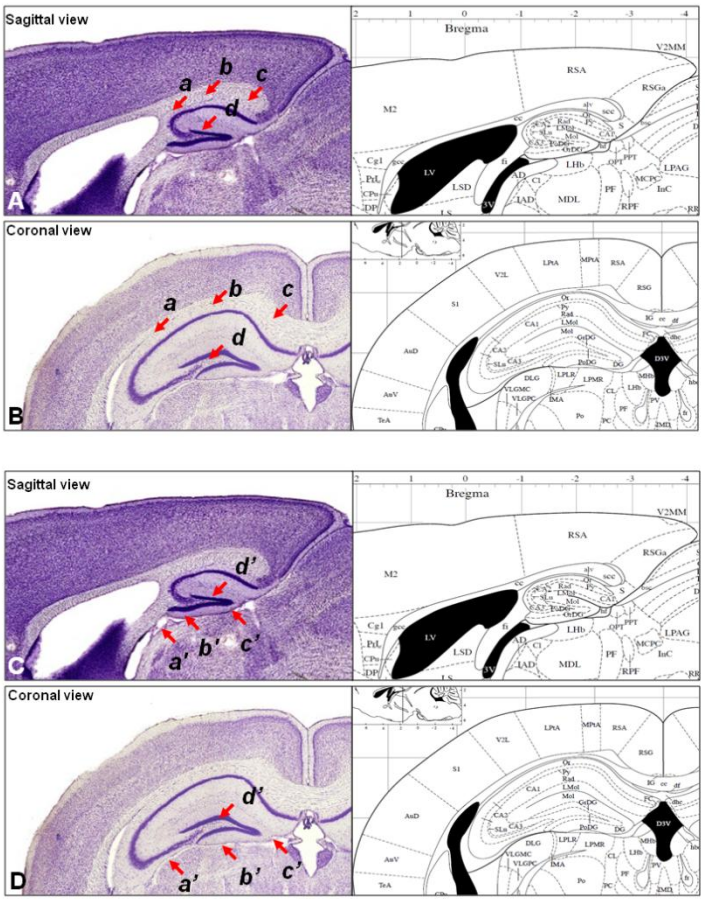

Figure 3-10. Paths of least resistance. Cells injected into *d* were consistently found along a horizontal stretch defined by arrows: *a, b, c* (A). Cells here appear stationary. This result is different from injections into *a,' b,' c'* because deposition of cells here can result in engraftments in *d'* (B). Coordinates that target *a*, may yield bilateral engraftment through the 3rd ventricle. Images modified from Paxinos Mouse Brain Atlas.

CHAPTER 4
THE EFFECT OF NEURONAL STEM CELLS ON AB PATHOLOGY AND THEIR UTILITY AS A THERAPEUTIC DELIVERY VEHICLE FOR THE AB DEGRADING PROTEASE, MMP9

Introduction

The use of stem cells that are engineered to produce molecules of therapeutic value holds much promise for the treatment of AD. The goal of this study was to explore their use for long-term delivery of candidate therapeutic molecules into mouse models of AD. Our aim was essentially to establish a foundation for *ex vivo* modified stem cells in the emerging clinical field of cell replacement therapy for AD.

We used SEZ derived NSCs because they are the only somatic cell that we know of that is endogenous to the brain, can be cultured for extended periods of time and may migrate millimeter distances when transplanted (Scheffler, et al., 2005, Walton, et al., 2006a, Zheng, et al., 2006). Other CNS cells such as neurons and glia are not suitable for *ex vivo* manipulation because they can only be cultured for a few weeks. Notably, direct injection of isolated microglia does not result in long-term grafts (G. Marshall, personal communication).

To show the feasibility of genetic manipulation of NSCs to overexpress Aβ disrupting factors, we transduced them with lentiviruses carrying transgenes for secreted Metalloprotease 9, membrane bound Heparanase and membrane bound Neprilysin. Because cultured NSCs are mitotic cells, lentiviral transduction was particularly suitable for this study. This is because these viruses integrate their genetic load into the host's chromosome and thus obviate [episomal] gene dilution with each cell division. The high efficiency of lentiviral transduction results in a transgene

expressing cells (Blits, et al., 2005). These cells were further purified using fluorescent activated cell sorting (FACS).

We focused most of our studies on MMP9 over other competing anti-Aβ candidate molecules because 1) it is naturally secreted, 2) it is overexpressed by astrocytes reactive to Aβ plaques, and 3) it has previously been demonstrated to degrade Aβ plaques *in situ* (Yan, et al., 2006, Yin, et al., 2006).

Methods

Lentivirus Construction

3rd generation self-inactivating lentiviruses (Dull, et al., 1998, Englund, et al., 2000) containing cDNA's for human MMP9, HPSE & Nep were created using the pCDH cloning and expression system (SBI, Mountain View, CA). Briefly, MMP9 (2.54kB insert) and HPSE (1.8kB) cDNA's contained within pCMV6-XL4 plasmid vectors (4.7kB empty vector) were purchased from Origene (Rockville, MD). We already had Neprilysin cDNA within the pCDNA 3.1 vector. All three constructs were amplified to provide enough material for removing and then transferring the cDNA insert's into 3rd generation GFP containing lentiviral vectors. The pCMV6 vector has Not1 restriction sites flanking the MMP9 and HPSE cDNA's, so we isolated MMP9 and HPSE inserts using Not1 restriction enzyme digest (New England Biolabs, Ipswich, MA). Nep cDNA was isolated from the pCDNA 3.1 vector using Nhe1 and Not1 restriction enzyme digests. These inserts were ligated into the pCDH lentiviral vector (SBI, Mountain View, CA). Viruses were packaged by transiently co-transfecting HEK293 cells with the pCDH construct (containing MMP9, HPSE, Nep inserts) along with plasmids for the creation of lentiviral structural and integration proteins, and VSV-G pseudotype (courtesy of S.S. Rowland). The VSV-G envelope protein enables lentiviruses to transduce a broad

range of mammalian cells. Viruses packaged by the 293 cells were concentrated to ~1 x 10^{11} particles/ul by centrifugation and minimal dilution.

Lentivirus Transduction

1 x 10^5 trypsinized NSCs and 293FT cells from confluent cultures were resuspended in 100ul dPBS. These cells were transduced by exposure to 6ul volume of virus concentrate for 1 hr in 37°C, with agitation every 10-15 min. This ratio of virus to cells was found to most optimally and consistently yield NSCs expressing the GFP reporter.

Fluorescence Activated Cell Sorting

Transduced cells were grown to confluent cultures in T25 flasks. Cells were trypsinized and resuspended in 5mls of PBS with 2% fetal bovine serum. GFP intensity cut-off points of A.U. 10^3 and 10^4 were used to obtain cells varying in transgene expression.

Isolation of NSCs

The protocols for isolating NSCs are contained in the literature (Marshall, et al., 2006, Zheng, et al., 2006). NSCs were cultured as described in Chapter 3.

Transplantation into Amyloid Beta AD Mice

The Line 85, which constitutively overexpress human Aβ, have been previously described to model the Aβ physiology that is a hallmark AD pathology. Surgeries were performed as described in Chapter 3. Briefly, a Hamilton 33 gauge needle (Hamilton Company, Reno, NV) was then loaded with NSCs prepared at ~5 x 10^4 cells/ul in 1x dPBS. The cells were derived from a trypsinized and pelleted monolayer of NSCs, washed twice with 200ul 1x dPBS and diluted to the appropriate volume using a reference cell count done on a hemacytometer. Cells were deposited at -2.0mm, -

2.3mm and -2.5mm into the hippocampus. 1.25 x 10^5 cells were deposited at -2.0mm and -2.3mm, while 2.5 x 10^5 cells were deposited at -2.5mm. Typically, 4-8ul total volume was deposited at the rate of 0.25ul per 15 seconds (dependant on cell concentration). 20um coronal sections were processed from whole brains and stored in anti-freeze media at -20C until further processing.

Immunochemistry

4% paraformaldehyde fixed cells or tissue sections processed for immunofluorescence in solutions containing 0.1% Triton-X, 10% goat serum in 1x PBS. Primary antibodies used in this study include copGFP (1:2000, Evrogen, Moscow, Russia), anti human MMP9 Clone 56-2A4 (Abcam, Cambridge, MA), anti human MMP9 Clone 6-6B (EMD, Gibbstown, NJ), anti human MMP9 Clone 7-11c (Santa Cruz Biotech, Santa Cruz, CA), anti mouse MMP9 (courtesy of R. Senior, Washington University, St. Louis, MO), anti-Aβ 6E10 (1:2000, Signet, Dedham, MA), microglial antigen Iba1 (1:1000, Wako, Richmond, VA), astrocyte antigen GFAP (1:1000, Dako Corporation, Carpinteria, CA). Cells were rinsed and incubated with goat secondary antibodies Alexa 488, 568 (Invitrogen, Carlsbard, CA). Cells were photographed with an Olympus DP71 camera mounted on an Olympus BX60 microscope. For western blot analysis, samples were diluted in Laemmli sample buffer containing 2% sodium dodecyl sulfate and loaded in 4-20% TG-SDS gels (Invitrogen, Carlsbad, CA) for standard SDS-PAGE. Immunoblots were probed with anti mouse/human MMP9 Clone 38898 (1:5000 Abcam) and Abcam anti human MMP9 Clone 56-2A4 (1:500 (Abcam). Gel blots were photographed using a Fugi imaging system (Fugifilm Life Science, Stamford, CT).

Analysis of Aβ Plaque Number

Image Pro Plus software (MediaCybernetics, Bethesda, MD) was used to quantify intensity over background for images of plaques in coronal sections (Dolev and Michaelson, 2004, Podoly, et al., 2008). Because transplanted cells largely settled in the subcortical and corpus callosum white matter tracks, we focused on a region of interest (ROI A) that included the dorsal hippocampus below the site of engraftment and the cortex above the site of engraftment (1.25mm x 2mm. To be consistent across mice, the vertical boundary for ROI A was the meeting of the dentate arms. The lateral blade of the dentate gyrus was the horizontal boundary. Only sections containing needle tracks were analyzed. Comparison was done on the equivalent region on the contralateral side. For statistical comparison, contralateral areas were analyzed using paired, two-tailed Student's t-test using Microsoft Excel. An unpaired, two-tailed Student's t-test was used for comparison between transplants of GFP NSC and MMP9 NSC transplants. A p-value of <0.05 was considered statistically significant.

Reverse Transcriptase Polymerase Chain Reaction (RT-PCR) of Human MMP9

Human immortalized 293FT cells, mouse immortalized 3T3 cells and NSCs were transduced in simultaneous 100ul reactions that contained 1×10^5 cells and 6ul of MMP9 virus concentrate as described above. Cells were allowed to grow for 6 days before being lysed with Trizol (Invitrogen, Carlsbard, CA). Because there were cell-type specific differences in growth rate, lysates were normalized for total protein using a bicinchoninic acid assay (BCA) (Peierce, Rockford, IL). RT-PCR reactions utilized primers specific to β-actin (400bp) and human MMP9 (600bp). Reagents from a Superscript One-Step RT-PCR System were used according to manufacturer

instructions (Invitrogen, Carlsbard, CA). Because of limited supplies of virus, we could not repeat transduction of cells. However, RT-PCR reactions were repeated 3x.

In Vitro MMP Gelatinase Activity

Conditioned media (C.M.) was collected from transduced and mock transduced NSCs 6 days after transduction (~75% confluent). To eliminate contamination by floating cells in our experiments, C.M. was centrifuged at 1000 x g for 10 min before being applied to 50ug/ml DQ gelatin (Invitrogen, Carlsbard, CA) at a 1:4 dilution. Reactions were incubated overnight at room temperature. Fluorescence increases upon degradation of DQ gelatin due to release of quenched fluorescein. To show gelatin degradation is due to MMP activity, the general MMP inhibitor 1, 10, phenanthroline (1, 10 PNTL) was applied at a 0.8mM concentration. Collagenase activity was used as a positive control. Triplicate reactions of each sample were measured with the excitation/emission spectra of 495nm/515nm using a spectrophotometer (Bio-Tek, Winooski, VT).

In Situ MMP Gelatinase Activity

Fixed brain sections were treated with a protocol modified from Yan et al. (Yan, et al., 2006). Briefly, a PBS solution with 0.1% Triton-X100 and 1% agarose (w/v) was made homogeneous by 2 to 4 rounds of short 10 sec microwave pulses and brief vortexing. The following additions were made to this solution in order to visualize or inhibit MMP activity: DQ gelatin (100ug/ml, warmed to 37°C), DAPI nuclear counterstain (1:1000), 1,10 PNTL (0.8mM), and EDTA (20mM). 300ul of DQ gelatin mixture was quickly added per section. After an overnight incubation in room temperature, green fluorescence of sections was captured with an Olympus DP71 camera mounted on an Olympus BX60 microscope.

Chemical Activation of secreted MMP9

Organomercurial compounds such as *p*-aminophenylmercuric acetate (AMPA) induce autoactivation of MMPs including MMP9 (Ramos-DeSimone, et al., 1999, Yan, et al., 2006). A 1mM concentration of AMPA was added to conditioned media from transduced and mock transduced NSCs. Commercially available MMP9 proenzyme (Perkin Elmer, Waltham, MA) was similarly treated as a positive control. The reaction volume was incubated overnight at 37°C before Western blot analysis with antibodies specific to human MMP9.

Results

GFP NSCs were transplanted into the hippocampus of four mice symptomatic for Aβ pathology using coordinates that resulted in primary corpus callosum engraftment and in some mice, secondary hippocampal fissure engraftment. This pattern of engraftment allowed us to ask whether NSCs have effects in the hippocampus and the cortex. After a month survival period, mice were harvested and their brains processed with antibodies reactive to Aβ and GFP. Needle track containing sections contained the largest engraftments. We analyzed five to seven such sections per animal for amyloid burden (Aβ plaque number) with Image Pro Plus software previously used in a similar capacity (Dolev and Michaelson, 2004, Podoly, et al., 2008). A region of interest (ROI A) proximal to white matter engrafted cells was studied (see Chapter 3). This area included the cortex above the white matter tracks and the dorsal hippocampus below (Fig. 4-1A). Compared to the equivalent contralateral region, we observed a 26.4% ($p=0.04$, paired t-test) reduction in Aβ plaque number in this ROI. Though there was variability in the number of Aβ plaques found per section (Fig. 4-1C), all mice had reduced Aβ plaque numbers (Fig. 4-1D).

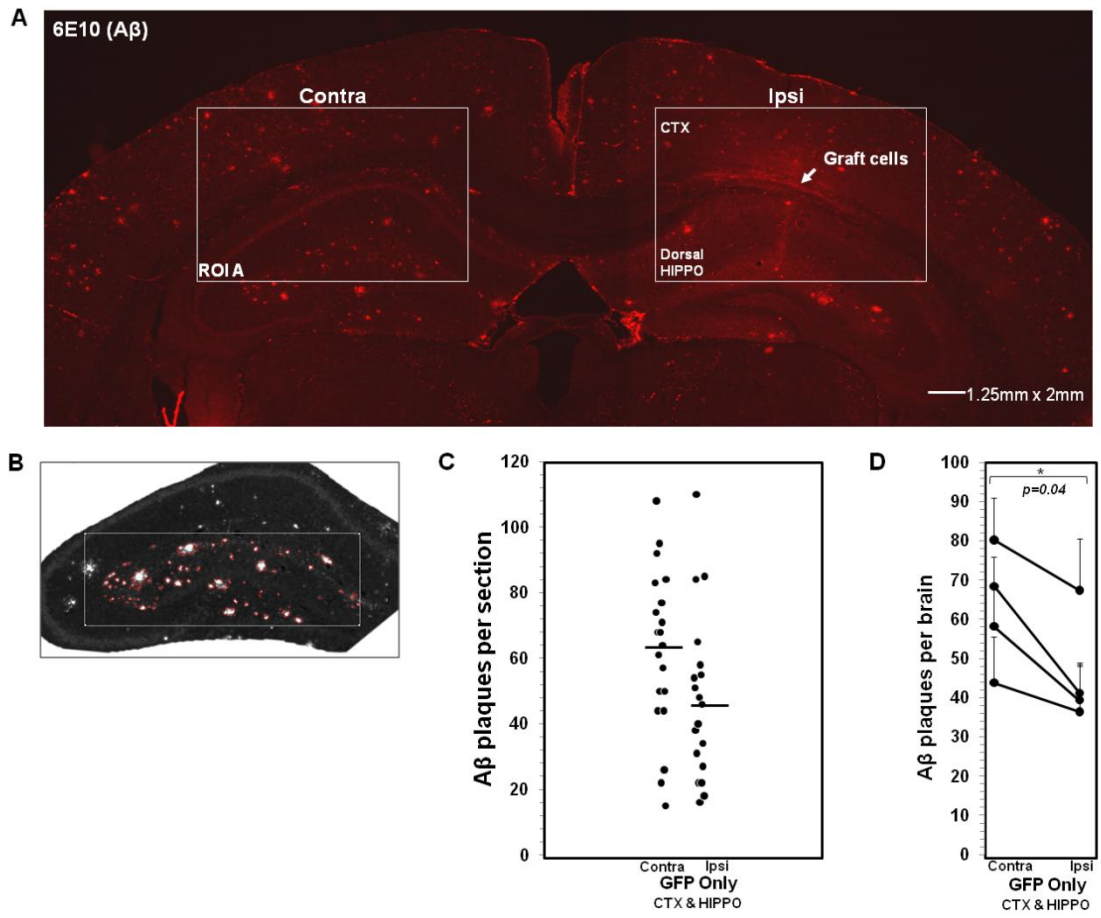

Figure 4-1. Transplantation of NSCs is associated with reduced amyloid burden. Example of Aβ immunostained section shows reduced Aβ plaque numbers in the region of engraftment of 10^3 GFP NSCs a month post-transplantation (A). Representative image demonstrating the sensitivity of software used to count Aβ plaques in sections (B). Plot of results where each dot indicates the number of Aβ plaques on a section. Compared to the contralateral side, the number of Aβ plaques was reduced in ROI A by 26.4% (p=0.03, paired t-test) (C). All mice had reduced Aβ plaque numbers (n=4) (D). *, p<0.05

To understand this result, we have performed preliminary experiments to determine whether 1) NSCs were directly clearing Aβ, 2) NSCs were producing diffusible factors that cleared Aβ or 3) NSCs were interacting with host cells to clear Aβ. Pulse-chase experiments similar to those described in Chapter 2 determined that NSCs were capable of internalizing 0.52ng/ml of Aβ42 in a period of 3 hours (n=4), (Fig. 4-2A). In comparison, neonatal mouse microglia internalized about twice as much Aβ42

(1.1ng/ml), but then expelled most of what was internalized (see Chapter 2) (Njie, et al., 2010). Interestingly, NSCs appear to process Aβ differently as internalization of Aβ was not followed by expulsion (Fig. 4-2B). This suggests that NSCs biophysically degrade Aβ *in vitro* and possibly *in vivo*.

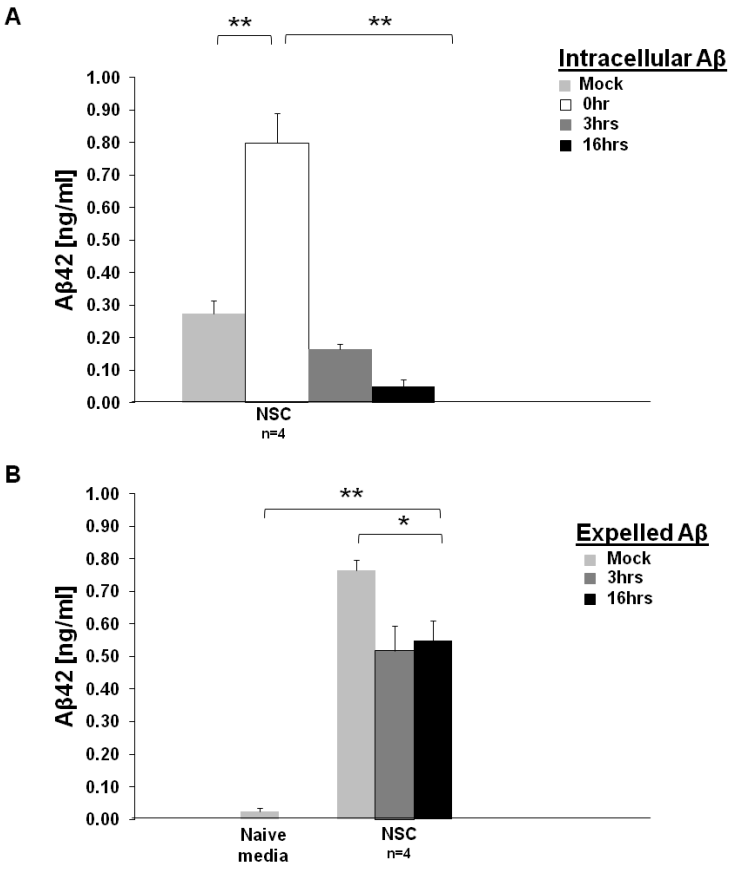

Figure 4-2. Fate of Aβ internalized by NSCs. GFP NSCs were exposed to Aβ42 in pulse-chase experiments (n=4). GFP NSCs internalized 0.52ng/ml within 3hrs (A). In contrast to microglia (Fig. 2-9), GFP NSCs did not expel internalized Aβ42 (B). This suggests NSCs engage in biophysical degradation of Aβ42 following phagocytosis. The ability of GFP NSCs to degrade Aβ42 provides a possible mechanism for reductions in *in vivo* Aβ plaques following transplantation (see Fig. 4-1). Mock data (gray) represents experiments without the presence of cells to control for non-specific adherence of Aβ to culture wells. Detection of Aβ42 requires the presence of both NH2 and COOH terminals of Aβ42, thus only intact Aβ42 peptides are quantified in the above experiments. *, $p<0.05$; **, $p<0.01$.

We found that NSC monolayers are reactive to an antibody against mouse MMP9 (n=3), (Fig. 4-3A). *In vivo*, astrocytes reacting to Aβ plaques overexpress mouse MMP9 as part of a general glial reaction to Aβ pathology (Fig. 4-3B). It may be that MMP9 and other NSC derived diffusible factors contribute to the clearance of Aβ. The lack of MMP9 specific chemical inhibitors makes this difficult to confirm *in vivo*. However, infusion of antibodies known to stop MMP9 gelatinase activity is a possible alternate approach that we may explore in the future.

Previously, degradation of DQ gelatin has been used to show MMP activity around Aβ plaques (Yan, et al., 2006). We verified this finding in mice that have continuous overexpression of Aβ (Fig. 4-4). This result suggests endogenous pathways to regulate Aβ plaques are active. However, recent work from our lab has shown that once formed, Aβ plaques are not removed by endogenous processes (Jankowsky, et al., 2005) - which include MMPs. We therefore wondered whether this is due to an overwhelming rate of amyloid formation. To shed light on this question, we stopped new Aβ production in mice with amyloid precursor protein under a tetracycline regulatory element. Following a month, we found similar levels of MMP activity around Aβ plaques (n=3), (Fig. 4-4B, C). This result suggests that endogenous processes continue to regulate actively Aβ plaque burden in the absence of new deposition. Since this activity does not result in eventual Aβ plaque clearance, it is perhaps the level of MMP anti-Aβ activity rather than the rate of new amyloid deposition that may be responsible for the permanence of Aβ plaques.

We decided to genetically modify NSCs to increase the amount of MMP9 in mice expressing Aβ pathology. To do so, we transduced NSCs with VSV-G serotype lentiviruses carrying the human MMP9 transgene. These lentiviruses, which carry GFP under a separate promoter (Fig. 4-5A) and are able to transduce mammalian cells, conferred GFP fluorescence to NSCs ~3 days post-transduction and 293FTs within 2 days post-transduction. No remnant virus genome was detected in NSC cultures following 2 washes (Fig. 4-5C). Enrichment of NSCs (described below), yielded cultures reactive to two antibodies specific to human MMP9 (Fig 4-5D). 293FT cells produced noticeably more GFP compared to NSCs (Fig. 4-6A, B). This result occurred in 3 independent transductions with independent lots of virus. Several possibilities were considered to explain this observation. These included a species effect, an immortal cell line effect, NSC quiescence, transcription versus translation and lack of uniformity in transduction conditions. To shed light on some of these possibilities, human [immortal] 293FT cells, mouse NSCs as well as mouse [immortal] 3T3 cells were transduced in parallel and analyzed for mRNA transcript production. We were unable to include human NSCs in this experiment due to the limited availability of these cells. This experiment was performed once due to a limited supply of virus, however RT-PCR reactions were repeated three times to reveal variability in analysis. Our results indicate that mouse 3T3 immortal cells had similar levels of transgene mRNA as NSCs (Fig. 4-6C, D). This result suggests that our observations in (A) are not unique to NSCs. Perhaps translational properties unique to 293FT's or human cells in general, may account for enhanced transgene overexpression in 293FT cells.

Though transduced NSCs do not match 293FT cells in transgene production, they nonetheless express human MMP9 which complements the endogenous mouse MMP9 they produce. These cells therefore overexpress total MMP9. Similar to previous reports (Ramos-DeSimone, et al., 1999), transgene directed MMP9 mRNA is translated to a secreted 92kDa zymogen (proenzyme). Mock treated NSCs have intrinsic MMP activity on gelatin that is chemically inhibited by 1,10 phenanthroline (Fig. 4-7A). The secretion of MMP9 zymogen by transduced NSCs is associated with a 3.5x increase in gelatinase activity (Fig. 4-7A). We did not observe degradation of Aβ42 in conditioned media from 10^3 MMP9 NSCs (10^3 cells, data not shown). However, the 39kDa catalytic subunit of MMP9 (ctMMP9) reduced Aβ detectable by Western blot by approximately 75% in overnight reactions (Fig. 4-7B). The amount of ctMMP9 needed to achieve this degradation was less than ideal: ~20:1 ratio of enzyme to substrate. However the observation that truncated MMP9 is the isoform capable of degrading Aβ is consistent with previous reports (Yan, et al., 2006). This suggests *in vivo* autoactivation of NSC produced MMP9 is required for anti-Aβ activity.

To determine if NSC produced MMP9 is capable of undergoing such autoactivation, conditioned media was treated to *p*-aminophenylmercuric acetate (AMPA). This organomercurial compound disrupts the interaction of an unpaired, N-terminal cysteine with the zinc ion of the MMP9 catalytic center. Such disruption initiates autoproteolytic N-terminal shedding that generates the MMP9 isoform shown to degrade Aβ in the literature (Yan, et al., 2006). We applied a 1mM concentration of AMPA to conditioned media and detected only the truncated (active) form of MMP9 following 24hrs (100% conversion) (Fig. 4-7C). We therefore concluded that transgene

directed MMP9 secreted by NSCs is capable of undergoing autoactivation. There are a number of proteases thought to mimic the action of AMPA *in vivo* (Ramos-DeSimone, et al., 1999). On the other hand, tissue inhibitors of metalloproteases (TIMP1-4) inhibit MMP9 but are limited by stoichiometric binding (Ramos-DeSimone, et al., 1999). TIMP levels have been shown to increase in AD (Lorenzl, et al., 2003, Peress, et al., 1995) and in one mouse model of AD (Hoe, et al., 2007). However, the concentration of TIMPs in mice with Aβ pathology has not been quantified. We therefore aimed to introduce as much MMP9 into the brain as possible in order to saturate endogenous activators of MMP9 and overcome inhibitors of MMP9.

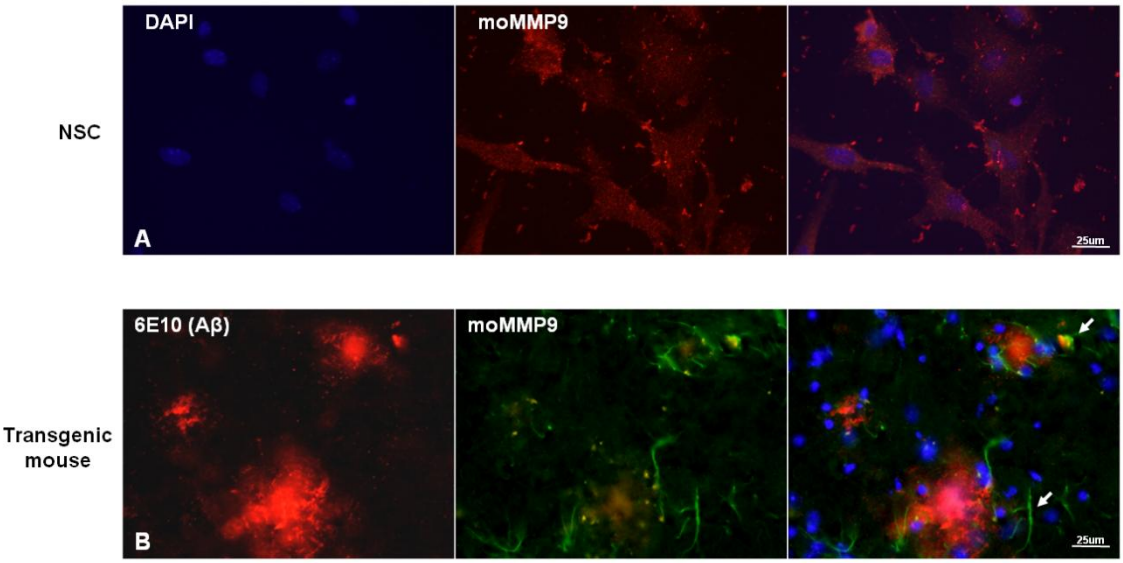

Figure 4-3. NSCs express endogenous mouse MMP9. NSCs were reactive to antibodies against mouse MMP9 (n=3) (A). It is possible that transplant derived mouse MMP9 adds to the concentration of MMP9 secreted by endogenous astrocytes reacting to Aβ plaques (n=2) (B, arrows).

Cultures of transduced NSCs had a non-uniform distribution of GFP. This suggested that in our population of transduced cells, transgene copies were varied from cell to cell. Peripheral drug treatment paradigms typically tailor dosage to optimally balance between desired effects and side effects. To emulate this preclinically, we

used FACS technology to take advantage of the differential transduction of NSCs by selecting for cells whose GFP intensity was A.U>10^3 or 10^4 (Fig. 4-8). The conditioned media from the resulting cultures was analyzed with Western blot using an antibody that detects commercially available human proMMP9 and verified with an antibody cross-reactive to both human and mouse MMP9. *In vitro*, a confluent layer of 10^3 cells secreted 0.51ug/ml of human MMP9 in a T25 flask with 5mls of media over 3 weeks. 10^4 cells treated similarity, secreted 0.66ug/ml over only 1 week (Fig. 4-9A). Non-transduced and non FACS sorted cells had no detectable secretion of human MMP9. We project that over 4 weeks, 10^3 and 10^4 cells will secrete 0.7ug/ml and 2.7ug/ml of MMP9, respectively (Fig. 4-9B). This demonstrates that we can create NSC cultures with low and high doses of MMP9 with FACS technology.

This result, though promising, is limited by yield. A confluent T25 flask holds a monolayer of ~5 x 10^6 NSCs. The average yield of 10^3 NSCs is 8.9 x 10^5 cells/flask. This is reduced 6-fold, or 1.4 x 10^5 cells/flask for 10^4 cells (n=7) (Fig. 4-8E). 10^4 cells are only 4.5% +/-0.8% (n=8) of the original population of transduced cells (Fig. 4-8D). Further selection exponentially diminishes yield. Therefore, we are confident that our enrichment protocol approached theoretical limits of selection. We reasoned that these highly enriched MMP9 expressing NSCs stand the best chance of overcoming endogenous MMP9 repressors and acting against Aβ. However, MMP9 expression can lead to negative consequences (Chambers and Matrisian, 1997, Lubbe, et al., 2006, Moll, et al., 1990). Therefore, we first worked with 10^3 cells in transplant studies in hopes of establishing safety as well as efficacy.

MMP9 expressing 10^3 NSCs were injected into five Aβ transgenic mice. We confirmed that NSCs continued MMP9 overexpression a month post-surgery (Fig. 4-10). Graft derived MMP9 had N-terminal shedding that is associated with activation (Fig. 4-10E). We have ongoing studies to determine the endogenous proteins that activated graft derived-MMP9. Analyses of *in vivo* MMP9 overexpression utilized antibodies specific to human MMP9 for immunocytochemistry (n=3), 1um z-plane confocal histology (n=2), and western blot (n=3).

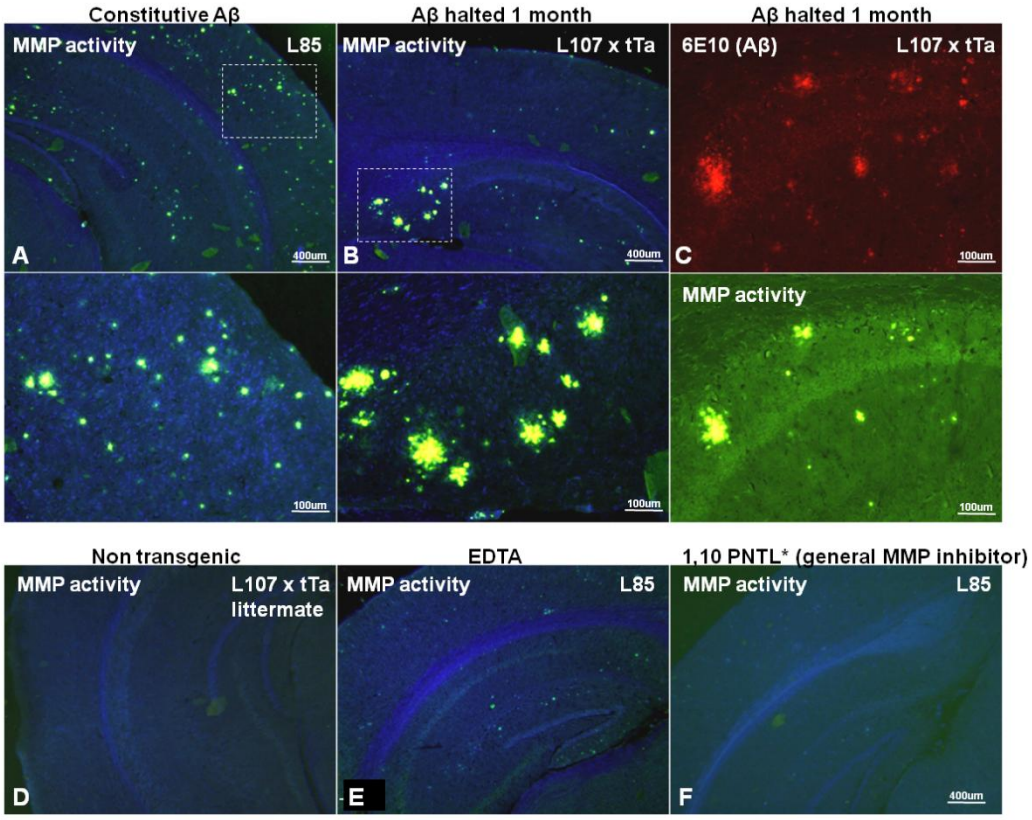

Figure 4-4. Endogenous MMP activity in mice with Aβ plaque burden. Sections incubated overnight with DQ gelatin demonstrate persistent MMP activity on Aβ plaques 4 weeks after cessation of Aβ production (n=3) (A-B). Controls show DQ gelatin fluorescence is specific to Aβ plaques (C), does not occur in non transgenic mice (D), and is dependent on MMP activity (E, F).

Mice receiving MMP9 NSC transplants were examined for Aβ plaque burden with methodology described above for GFP NSCs. A sham injection on the contralateral

side was performed in order to control for the effect of needle injury on the cell injected side. Compared to the needle injury on the contralateral side, we did not notice additional death of neuronal cells or otherwise abnormal cytoarchitecture in the side of the brain containing MMP9 NSCs. We observed a 28.6% ($p=0.03$, paired t-test) reduction in Aβ plaque number within ROI A (Fig. 4-11A, B).

MMP9 NSC and GFP NSC transplants had comparatively similar percent reductions in Aβ plaque number (Fig. 4-11C). Since Aβ plaque number reductions were statistically significant in both groups, we asked whether there was change in the amount of Aβ plaques cleared in mice receiving GFP NSCs and MMP9 NSCs. We subtracted the averaged contralateral Aβ plaque number in each animal from the averaged ipsilateral Aβ plaque number and then compared across the two transplant groups. MMP9 NSC transplants were associated with clearance of 31% more Aβ plaques compared to GFP NSC transplants ($p=0.47$, unpaired t-test), (Fig 4-11E). This trend, though non-statistically significant, is promising. It should be noted that mice hosting MMP9 NSC transplants were a month older and consequently had 25% greater Aβ plaque numbers (Fig. 4-11D). The lack of a uniform baseline of Aβ plaque number due to age-related changes is confounding. The increased engraftment of MMP9 NSCs relative to GFP NSCs further complicates interpretation. Though our data indicates a trend of more Aβ plaque clearance in 10^3 MMP9 NSCs, further experimentation with 10^4 cells that more robustly express MMP9 is needed with special attention to address the confounding variables described above.

Discussion

In this study, we aimed to determine whether NSCs could be used to reduce Aβ pathology either without modification or as a vehicle to deliver molecules that have

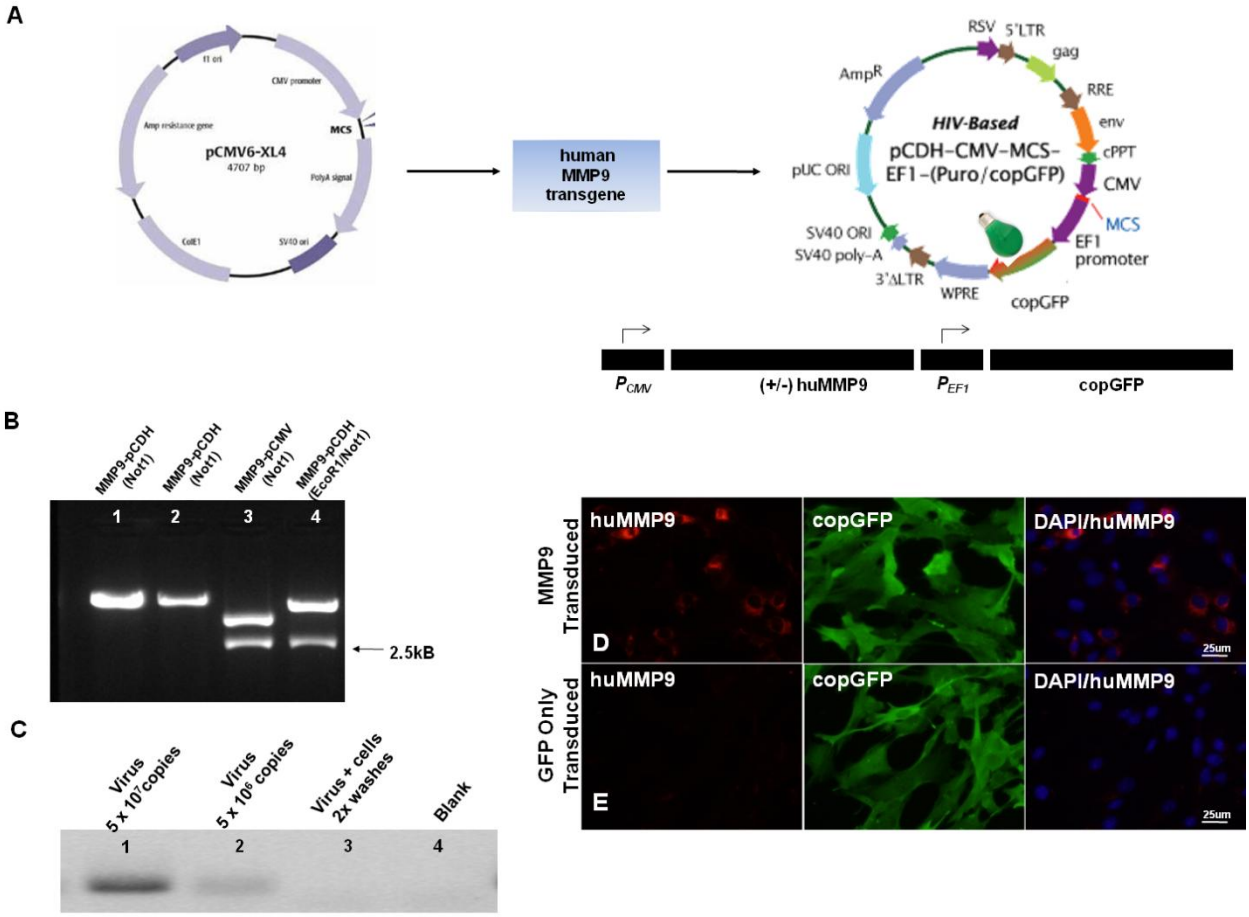

Figure 4-5. Genetic modification of NSCs for MMP9 overexpression. Vector diagram of MMP9 transgene illustrates subcloning of human MMP9 cDNA from a pCMV vector (4.7kB) to a pCDH vector (7.5kB). The pCDH vector contains plankton derived GFP reporter gene and components necessary for the packaging of self-inactivating lentiviruses. The dual promoter design of pCDH meant MMP9 was independently driven by the CMV promoter while copGFP was driven by the EF1 promoter (A). Restriction enzyme digests yielded MMP9 transgene of correct size (2.5kB) at the end of the cloning process (B, Lanes 3 & 4). Real-time PCR showed no evidence of viral genome in media in transduced cultures washed with dPBS (C). Transduction resulted in GFP reporter gene expression (D, E middle panels). GFP NSCs (D) and MMP9 NSCs (E) differed only in MMP9 expression. GFP and MMP9 immunoreactivity did not always colocalize (D, compare left and middle panels).

promising anti-Aβ qualities. Unlike our results with microglia (see Chapter 2), NSCs *in vitro* biophysically degrade Aβ. Transplantation of NSCs is associated with close to a one-third reduction in Aβ plaque numbers in the cortex and hippocampus. Genetically

modifying NSCs to overexpress MMP9 is associated with a trend of more clearance of Aβ plaques; however a statistically significant difference was not found. It is possible that greater overexpression of MMP9 may yield more robust reductions in Aβ plaque numbers. We developed a method to enrich for MMP9 production in NSCs cultures by utilizing FACS selection to take advantage of the plurality of gene dosage associated with lentiviral transduction. This positive selection scheme approaches the theoretical limit of enrichment and has resulted in improvement from initially undetectable levels of MMP9 in NSC conditioned media to detection of ug/ml amounts of MMP9. We were also able to demonstrate enrichment of heparanase overexpressing NSCs. Therefore, this method of enrichment is generally applicable to emerging therapies using NSCs. Our future studies will concentrate on NSCs four-fold more enriched that those utilized for the transplant studies described in this report.

Endogenous MMP Activity

Our current findings show that the brain continues to use MMPs to regulate pre-existing Aβ plaques suggesting that endogenous processes do not cease actively mitigating Aβ plaque burden. These processes appear insufficient as Aβ plaques persist six months after genetic cessation of new Aβ production (Jankowsky, et al., 2005). However, once formed, Aβ plaques resist biophysical removal despite persistence of these endogenous efforts. This underscores the need for exogenous intervention to clear Aβ plaques in mice and perhaps in humans.

Aβ plaque Burden is Lowered Following NSC Transplantation

We introduced GFP NSCs and MMP9 NSCs into the brain and found both cell types reduced Aβ plaque numbers. This result suggests that transplanted NSCs or uncharacterized biology associated with their engraftment, reduces the prevalence of

otherwise permanent Aβ plaque burden. Our findings contradict recent work by Blurton-Jones and colleagues (Blurton-Jones, et al., 2009). In their observations, Aβ content was not reduced in hippocampal injections of NSCs. The discrepancy with our findings may perhaps be explained by unknown factors unique to their model --a triple-transgenic mouse with tauopathy, versus our models which strictly model amyloidosis (Oddo, et al., 2003). Secondly, the cells used by Blurton-Jones et al., were created without region-specificity; they were derived from neurospheres obtained from whole brain homogenates. It is possible that the SEZ origin of our NSCs enabled unique anti-Aβ effects. If true, our finding may mean that some but not all populations of NSCs exhibit anti-Aβ activity.

NSCs as a Platform to Deliver MMP9 and Other Candidate Therapeutics *In Vivo*

We hypothesized that constitutive MMP9 secretion by NSCs proteolytically will act on fibrillar Aβ and confer further decreases in Aβ plaque burden. Since *ex vivo* manipulation of NSCs for use as delivery vehicles of therapeutics is a field still in its infancy, our work sheds light on several important questions regarding NSCs in this paradigm. These questions include: do NSCs retain stem cell qualities if genetically manipulated *in vitro?* Do NSCs express active, transgene directed proteins of interest? Are such proteins produced in sufficient amounts? Can NSCs be genetically modified with a repertoire of candidate molecules? New molecules with interesting anti-Aβ effects continue to be published. For instance MT1-MMP has recently been shown to degrade Aβ *in vitro* (Liao and Van Nostrand, 2010). Our observations on genetically manipulating and purifying NSCs and the *in vivo* effects of MMP9 NSCs demonstrate potential positive effects as well as pitfalls that may apply to emerging candidate molecules.

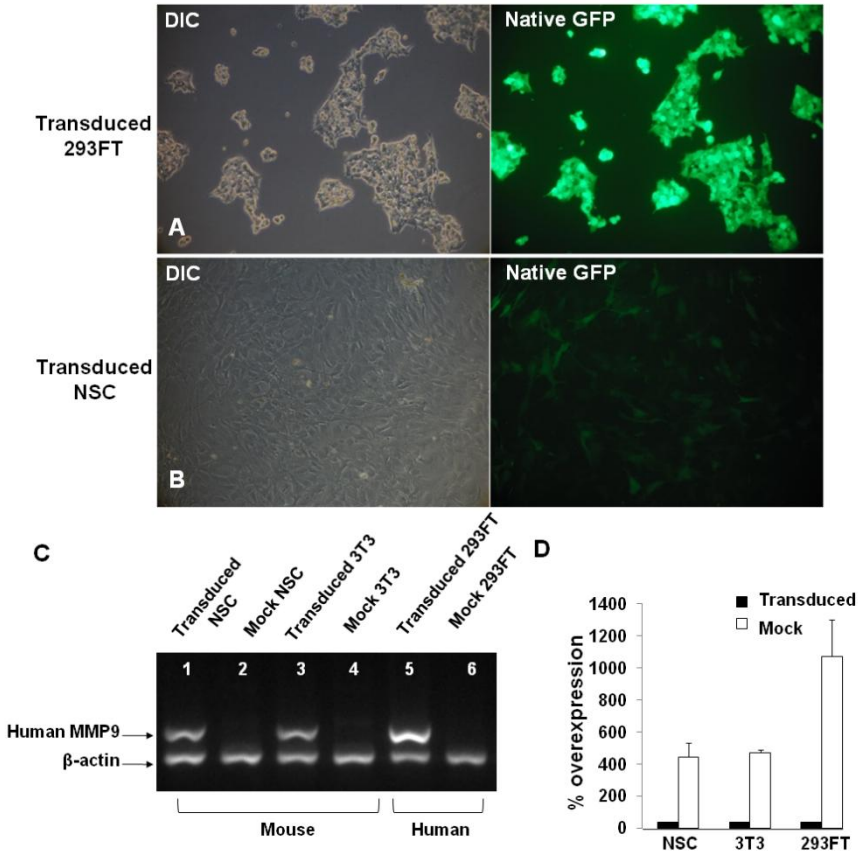

Figure 4-6. Cell type differences in transduction efficiency. 293FT cells produced significantly more GFP protein relative to equivalently treated NSCs (n=2) (A, B). Semi-quantitative RT-PCR analysis of transduced cells indicated mouse 3T3 immortal cells had comparable amounts of MMP9 mRNA as NSCs, suggesting low levels of transgene expression is not NSC specific (C). This comparative transduction experiment was not investigated further due to the limited supply of lentiviral stocks. Error bars reflective RT-PCR analyses (D).

Characteristics of NSCs overexpressing transgenes

Regarding the maintenance of 'stemness' following genetic manipulation, our transgene receiving NSCs continued expression of BIII-Tubulin (data not shown), a immunological marker commonly associated with precursor cells (Walton, et al., 2006a). Interestingly, transplanted NSCs in white matter tracks do not stain for BIII-Tubulin (see Chapter 3). Studies have shown that microglia are associated with the maintenance of

the self-renewal capacity of NSC cultures (Walton, et al., 2006b). We do not see obvious changes in the microglial subpopulation following MMP9 genetic modification.

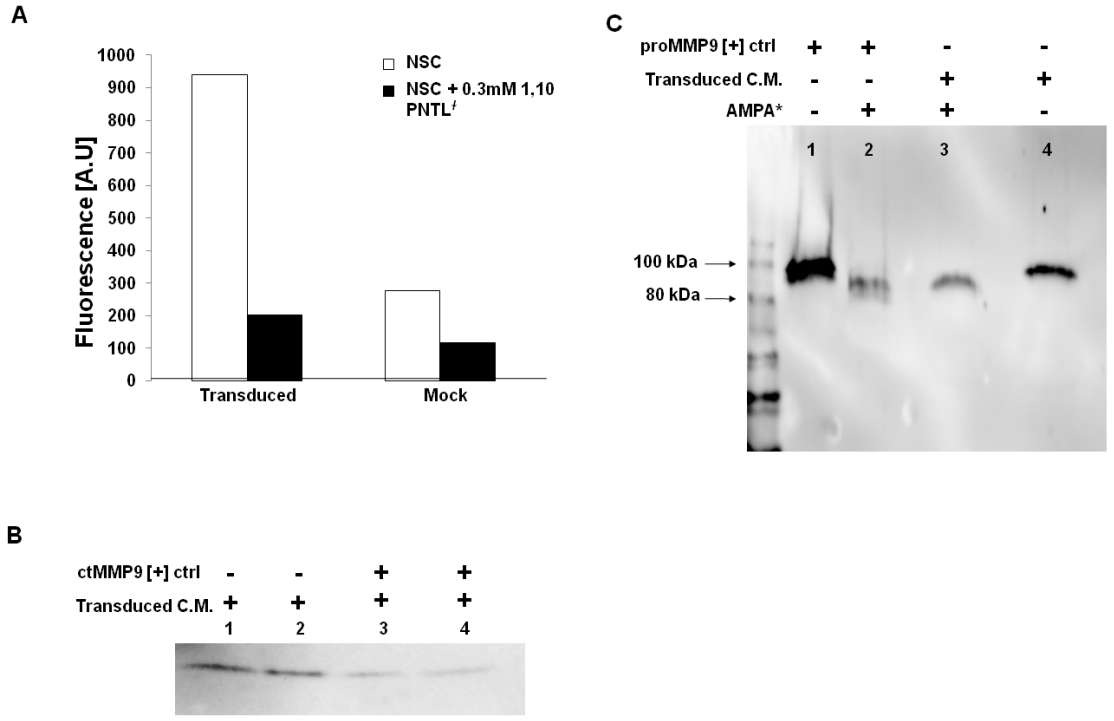

Figure 4-7. Secreted MMP9 has zymogen activity and can undergo autoactivation. Conditioned media (C.M.) from transduced NSCs has 3-fold more gelatinase activity compared to media from mock treated NSCs (A). MMP9 NSC conditioned media was not associated with degradation of Aβ (data not shown). Commercially available catalytic subunit of MMP9 (39kDa) was able to degrade Aβ (B). Application of *p*-aminophenylmercuric acetate (AMPA) to conditioned media results in conversion (autoactivation) of transgene derived 92kDa MMP9 zymogen to ~84kDa isoform that is associated with Aβ degradation (C). Mouse MMP9 (105kDa) not detected here. Human specific MMP9 antibody used.

In vivo, NSCs transition between states of quiescence and proliferation (Chambers and Matrisian, 1997, Lubbe, et al., 2006, Moll, et al., 1990). In a quiescent state, it is likely that the metabolic rate of NSCs is reduced. This may effect NSC drug delivery as transgene transcription or translation may be affected negatively. In our experience, NSC consistently secreted appropriately folded MMP9 that is capable of N-terminal shedding and gelatinase activity. Following transduction, we found an assortment of

GFP expression in a population of cells that did not yield detectable levels of MMP9 (cell associated antibody reactivity). We attribute this variability in reporter gene expression to the randomness of lentiviral infection, regions of transgene integration and unknown promoter effects. However, NSC quiescence may contribute to the assorted expression of GFP. Nonetheless, we were able to select for the brightest cells and improve our yields of transgene protein to ug/ml quantities. The success of our selection suggests that in a clinical setting, similar methodology may be used to obtain populations of cells that yield appropriate doses of candidate drugs.

Whether transgene expression changes once NSCs are transplanted remains unanswered. Further exploration of temporal changes in transgene expression as well as studies to understand endogenous activators and inhibitors are needed. MMP9 NSCs form significantly larger grafts than GFP NSCs (see Chapter 3). Yet, both cell types are associated with similar reductions in amyloid burden. It is possible that subpopulations of NSCs that are responsible for anti-Aβ activity are also prone to Aβ toxicity. Previous studies have shown Aβ to be selectively toxic to certain populations of the hippocampal stem cell niche (Verret, et al., 2007). If a similar scenario applies to transplanted NSCs, it may be that a subpopulation within MMP9 NSC grafts was ablated after a bolus of anti-Aβ activity commensurate with that of GFP NSCs. Remaining MMP9 NSCs lacking anti-Aβ activity may then have continued surviving due to MMP9 overexpression. Determining whether this hypothesis is true is complicated by the fact that large numbers of transplanted NSCs do not display common immunological markers (T. Zheng, personal communication), (Verret, et al., 2007) and what researchers know about transplanted NSCs is largely based on snapshots (histology,

etc) of dynamic graft environments. Temporal studies of graft survival and better markers of NSCs would facilitate more granular understanding of NSC grafts.

NSCs showed reporter gene expression when transduced with neprilysin and heparanase. We discontinued our work with neprilysin because NSC cultures repeatedly died days after transduction. However, heparanase NSCs have been passaged multiple times. These cells are reactive to an antibody against heparanase (data not shown), suggesting transgene expression. MMP9 and heparanase NSCs both display two populations of GFP intensity when analyzed with FACS. Consequently, we have been able to isolate 10^3 and 10^4 heparanase NSCs. This data suggests that neprilysin expression may be uniquely toxic to NSC cultures. However our experience with MMP9 and heparanase expression indicates that NSCs are capable of producing a diverse pallet of anti-Aβ molecules.

Concluding Comments

In this preclinical study, we took advantage of interesting stem cell properties in a disease setting. Our experiments demonstrate that NSCs can be genetically manipulated *ex vivo* and yield robust grafts when transplanted into the hippocampus of diseased mice. Such grafts are associated with reductions of Aβ plaques in a mouse model of AD. This result provides evidence of a novel attribute of transplanted NSCs. We attempted to further enhance NSC anti-Aβ activity by inducing MMP9 overexpression. However, only a trend towards further reductions in Aβ plaques was observed. It is possible that enriched NSCs will produce enough MMP9 to overcome endogenous tissue inhibitors of MMP9. We describe an enrichment method that has yielded NSCs cultures able to produce ug/ml concentrations of MMP9. This method has been generalized to NSCs expressing other candidate molecules. Our future

studies aim to find the right dose of MMP9 or alternatively, the right drug to maximally reduce Aβ pathology. Together, data presented here demonstrates that NSCs can be used as a platform for testing novel therapeutic molecules *in vivo*.

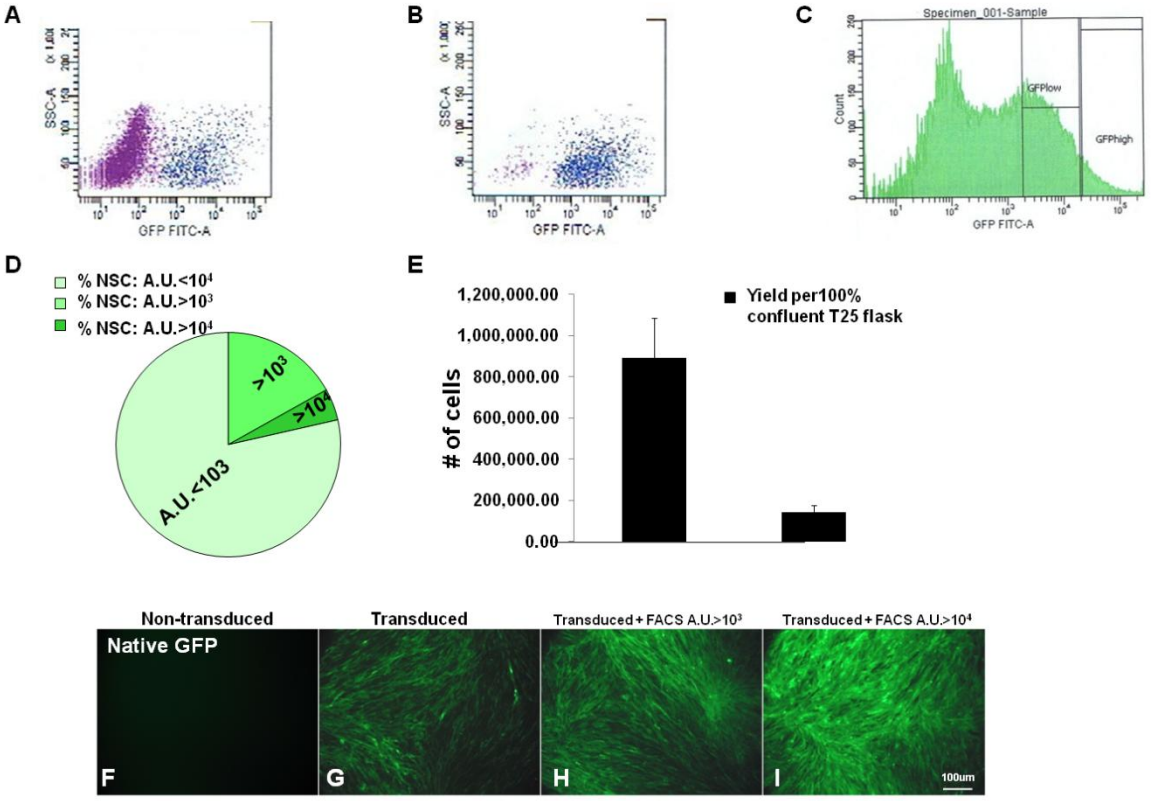

Figure 4-8. Enrichment of NSC cultures. FACS analysis demonstrated two populations of cells in transduced cultures that vary in reporter gene expression (A, C). Within the population of brightest cells (B), we selected for intensity greater than10^3 or 10^4 (C, GFP low, GFP high). The resultant cells represent 16% and 4.5% of the overall transduced population, respectively (n=8) (D). These cells are referred to as 10^3 NSCs and 10^4 NSCs. Yields of10^3 NSCs and 10^4 NSCs attained per T25 flask holding ~5 x 10^6 NSCs (n=7) (E). The methodology used here resulted in highly enriched cultures (compare G, I, equally exposed images of similarly confluent cultures) and can be used for NSCs expressing other transgenes: Chromatogram in (C) is from heparanase overexpressing NSCs. Characteristic double hump is also exhibited by GFP NSCs and MMP9 NSCs (data not shown).

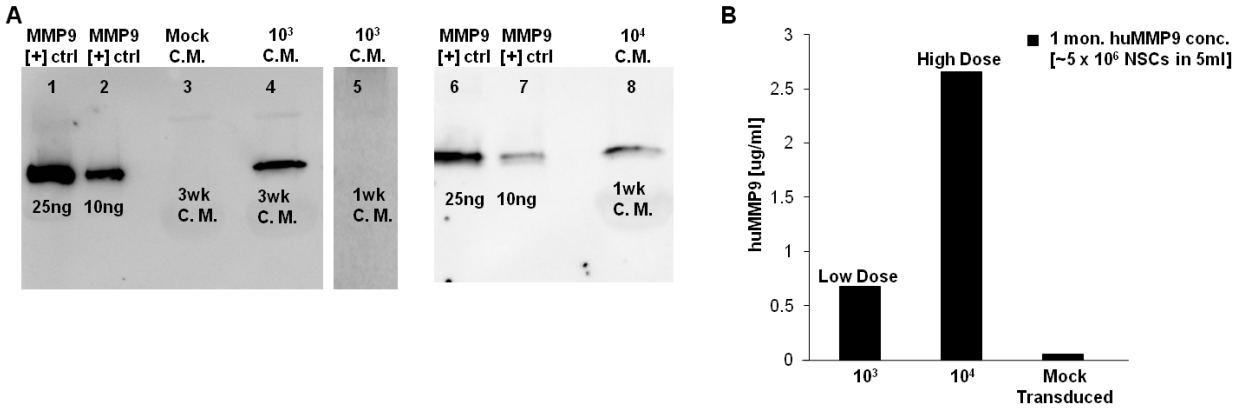

Figure 4-9. NSC enrichment is associated with rate of MMP9 secretion. MMP9 from 10^3 NSCs is detectable at 3 weeks while MMP9 from similarly confluent 10^4 NSCs is detectable at 1 week (n=3) (A). Projected concentration of MMP9 that a confluent layer of NSCs will secrete in a 5ml volume during the course of a month (B) is derived from densitometric analysis of data in (A).

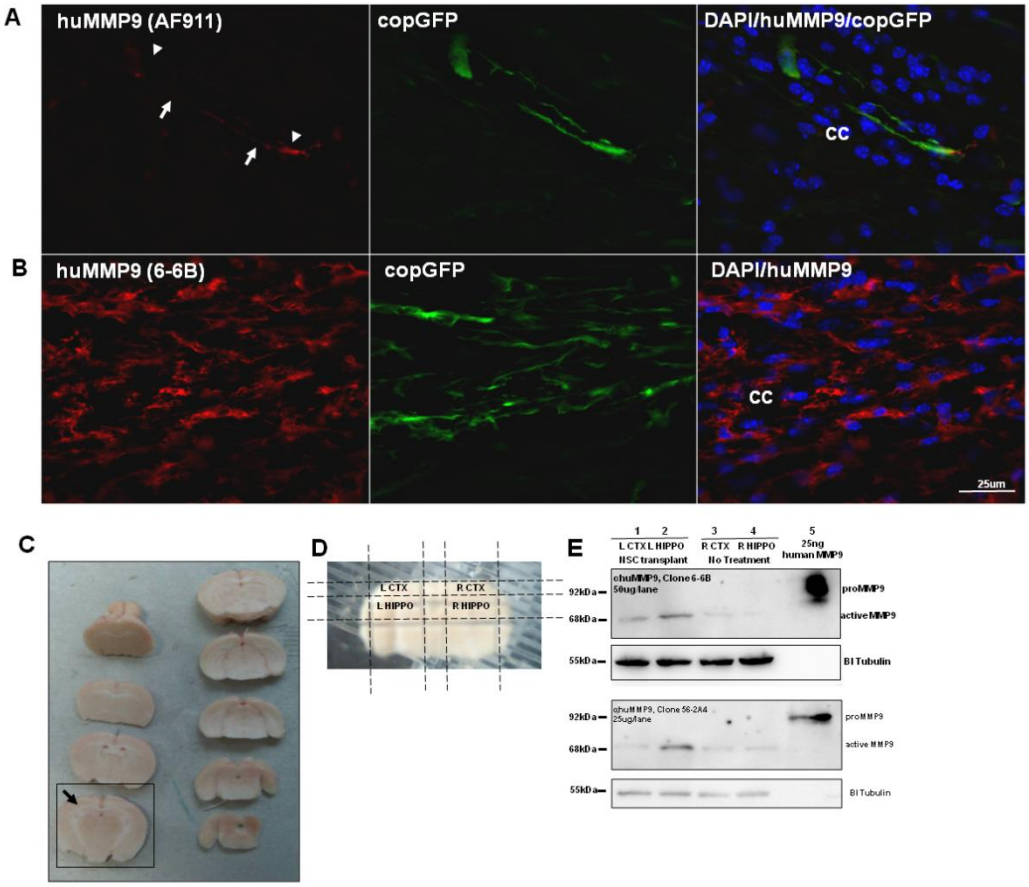

Figure 4-10. NSC overexpression and activation of MMP9 *in vivo.* 1um z-plane depth confocal images indicate NSCs overexpressed huMMP9 a month following transplantation (A-B). MMP9 was observed in cell bodies (arrowheads) as well as processes (arrows) extended by NSCs within the white matter of Aβ transgenic mice (n=3) and not in the contralateral [non-injected] hemisphere (not shown) (A). To gain insight on the distribution of MMP9 secreted by NSCs, the brains of non transgenic mice with one month MMP9 NSC engraftments were sectioned at 1mm intervals (C). Cortical and hippocampal regions were then dissected (D) and analyzed with western blot using antibodies against human MMP9. Immunoreactivity was strongest in the hippocampus of the hemisphere where NSCs were injected into (n=2). NSCs *in vitro* secrete proMMP9 (Fig. 4-9A). However, MMP9 *in vivo* is of a lower molecular weight indicating activation by endogenous factors. Mouse MMP9 is >100kDa and not detected by antibodies used here.

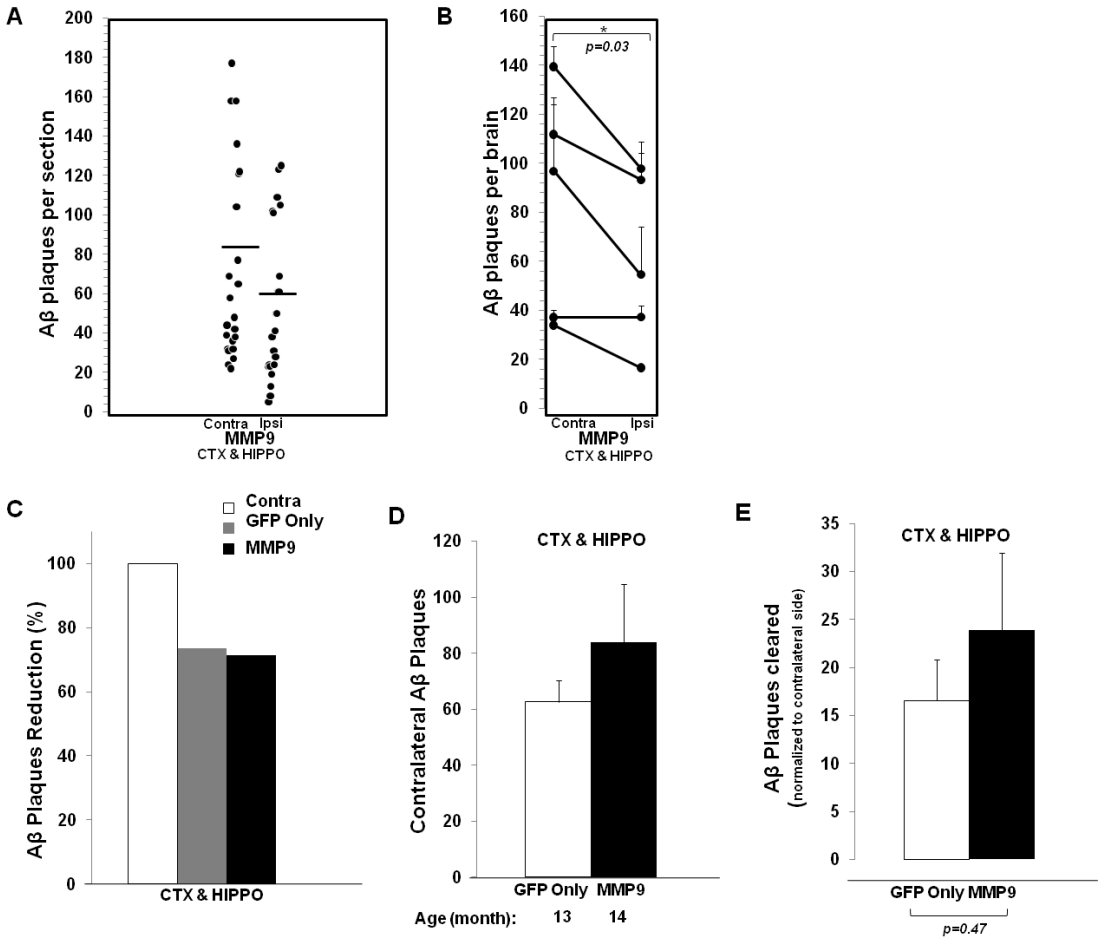

Figure 4-11. Transplantation of MMP9 NSCs and GFP NSCs results in similar reductions in amyloid burden. Compared to the contralateral side, the number of Aβ plaques in Aβ transgenic mice with one month 10^3 MMP9 NSC engraftments was reduced by 28.5% (p=0.04, paired t-test) (A). All mice receiving MMP9 NSCs had reduced Aβ plaque numbers (n=5) (B). GFP NSC and MMP9 NSCs had similar reductions of Aβ plaque numbers (C), (see Fig. 4-1). Due to age-related effects, contralateral Aβ plaque burden was 25% greater in mice receiving MMP9 NSCs (D). Therefore, percentage reduction is not indicative of total Aβ plaques cleared between the two groups of mice. To determine if MMP9 overexpression is associated with greater clearance of Aβ plaques, we compared the absolute number of Aβ plaques cleared across groups. The results indicate MMP9 overexpression by NSCs is associated with a non-statistically significant trend of 31% more Aβ plaques cleared (p=0.47, unpaired t-test) (E). *, p<0.05

CHAPTER 5
CONCLUSIONS

Beyond the treatment of Alzheimer's disease, our studies may hold relevance to other brain diseases that feature protein aggregation. For instance, Amyloid Lateral Sclerosis (ALS) and Parkinson's disease have aggregates of superoxide dismutase (SOD1) and α-synuclein, respectively. Recently, elegant studies by Don Cleveland and others show that microglia expressing mutated SOD1 play an important role in the end stage of ALS. This evidence fits with our findings: the perturbation of microglial functionality with age may contribute to neurodegeneration in mouse models and perhaps in diseased humans. However, therapeutic manipulation of endogenous microglia is difficult. This is evidenced by the lack of robust outcomes in clinical trials that aimed to reduce glial activity (ex. non steroidal anti-inflammatory drug trials) (Sabbagh, 2009) or enhance glial activity (Aβ immunization trials) (Patton, et al., 2006).

Stem cell transplants present an alternative avenue to directly target amyloid burden. In work presented in here, we were unable to modify NSCs to reduce Aβ. It is likely that we haven't found the right dose or the right drug to elicit a change in pathology. However, this negative result shouldn't detract from other relevant observations. First, transplantation of NSCs is associated with reduced Aβ burden. Second, injection of NSCs into the hippocampus results consistently in engraftment in defined regions of the hippocampus and surrounding white matter. Finally, transgene overexpression modified NSC engraftment patterns. These findings have significant implications for proposals for the use of stem cells to restore dying cells or to deliver drugs to sites of injury.

In our studies, we focus on the Aβ pathology of AD. Currently, there is intense debate regarding the importance of Aβ in AD. The different schools of thought have noteworthy evidence to cite. For instance, a recent drug trial with an anti-tau compound has yielded perhaps the most promising clinical outcomes in AD drug trials history (TauRx, Rember trials). This suggests a causative role for tau in AD etiology. On the other hand, research published this month shows fibrillar Aβ in non demented individuals who have parents with late-onset (sporadic) AD (Mosconi, et al.). This buttresses already strong genetic data from Down's syndrome cases and mutations in the amyloid precursor protein and presenilin loci. The ubiquity of data to support the different schools of thought of how AD arises is remarkable and unique amongst neurodegenerative diseases. This ubiquity also highlights the fact that success has not been had with removal of any of the pathologies found in AD. Until this occurs, and clinical outcome is observed, arguments on the role of Aβ versus tau are inherently academic. They are based on correlation, not causation.

Removing the pathologies of AD has proven difficult partly because of difficulties with delivering drugs into the brain. The use of NSCs, as demonstrated here, presents a novel approach to overcome this difficulty. The scope of this approach is not limited to AD, as research on treatments for most diseases of the brain is hindered by the inability to deliver drugs into the brain.

In the course of human history, medical practice on the brain has typically involved the removal of tissue. At this junction in history, NSCs transplants represent a bifurcation point. What happens after the introduction of new tissue into the brain is largely unknown. The work presented here adds to our understanding of the behavior

of implanted brain tissue and the manipulation of said tissue to counter disease pathology.

LIST OF REFERENCES

Armstrong, R.A., Cairns, N.J., Myers, D., Smith, C.U., Lantos, P.L., Rossor, M.N. 1996. A comparison of beta-amyloid deposition in the medial temporal lobe in sporadic Alzheimer's disease, Down's syndrome and normal elderly brains. Neurodegeneration 5(1), 35-41.

Association, A.s. 2007. Alzheimer's Disease Facts and Figures 2007. Alzheimer's Association.

Astary, G.W., Kantorovich, S., Carney, P.R., Mareci, T.H., Sarntinoranont, M. Regional convection-enhanced delivery of gadolinium-labeled albumin in the rat hippocampus in vivo. J Neurosci Methods 187(1), 129-37.

Astary, G.W., Kantorovich, S., Carney, P.R., Mareci, T.H., Sarntinoranont, M. 2010. Regional convection-enhanced delivery of gadolinium-labeled albumin in the rat hippocampus in vivo. J Neurosci Methods 187(1), 129-37.

Auld, D.S., Kornecook, T.J., Bastianetto, S., Quirion, R. 2002. Alzheimer's disease and the basal forebrain cholinergic system: relations to beta-amyloid peptides, cognition, and treatment strategies. Prog Neurobiol 68(3), 209-45.

Bales, K.R., Du, Y., Holtzman, D., Cordell, B., Paul, S.M. 2000. Neuroinflammation and Alzheimer's disease: critical roles for cytokine/Abeta-induced glial activation, NF-kappaB, and apolipoprotein E. Neurobiol Aging 21(3), 427-32; discussion 51-3.

Beckmann, N., Schuler, A., Mueggler, T., Meyer, E.P., Wiederhold, K.H., Staufenbiel, M., Krucker, T. 2003. Age-dependent cerebrovascular abnormalities and blood flow disturbances in APP23 mice modeling Alzheimer's disease. J Neurosci 23(24), 8453-9.

Bennett, L.B., Cai, J., Enikolopov, G., Iacovitti, L. 2010. Heterotopically transplanted CVO neural stem cells generate neurons and migrate with SVZ cells in the adult mouse brain. Neurosci Lett 475(1), 1-6.

Bjorklund, A., Dunnett, S.B., Brundin, P., Stoessl, A.J., Freed, C.R., Breeze, R.E., Levivier, M., Peschanski, M., Studer, L., Barker, R. 2003. Neural transplantation for the treatment of Parkinson's disease. Lancet Neurol 2(7), 437-45.

Blits, B., Kitay, B.M., Farahvar, A., Caperton, C.V., Dietrich, W.D., Bunge, M.B. 2005. Lentiviral vector-mediated transduction of neural progenitor cells before implantation into injured spinal cord and brain to detect their migration, deliver neurotrophic factors and repair tissue. Restor Neurol Neurosci 23(5-6), 313-24.

Blurton-Jones, M., Kitazawa, M., Martinez-Coria, H., Castello, N.A., Muller, F.J., Loring, J.F., Yamasaki, T.R., Poon, W.W., Green, K.N., LaFerla, F.M. 2009. Neural stem cells improve cognition via BDNF in a transgenic model of Alzheimer disease. Proc Natl Acad Sci U S A 106(32), 13594-9.

Boillee, S., Yamanaka, K., Lobsiger, C.S., Copeland, N.G., Jenkins, N.A., Kassiotis, G., Kollias, G., Cleveland, D.W. 2006. Onset and progression in inherited ALS determined by motor neurons and microglia. Science 312(5778), 1389-92.

Bolmont, T., Haiss, F., Eicke, D., Radde, R., Mathis, C.A., Klunk, W.E., Kohsaka, S., Jucker, M., Calhoun, M.E. 2008. Dynamics of the microglial/amyloid interaction indicate a role in plaque maintenance. J Neurosci 28(16), 4283-92.

Borchelt, D.R., Lee, M.K., Gonzales, V., Slunt, H.H., Ratovitski, T., Jenkins, N.A., Copeland, N.G., Price, D.L., Sisodia, S.S. 2002. Accumulation of proteolytic fragments of mutant presenilin 1 and accelerated amyloid deposition are co-regulated in transgenic mice. Neurobiol Aging 23(2), 171-7.

Borchelt, D.R., Taraboulos, A., Prusiner, S.B. 1992. Evidence for synthesis of scrapie prion proteins in the endocytic pathway. J Biol Chem 267(23), 16188-99.

Bouras, C., Hof, P.R., Giannakopoulos, P., Michel, J.P., Morrison, J.H. 1994. Regional distribution of neurofibrillary tangles and senile plaques in the cerebral cortex of elderly patients: a quantitative evaluation of a one-year autopsy population from a geriatric hospital. Cereb Cortex 4(2), 138-50.

Braak, H., Braak, E. 1995. Staging of Alzheimer's disease-related neurofibrillary changes. Neurobiol Aging 16(3), 271-8; discussion 8-84.

Braak, H., Braak, E., Bohl, J., Reintjes, R. 1996. Age, neurofibrillary changes, A beta-amyloid and the onset of Alzheimer's disease. Neurosci Lett 210(2), 87-90.

Brookmeyer, R., Corrada, M.M., Curriero, F.C., Kawas, C. 2002. Survival following a diagnosis of Alzheimer disease. Arch Neurol 59(11), 1764-7.

Brunello, A.G., Weissenberger, J., Kappeler, A., Vallan, C., Peters, M., Rose-John, S., Weis, J. 2000. Astrocytic alterations in interleukin-6/Soluble interleukin-6 receptor alpha double-transgenic mice. Am J Pathol 157(5), 1485-93.

Bruunsgaard, H., Andersen-Ranberg, K., Jeune, B., Pedersen, A.N., Skinhoj, P., Pedersen, B.K. 1999. A high plasma concentration of TNF-alpha is associated with dementia in centenarians. J Gerontol A Biol Sci Med Sci 54(7), M357-64.

Calafiore, M., Battaglia, G., Zappala, A., Trovato-Salinaro, E., Caraci, F., Caruso, M., Vancheri, C., Sortino, M.A., Nicoletti, F., Copani, A. 2006. Progenitor cells from the adult mouse brain acquire a neuronal phenotype in response to beta-amyloid. Neurobiol Aging 27(4), 606-13.

Carson, M.J., Reilly, C.R., Sutcliffe, J.G., Lo, D. 1998. Mature microglia resemble immature antigen-presenting cells. Glia 22(1), 72-85.

Carter, D.B., Dunn, E., McKinley, D.D., Stratman, N.C., Boyle, T.P., Kuiper, S.L., Oostveen, J.A., Weaver, R.J., Boller, J.A., Gurney, M.E. 2001. Human apolipoprotein E4 accelerates beta-amyloid deposition in APPsw transgenic mouse brain. Ann Neurol 50(4), 468-75.

Chambers, A.F., Matrisian, L.M. 1997. Changing views of the role of matrix metalloproteinases in metastasis. J Natl Cancer Inst 89(17), 1260-70.

Chung, H., Brazil, M.I., Irizarry, M.C., Hyman, B.T., Maxfield, F.R. 2001. Uptake of fibrillar beta-amyloid by microglia isolated from MSR-A (type I and type II) knockout mice. Neuroreport 12(6), 1151-4.

Cole, G.M., Beech, W., Frautschy, S.A., Sigel, J., Glasgow, C., Ard, M.D. 1999. Lipoprotein effects on Abeta accumulation and degradation by microglia in vitro. J Neurosci Res 57(4), 504-20.

Collins, J.S., Perry, R.T., Watson, B., Jr., Harrell, L.E., Acton, R.T., Blacker, D., Albert, M.S., Tanzi, R.E., Bassett, S.S., McInnis, M.G., Campbell, R.D., Go, R.C. 2000. Association of a haplotype for tumor necrosis factor in siblings with late-onset Alzheimer disease: the NIMH Alzheimer Disease Genetics Initiative. Am J Med Genet 96(6), 823-30.

Culpan, D., MacGowan, S.H., Ford, J.M., Nicoll, J.A., Griffin, W.S., Dewar, D., Cairns, N.J., Hughes, A., Kehoe, P.G., Wilcock, G.K. 2003. Tumour necrosis factor-alpha gene polymorphisms and Alzheimer's disease. Neurosci Lett 350(1), 61-5.

de Haas, A.H., Boddeke, H.W., Brouwer, N., Biber, K. 2007. Optimized isolation enables ex vivo analysis of microglia from various central nervous system regions. Glia 55(13), 1374-84.

Dolev, I., Michaelson, D.M. 2004. A nontransgenic mouse model shows inducible amyloid-beta (Abeta) peptide deposition and elucidates the role of apolipoprotein E in the amyloid cascade. Proc Natl Acad Sci U S A 101(38), 13909-14.

Dong, H., Goico, B., Martin, M., Csernansky, C.A., Bertchume, A., Csernansky, J.G. 2004. Modulation of hippocampal cell proliferation, memory, and amyloid plaque deposition in APPsw (Tg2576) mutant mice by isolation stress. Neuroscience 127(3), 601-9.

Donovan, M.H., Yazdani, U., Norris, R.D., Games, D., German, D.C., Eisch, A.J. 2006. Decreased adult hippocampal neurogenesis in the PDAPP mouse model of Alzheimer's disease. J Comp Neurol 495(1), 70-83.

Dringen, R. 2005. Oxidative and antioxidative potential of brain microglial cells. Antioxid Redox Signal 7(9-10), 1223-33.

Dull, T., Zufferey, R., Kelly, M., Mandel, R.J., Nguyen, M., Trono, D., Naldini, L. 1998. A third-generation lentivirus vector with a conditional packaging system. J Virol 72(11), 8463-71.

Edbauer, D., Willem, M., Lammich, S., Steiner, H., Haass, C. 2002. Insulin-degrading enzyme rapidly removes the beta-amyloid precursor protein intracellular domain (AICD). J Biol Chem 277(16), 13389-93.

El-Amouri, S.S., Zhu, H., Yu, J., Gage, F.H., Verma, I.M., Kindy, M.S. 2007. Neprilysin protects neurons against Abeta peptide toxicity. Brain Res 1152, 191-200.

El Khoury, J., Hickman, S.E., Thomas, C.A., Cao, L., Silverstein, S.C., Loike, J.D. 1996. Scavenger receptor-mediated adhesion of microglia to beta-amyloid fibrils. Nature 382(6593), 716-9.

El Khoury, J., Toft, M., Hickman, S.E., Means, T.K., Terada, K., Geula, C., Luster, A.D. 2007. Ccr2 deficiency impairs microglial accumulation and accelerates progression of Alzheimer-like disease. Nat Med 13(4), 432-8.

Englund, U., Ericson, C., Rosenblad, C., Mandel, R.J., Trono, D., Wictorin, K., Lundberg, C. 2000. The use of a recombinant lentiviral vector for ex vivo gene transfer into the rat CNS. Neuroreport 11(18), 3973-7.

Esen, N., Kielian, T. 2007. Effects of low dose GM-CSF on microglial inflammatory profiles to diverse pathogen-associated molecular patterns (PAMPs). J Neuroinflammation 4, 10.

Fagan, A.M., Bu, G., Sun, Y., Daugherty, A., Holtzman, D.M. 1996. Apolipoprotein E-containing high density lipoprotein promotes neurite outgrowth and is a ligand for the low density lipoprotein receptor-related protein. J Biol Chem 271(47), 30121-5.

Farris, W., Mansourian, S., Chang, Y., Lindsley, L., Eckman, E.A., Frosch, M.P., Eckman, C.B., Tanzi, R.E., Selkoe, D.J., Guenette, S. 2003. Insulin-degrading enzyme regulates the levels of insulin, amyloid beta-protein, and the beta-amyloid precursor protein intracellular domain in vivo. Proc Natl Acad Sci U S A 100(7), 4162-7.

Farris, W., Schutz, S.G., Cirrito, J.R., Shankar, G.M., Sun, X., George, A., Leissring, M.A., Walsh, D.M., Qiu, W.Q., Holtzman, D.M., Selkoe, D.J. 2007. Loss of neprilysin function promotes amyloid plaque formation and causes cerebral amyloid angiopathy. Am J Pathol 171(1), 241-51.

Fiala, M., Lin, J., Ringman, J., Kermani-Arab, V., Tsao, G., Patel, A., Lossinsky, A.S., Graves, M.C., Gustavson, A., Sayre, J., Sofroni, E., Suarez, T., Chiappelli, F., Bernard, G. 2005. Ineffective phagocytosis of amyloid-beta by macrophages of Alzheimer's disease patients. J Alzheimers Dis 7(3), 221-32; discussion 55-62.

Flanary, B.E., Sammons, N.W., Nguyen, C., Walker, D., Streit, W.J. 2007. Evidence that aging and amyloid promote microglial cell senescence. Rejuvenation Res 10(1), 61-74.

Floden, A.M., Combs, C.K. 2006. Beta-amyloid stimulates murine postnatal and adult microglia cultures in a unique manner. J Neurosci 26(17), 4644-8.

Floden, A.M., Li, S., Combs, C.K. 2005. Beta-amyloid-stimulated microglia induce neuron death via synergistic stimulation of tumor necrosis factor alpha and NMDA receptors. J Neurosci 25(10), 2566-75.

Frank, M.G., Wieseler-Frank, J.L., Watkins, L.R., Maier, S.F. 2006. Rapid isolation of highly enriched and quiescent microglia from adult rat hippocampus: immunophenotypic and functional characteristics. J Neurosci Methods 151(2), 121-30.

Frautschy, S.A., Yang, F., Irrizarry, M., Hyman, B., Saido, T.C., Hsiao, K., Cole, G.M. 1998. Microglial response to amyloid plaques in APPsw transgenic mice. Am J Pathol 152(1), 307-17.

Fryer, J.D., Simmons, K., Parsadanian, M., Bales, K.R., Paul, S.M., Sullivan, P.M., Holtzman, D.M. 2005. Human apolipoprotein E4 alters the amyloid-beta 40:42 ratio and promotes the formation of cerebral amyloid angiopathy in an amyloid precursor protein transgenic model. J Neurosci 25(11), 2803-10.

Fusetti, M., Fioretti, A.B., Silvagni, F., Simaskou, M., Sucapane, P., Necozione, S., Eibenstein, A. Smell and preclinical Alzheimer disease: study of 29 patients with amnesic mild cognitive impairment. J Otolaryngol Head Neck Surg 39(2), 175-81.

Games, D., Adams, D., Alessandrini, R., Barbour, R., Berthelette, P., Blackwell, C., Carr, T., Clemens, J., Donaldson, T., Gillespie, F., et al. 1995. Alzheimer-type neuropathology in transgenic mice overexpressing V717F beta-amyloid precursor protein. Nature 373(6514), 523-7.

Gao, C.Y., Stepp, M.A., Fariss, R., Zelenka, P. 2004. Cdk5 regulates activation and localization of Src during corneal epithelial wound closure. J Cell Sci 117(Pt 18), 4089-98.

German, D.C., Yazdani, U., Speciale, S.G., Pasbakhsh, P., Games, D., Liang, C.L. 2003. Cholinergic neuropathology in a mouse model of Alzheimer's disease. J Comp Neurol 462(4), 371-81.

Giulian, D. 1987. Ameboid microglia as effectors of inflammation in the central nervous system. J Neurosci Res 18(1), 155-71, 32-3.

Goate, A., Chartier-Harlin, M.C., Mullan, M., Brown, J., Crawford, F., Fidani, L., Giuffra, L., Haynes, A., Irving, N., James, L., et al. 1991. Segregation of a missense mutation in the amyloid precursor protein gene with familial Alzheimer's disease. Nature 349(6311), 704-6.

Hattiangady, B., Shuai, B., Cai, J., Coksaygan, T., Rao, M.S., Shetty, A.K. 2007. Increased dentate neurogenesis after grafting of glial restricted progenitors or neural stem cells in the aging hippocampus. Stem Cells 25(8), 2104-17.

He, B.P., Wen, W., Strong, M.J. 2002. Activated microglia (BV-2) facilitation of TNF-alpha-mediated motor neuron death in vitro. J Neuroimmunol 128(1-2), 31-8.

Heneka, M.T., O'Banion, M.K. 2007. Inflammatory processes in Alzheimer's disease. J Neuroimmunol 184(1-2), 69-91.

Hickman, S.E., Allison, E.K., El Khoury, J. 2008. Microglial dysfunction and defective beta-amyloid clearance pathways in aging Alzheimer's disease mice. J Neurosci 28(33), 8354-60.

Higgins, G.A., Jacobsen, H. 2003. Transgenic mouse models of Alzheimer's disease: phenotype and application. Behav Pharmacol 14(5-6), 419-38.

Hirrlinger, J., Gutterer, J.M., Kussmaul, L., Hamprecht, B., Dringen, R. 2000. Microglial cells in culture express a prominent glutathione system for the defense against reactive oxygen species. Dev Neurosci 22(5-6), 384-92.

Hoe, H.S., Cooper, M.J., Burns, M.P., Lewis, P.A., van der Brug, M., Chakraborty, G., Cartagena, C.M., Pak, D.T., Cookson, M.R., Rebeck, G.W. 2007. The metalloprotease inhibitor TIMP-3 regulates amyloid precursor protein and apolipoprotein E receptor proteolysis. J Neurosci 27(40), 10895-905.

Hsiao, K., Chapman, P., Nilsen, S., Eckman, C., Harigaya, Y., Younkin, S., Yang, F., Cole, G. 1996. Correlative memory deficits, Abeta elevation, and amyloid plaques in transgenic mice. Science 274(5284), 99-102.

Huang, F., Buttini, M., Wyss-Coray, T., McConlogue, L., Kodama, T., Pitas, R.E., Mucke, L. 1999. Elimination of the class A scavenger receptor does not affect amyloid plaque formation or neurodegeneration in transgenic mice expressing human amyloid protein precursors. Am J Pathol 155(5), 1741-7.

Imitola, J., Raddassi, K., Park, K.I., Mueller, F.J., Nieto, M., Teng, Y.D., Frenkel, D., Li, J., Sidman, R.L., Walsh, C.A., Snyder, E.Y., Khoury, S.J. 2004. Directed migration of neural stem cells to sites of CNS injury by the stromal cell-derived factor 1alpha/CXC chemokine receptor 4 pathway. Proc Natl Acad Sci U S A 101(52), 18117-22.

Irizarry, M.C., Cheung, B.S., Rebeck, G.W., Paul, S.M., Bales, K.R., Hyman, B.T. 2000. Apolipoprotein E affects the amount, form, and anatomical distribution of amyloid beta-peptide deposition in homozygous APP(V717F) transgenic mice. Acta Neuropathol (Berl) 100(5), 451-8.

Iwata, N., Tsubuki, S., Takaki, Y., Shirotani, K., Lu, B., Gerard, N.P., Gerard, C., Hama, E., Lee, H.J., Saido, T.C. 2001. Metabolic regulation of brain Abeta by neprilysin. Science 292(5521), 1550-2.

Jankowsky, J.L., Slunt, H.H., Gonzales, V., Savonenko, A.V., Wen, J.C., Jenkins, N.A., Copeland, N.G., Younkin, L.H., Lester, H.A., Younkin, S.G., Borchelt, D.R. 2005. Persistent amyloidosis following suppression of Abeta production in a transgenic model of Alzheimer disease. PLoS Med 2(12), e355.

Jin, K., Peel, A.L., Mao, X.O., Xie, L., Cottrell, B.A., Henshall, D.C., Greenberg, D.A. 2004. Increased hippocampal neurogenesis in Alzheimer's disease. Proc Natl Acad Sci U S A 101(1), 343-7.

Jung, S., Aliberti, J., Graemmel, P., Sunshine, M.J., Kreutzberg, G.W., Sher, A., Littman, D.R. 2000. Analysis of fractalkine receptor CX(3)CR1 function by targeted deletion and green fluorescent protein reporter gene insertion. Mol Cell Biol 20(11), 4106-14.

Kang, S.S., Kook, J.H., Hwang, S., Park, S.H., Nam, S.C., Kim, J.K. 2008. Inhibition of matrix metalloproteinase-9 attenuated neural progenitor cell migration after photothrombotic ischemia. Brain Res 1228, 20-6.

Klein, M.A., Moller, J.C., Jones, L.L., Bluethmann, H., Kreutzberg, G.W., Raivich, G. 1997. Impaired neuroglial activation in interleukin-6 deficient mice. Glia 19(3), 227-33.

Kukekov, V.G., Laywell, E.D., Thomas, L.B., Steindler, D.A. 1997. A nestin-negative precursor cell from the adult mouse brain gives rise to neurons and glia. Glia 21(4), 399-407.

Kumar-Singh, S., Theuns, J., Van Broeck, B., Pirici, D., Vennekens, K., Corsmit, E., Cruts, M., Dermaut, B., Wang, R., Van Broeckhoven, C. 2006. Mean age-of-onset of familial alzheimer disease caused by presenilin mutations correlates with both increased Abeta42 and decreased Abeta40. Hum Mutat 27(7), 686-95.

Laywell, E.D., Rakic, P., Kukekov, V.G., Holland, E.C., Steindler, D.A. 2000. Identification of a multipotent astrocytic stem cell in the immature and adult mouse brain. Proc Natl Acad Sci U S A 97(25), 13883-8.

Leal, M.C., Dorfman, V.B., Gamba, A.F., Frangione, B., Wisniewski, T., Castano, E.M., Sigurdsson, E.M., Morelli, L. 2006. Plaque-associated overexpression of insulin-degrading enzyme in the cerebral cortex of aged transgenic tg2576 mice with Alzheimer pathology. J Neuropathol Exp Neurol 65(10), 976-87.

Leissring, M.A., Farris, W., Chang, A.Y., Walsh, D.M., Wu, X., Sun, X., Frosch, M.P., Selkoe, D.J. 2003. Enhanced proteolysis of beta-amyloid in APP transgenic mice prevents plaque formation, secondary pathology, and premature death. Neuron 40(6), 1087-93.

Lewis, J., Dickson, D.W., Lin, W.L., Chisholm, L., Corral, A., Jones, G., Yen, S.H., Sahara, N., Skipper, L., Yager, D., Eckman, C., Hardy, J., Hutton, M., McGowan, E. 2001. Enhanced neurofibrillary degeneration in transgenic mice expressing mutant tau and APP. Science 293(5534), 1487-91.

Li, J.P., Galvis, M.L., Gong, F., Zhang, X., Zcharia, E., Metzger, S., Vlodavsky, I., Kisilevsky, R., Lindahl, U. 2005. In vivo fragmentation of heparan sulfate by heparanase overexpression renders mice resistant to amyloid protein A amyloidosis. Proc Natl Acad Sci U S A 102(18), 6473-7.

Li, L., Lu, J., Tay, S.S., Moochhala, S.M., He, B.P. 2007. The function of microglia, either neuroprotection or neurotoxicity, is determined by the equilibrium among factors released from activated microglia in vitro. Brain Res 1159, 8-17.

Liao, M.C., Van Nostrand, W.E. 2010. Degradation of soluble and fibrillar amyloid beta-protein by matrix metalloproteinase (MT1-MMP) in vitro. Biochemistry 49(6), 1127-36.

Licastro, F., Pedrini, S., Caputo, L., Annoni, G., Davis, L.J., Ferri, C., Casadei, V., Grimaldi, L.M. 2000. Increased plasma levels of interleukin-1, interleukin-6 and alpha-1-antichymotrypsin in patients with Alzheimer's disease: peripheral inflammation or signals from the brain? J Neuroimmunol 103(1), 97-102.

Lindenau, J., Noack, H., Asayama, K., Wolf, G. 1998. Enhanced cellular glutathione peroxidase immunoreactivity in activated astrocytes and in microglia during excitotoxin induced neurodegeneration. Glia 24(2), 252-6.

Loddick, S.A., Turnbull, A.V., Rothwell, N.J. 1998. Cerebral interleukin-6 is neuroprotective during permanent focal cerebral ischemia in the rat. J Cereb Blood Flow Metab 18(2), 176-9.

Lopez-Toledano, M.A., Shelanski, M.L. 2004. Neurogenic effect of beta-amyloid peptide in the development of neural stem cells. J Neurosci 24(23), 5439-44.

Lorenzl, S., Albers, D.S., LeWitt, P.A., Chirichigno, J.W., Hilgenberg, S.L., Cudkowicz, M.E., Beal, M.F. 2003. Tissue inhibitors of matrix metalloproteinases are elevated in cerebrospinal fluid of neurodegenerative diseases. J Neurol Sci 207(1-2), 71-6.

Lu, W.G., Chen, H., Wang, D., Li, F.G., Zhang, S.M. 2007. Regionspecific survival and differentiation of mouse embryonic stem cell-derived implants in the adult rat brain. Sheng Li Xue Bao 59(1), 51-7.

Lubbe, W.J., Zhou, Z.Y., Fu, W., Zuzga, D., Schulz, S., Fridman, R., Muschel, R.J., Waldman, S.A., Pitari, G.M. 2006. Tumor epithelial cell matrix metalloproteinase 9 is a target for antimetastatic therapy in colorectal cancer. Clin Cancer Res 12(6), 1876-82.

Lue, L.F., Walker, D.G. 2002. Modeling Alzheimer's disease immune therapy mechanisms: interactions of human postmortem microglia with antibody-opsonized amyloid beta peptide. J Neurosci Res 70(4), 599-610.

Lundberg, C., Martinez-Serrano, A., Cattaneo, E., McKay, R.D., Bjorklund, A. 1997. Survival, integration, and differentiation of neural stem cell lines after transplantation to the adult rat striatum. Exp Neurol 145(2 Pt 1), 342-60.

Majumdar, A., Chung, H., Dolios, G., Wang, R., Asamoah, N., Lobel, P., Maxfield, F.R. 2007a. Degradation of fibrillar forms of Alzheimer's amyloid beta-peptide by macrophages. Neurobiol Aging.

Majumdar, A., Cruz, D., Asamoah, N., Buxbaum, A., Sohar, I., Lobel, P., Maxfield, F.R. 2007b. Activation of microglia acidifies lysosomes and leads to degradation of Alzheimer amyloid fibrils. Mol Biol Cell 18(4), 1490-6.

Marr, R.A., Rockenstein, E., Mukherjee, A., Kindy, M.S., Hersh, L.B., Gage, F.H., Verma, I.M., Masliah, E. 2003. Neprilysin gene transfer reduces human amyloid pathology in transgenic mice. J Neurosci 23(6), 1992-6.

Marshall, G.P., 2nd, Laywell, E.D., Zheng, T., Steindler, D.A., Scott, E.W. 2006. In vitro-derived "neural stem cells" function as neural progenitors without the capacity for self-renewal. Stem Cells 24(3), 731-8.

Marz, P., Cheng, J.G., Gadient, R.A., Patterson, P.H., Stoyan, T., Otten, U., Rose-John, S. 1998. Sympathetic neurons can produce and respond to interleukin 6. Proc Natl Acad Sci U S A 95(6), 3251-6.

McDermott, J.R., Bartram, R.E., Knight, P.A., Miller, H.R., Garrod, D.R., Grencis, R.K. 2003. Mast cells disrupt epithelial barrier function during enteric nematode infection. Proc Natl Acad Sci U S A 100(13), 7761-6.

McGeer, P.L., McGeer, E.G. 2001. Polymorphisms in inflammatory genes and the risk of Alzheimer disease. Arch Neurol 58(11), 1790-2.

Meyer-Luehmann, M., Spires-Jones, T.L., Prada, C., Garcia-Alloza, M., de Calignon, A., Rozkalne, A., Koenigsknecht-Talboo, J., Holtzman, D.M., Bacskai, B.J., Hyman, B.T. 2008. Rapid appearance and local toxicity of amyloid-beta plaques in a mouse model of Alzheimer's disease. Nature 451(7179), 720-4.

Miller, K.R., Streit, W.J. 2007. The effects of aging, injury and disease on microglial function: a case for cellular senescence. Neuron Glia Biol 3(3), 245-53.

Milton, R.H., Abeti, R., Averaimo, S., DeBiasi, S., Vitellaro, L., Jiang, L., Curmi, P.M., Breit, S.N., Duchen, M.R., Mazzanti, M. 2008. CLIC1 function is required for beta-amyloid-induced generation of reactive oxygen species by microglia. J Neurosci 28(45), 11488-99.

Moll, U.M., Youngleib, G.L., Rosinski, K.B., Quigley, J.P. 1990. Tumor promoter-stimulated Mr 92,000 gelatinase secreted by normal and malignant human cells: isolation and characterization of the enzyme from HT1080 tumor cells. Cancer Res 50(19), 6162-70.

Moolman, D.L., Vitolo, O.V., Vonsattel, J.P., Shelanski, M.L. 2004. Dendrite and dendritic spine alterations in Alzheimer models. J Neurocytol 33(3), 377-87.

Mosconi, L., Rinne, J.O., Tsui, W.H., Berti, V., Li, Y., Wang, H., Murray, J., Scheinin, N., Nagren, K., Williams, S., Glodzik, L., De Santi, S., Vallabhajosula, S., de Leon, M.J. Increased fibrillar amyloid-{beta} burden in normal individuals with a family history of late-onset Alzheimer's. Proc Natl Acad Sci U S A.

Motte, J., Williams, R.S. 1989. Age-related changes in the density and morphology of plaques and neurofibrillary tangles in Down syndrome brain. Acta Neuropathol (Berl) 77(5), 535-46.

Munger, J.S., Haass, C., Lemere, C.A., Shi, G.P., Wong, W.S., Teplow, D.B., Selkoe, D.J., Chapman, H.A. 1995. Lysosomal processing of amyloid precursor protein to A beta peptides: a distinct role for cathepsin S. Biochem J 311 (Pt 1), 299-305.

Nagaraja, T.N., Patel, P., Gorski, M., Gorevic, P.D., Patlak, C.S., Fenstermacher, J.D. 2005. In normal rat, intraventricularly administered insulin-like growth factor-1 is rapidly cleared from CSF with limited distribution into brain. Cerebrospinal Fluid Res 2, 5.

Naidu, A., Xu, Q., Catalano, R., Cordell, B. 2002. Secretion of apolipoprotein E by brain glia requires protein prenylation and is suppressed by statins. Brain Res 958(1), 100-11.

Njie, E.G., Boelen, E., Stassen, F.R., Steinbusch, H.W., Borchelt, D.R., Streit, W.J. 2010. Ex vivo cultures of microglia from young and aged rodent brain reveal age-related changes in microglial function. Neurobiol Aging.

Oddo, S., Caccamo, A., Shepherd, J.D., Murphy, M.P., Golde, T.E., Kayed, R., Metherate, R., Mattson, M.P., Akbari, Y., LaFerla, F.M. 2003. Triple-transgenic model of Alzheimer's disease with plaques and tangles: intracellular Abeta and synaptic dysfunction. Neuron 39(3), 409-21.

Olstorn, H., Moe, M.C., Roste, G.K., Bueters, T., Langmoen, I.A. 2007. Transplantation of stem cells from the adult human brain to the adult rat brain. Neurosurgery 60(6), 1089-98; discussion 98-9.

Paresce, D.M., Chung, H., Maxfield, F.R. 1997. Slow degradation of aggregates of the Alzheimer's disease amyloid beta-protein by microglial cells. J Biol Chem 272(46), 29390-7.

Park, K.I., Teng, Y.D., Snyder, E.Y. 2002. The injured brain interacts reciprocally with neural stem cells supported by scaffolds to reconstitute lost tissue. Nat Biotechnol 20(11), 1111-7.

Parsons, C.G., Stoffler, A., Danysz, W. 2007. Memantine: a NMDA receptor antagonist that improves memory by restoration of homeostasis in the glutamatergic system - too little activation is bad, too much is even worse. Neuropharmacology 53(6), 699-723.

Patton, R.L., Kalback, W.M., Esh, C.L., Kokjohn, T.A., Van Vickle, G.D., Luehrs, D.C., Kuo, Y.M., Lopez, J., Brune, D., Ferrer, I., Masliah, E., Newel, A.J., Beach, T.G., Castano, E.M., Roher, A.E. 2006. Amyloid-beta peptide remnants in AN-1792-immunized Alzheimer's disease patients: a biochemical analysis. Am J Pathol 169(3), 1048-63.

Peress, N., Perillo, E., Zucker, S. 1995. Localization of tissue inhibitor of matrix metalloproteinases in Alzheimer's disease and normal brain. J Neuropathol Exp Neurol 54(1), 16-22.

Pihlaja, R., Koistinaho, J., Malm, T., Sikkila, H., Vainio, S., Koistinaho, M. 2008. Transplanted astrocytes internalize deposited beta-amyloid peptides in a transgenic mouse model of Alzheimer's disease. Glia 56(2), 154-63.

Podoly, E., Bruck, T., Diamant, S., Melamed-Book, N., Weiss, A., Huang, Y., Livnah, O., Langermann, S., Wilgus, H., Soreq, H. 2008. Human recombinant butyrylcholinesterase purified from the milk of transgenic goats interacts with beta-amyloid fibrils and suppresses their formation in vitro. Neurodegener Dis 5(3-4), 232-6.

Ponomarev, E.D., Novikova, M., Maresz, K., Shriver, L.P., Dittel, B.N. 2005. Development of a culture system that supports adult microglial cell proliferation and maintenance in the resting state. J Immunol Methods 300(1-2), 32-46.

Prajerova, I., Honsa, P., Chvatal, A., Anderova, M. Neural stem/progenitor cells derived from the embryonic dorsal telencephalon of D6/GFP mice differentiate primarily into neurons after transplantation into a cortical lesion. Cell Mol Neurobiol 30(2), 199-218.

Price, J.L., McKeel, D.W., Jr., Buckles, V.D., Roe, C.M., Xiong, C., Grundman, M., Hansen, L.A., Petersen, R.C., Parisi, J.E., Dickson, D.W., Smith, C.D., Davis, D.G., Schmitt, F.A., Markesbery, W.R., Kaye, J., Kurlan, R., Hulette, C., Kurland, B.F., Higdon, R., Kukull, W., Morris, J.C. 2009. Neuropathology of nondemented aging: presumptive evidence for preclinical Alzheimer disease. Neurobiol Aging 30(7), 1026-36.

Qin, L., Liu, Y., Wang, T., Wei, S.J., Block, M.L., Wilson, B., Liu, B., Hong, J.S. 2004. NADPH oxidase mediates lipopolysaccharide-induced neurotoxicity and proinflammatory gene expression in activated microglia. J Biol Chem 279(2), 1415-21.

Qiu, W.Q., Walsh, D.M., Ye, Z., Vekrellis, K., Zhang, J., Podlisny, M.B., Rosner, M.R., Safavi, A., Hersh, L.B., Selkoe, D.J. 1998. Insulin-degrading enzyme regulates extracellular levels of amyloid beta-protein by degradation. J Biol Chem 273(49), 32730-8.

Radojevic, V., Kapfhammer, J.P. 2009. Directed fiber outgrowth from transplanted embryonic cortex-derived neurospheres in the adult mouse brain. Neural Plast 2009, 852492.

Raedt, R., Van Dycke, A., Waeytens, A., Wyckhuys, T., Vonck, K., Wadman, W., Boon, P. 2009. Unconditioned adult-derived neurosphere cells mainly differentiate towards astrocytes upon transplantation in sclerotic rat hippocampus. Epilepsy Res 87(2-3), 148-59.

Ramos-DeSimone, N., Hahn-Dantona, E., Sipley, J., Nagase, H., French, D.L., Quigley, J.P. 1999. Activation of matrix metalloproteinase-9 (MMP-9) via a converging plasmin/stromelysin-1 cascade enhances tumor cell invasion. J Biol Chem 274(19), 13066-76.

Raponi, E., Agenes, F., Delphin, C., Assard, N., Baudier, J., Legraverend, C., Deloulme, J.C. 2007. S100B expression defines a state in which GFAP-expressing cells lose their neural stem cell potential and acquire a more mature developmental stage. Glia 55(2), 165-77.

Reynolds, B.A., Weiss, S. 1992. Generation of neurons and astrocytes from isolated cells of the adult mammalian central nervous system. Science 255(5052), 1707-10.

Rogers, J., Strohmeyer, R., Kovelowski, C.J., Li, R. 2002. Microglia and inflammatory mechanisms in the clearance of amyloid beta peptide. Glia 40(2), 260-9.

Ross, J. 1995. mRNA stability in mammalian cells. Microbiol Rev 59(3), 423-50.

Rovelet-Lecrux, A., Hannequin, D., Raux, G., Le Meur, N., Laquerriere, A., Vital, A., Dumanchin, C., Feuillette, S., Brice, A., Vercelletto, M., Dubas, F., Frebourg, T., Campion, D. 2006. APP locus duplication causes autosomal dominant early-onset Alzheimer disease with cerebral amyloid angiopathy. Nat Genet 38(1), 24-6.

Ruiz-Opazo, N., Kosik, K.S., Lopez, L.V., Bagamasbad, P., Ponce, L.R., Herrera, V.L. 2004. Attenuated hippocampus-dependent learning and memory decline in transgenic TgAPPswe Fischer-344 rats. Mol Med 10(1-6), 36-44.

Ryu, J.K., Cho, T., Wang, Y.T., McLarnon, J.G. 2009. Neural progenitor cells attenuate inflammatory reactivity and neuronal loss in an animal model of inflamed AD brain. J Neuroinflammation 6, 39.

Sabbagh, M.N. 2009. Drug development for Alzheimer's disease: where are we now and where are we headed? Am J Geriatr Pharmacother 7(3), 167-85.

Savonenko, A., Xu, G.M., Melnikova, T., Morton, J.L., Gonzales, V., Wong, M.P., Price, D.L., Tang, F., Markowska, A.L., Borchelt, D.R. 2005. Episodic-like memory deficits in the APPswe/PS1dE9 mouse model of Alzheimer's disease: relationships to beta-amyloid deposition and neurotransmitter abnormalities. Neurobiol Dis 18(3), 602-17.

Sawaya, M.R., Sambashivan, S., Nelson, R., Ivanova, M.I., Sievers, S.A., Apostol, M.I., Thompson, M.J., Balbirnie, M., Wiltzius, J.J., McFarlane, H.T., Madsen, A.O., Riekel, C., Eisenberg, D. 2007. Atomic structures of amyloid cross-beta spines reveal varied steric zippers. Nature 447(7143), 453-7.

Scheffler, B., Walton, N.M., Lin, D.D., Goetz, A.K., Enikolopov, G., Roper, S.N., Steindler, D.A. 2005. Phenotypic and functional characterization of adult brain neuropoiesis. Proc Natl Acad Sci U S A 102(26), 9353-8.

Schmidt, S.D., Nixon, R.A., Mathews, P.M. 2005. ELISA method for measurement of amyloid-beta levels. Methods Mol Biol 299, 279-97.

Schwab, C., Hosokawa, M., McGeer, P.L. 2004. Transgenic mice overexpressing amyloid beta protein are an incomplete model of Alzheimer disease. Exp Neurol 188(1), 52-64.

Shagin, D.A., Barsova, E.V., Yanushevich, Y.G., Fradkov, A.F., Lukyanov, K.A., Labas, Y.A., Semenova, T.N., Ugalde, J.A., Meyers, A., Nunez, J.M., Widder, E.A., Lukyanov, S.A., Matz, M.V. 2004. GFP-like proteins as ubiquitous metazoan superfamily: evolution of functional features and structural complexity. Mol Biol Evol 21(5), 841-50.

Shen, Y., Joachimiak, A., Rosner, M.R., Tang, W.J. 2006. Structures of human insulin-degrading enzyme reveal a new substrate recognition mechanism. Nature 443(7113), 870-4.

Shetty, A.K., Rao, M.S., Hattiangady, B. 2008. Behavior of hippocampal stem/progenitor cells following grafting into the injured aged hippocampus. J Neurosci Res 86(14), 3062-74.

Sierra, A., Gottfried-Blackmore, A.C., McEwen, B.S., Bulloch, K. 2007. Microglia derived from aging mice exhibit an altered inflammatory profile. Glia 55(4), 412-24.

Simard, A.R., Soulet, D., Gowing, G., Julien, J.P., Rivest, S. 2006. Bone marrow-derived microglia play a critical role in restricting senile plaque formation in Alzheimer's disease. Neuron 49(4), 489-502.

Simmons, D.A., Casale, M., Alcon, B., Pham, N., Narayan, N., Lynch, G. 2007. Ferritin accumulation in dystrophic microglia is an early event in the development of Huntington's disease. Glia 55(10), 1074-84.

Stalder, M., Phinney, A., Probst, A., Sommer, B., Staufenbiel, M., Jucker, M. 1999. Association of microglia with amyloid plaques in brains of APP23 transgenic mice. Am J Pathol 154(6), 1673-84.

Storm van's Gravesande, K., Layne, M.D., Ye, Q., Le, L., Baron, R.M., Perrella, M.A., Santambrogio, L., Silverman, E.S., Riese, R.J. 2002. IFN regulatory factor-1 regulates IFN-gamma-dependent cathepsin S expression. J Immunol 168(9), 4488-94.

Streit, W.J., Hurley, S.D., McGraw, T.S., Semple-Rowland, S.L. 2000. Comparative evaluation of cytokine profiles and reactive gliosis supports a critical role for interleukin-6 in neuron-glia signaling during regeneration. J Neurosci Res 61(1), 10-20.

Streit, W.J., Miller, K.R., Lopes, K.O., Njie, E. 2008. Microglial degeneration in the aging brain--bad news for neurons? Front Biosci 13, 3423-38.

Streit, W.J., Mrak, R.E., Griffin, W.S. 2004. Microglia and neuroinflammation: a pathological perspective. J Neuroinflammation 1(1), 14.

Sturchler-Pierrat, C., Abramowski, D., Duke, M., Wiederhold, K.H., Mistl, C., Rothacher, S., Ledermann, B., Burki, K., Frey, P., Paganetti, P.A., Waridel, C., Calhoun, M.E., Jucker, M., Probst, A., Staufenbiel, M., Sommer, B. 1997. Two amyloid precursor protein transgenic mouse models with Alzheimer disease-like pathology. Proc Natl Acad Sci U S A 94(24), 13287-92.

Svendsen, C.N., Clarke, D.J., Rosser, A.E., Dunnett, S.B. 1996. Survival and differentiation of rat and human epidermal growth factor-responsive precursor cells following grafting into the lesioned adult central nervous system. Exp Neurol 137(2), 376-88.

Takaki, Y., Iwata, N., Tsubuki, S., Taniguchi, S., Toyoshima, S., Lu, B., Gerard, N.P., Gerard, C., Lee, H.J., Shirotani, K., Saido, T.C. 2000. Biochemical identification of the neutral endopeptidase family member responsible for the catabolism of amyloid beta peptide in the brain. J Biochem (Tokyo) 128(6), 897-902.

Tan, J., Town, T., Paris, D., Mori, T., Suo, Z., Crawford, F., Mattson, M.P., Flavell, R.A., Mullan, M. 1999. Microglial activation resulting from CD40-CD40L interaction after beta-amyloid stimulation. Science 286(5448), 2352-5.

Tang, J., Xu, H., Fan, X., Li, D., Rancourt, D., Zhou, G., Li, Z., Yang, L. 2008. Embryonic stem cell-derived neural precursor cells improve memory dysfunction in Abeta(1-40) injured rats. Neurosci Res 62(2), 86-96.

Tanzi, R.E., Bertram, L. 2005. Twenty years of the Alzheimer's disease amyloid hypothesis: a genetic perspective. Cell 120(4), 545-55.

Tarkowski, E., Blennow, K., Wallin, A., Tarkowski, A. 1999. Intracerebral production of tumor necrosis factor-alpha, a local neuroprotective agent, in Alzheimer disease and vascular dementia. J Clin Immunol 19(4), 223-30.

Tchaikovskaya, T., Fraifeld, V., Urphanishvili, T., Andorfer, J.H., Davies, P., Listowsky, I. 2005. Glutathione S-transferase hGSTM3 and ageing-associated neurodegeneration: relationship to Alzheimer's disease. Mech Ageing Dev 126(2), 309-15.

Terry, A.V., Jr., Buccafusco, J.J. 2003. The cholinergic hypothesis of age and Alzheimer's disease-related cognitive deficits: recent challenges and their implications for novel drug development. J Pharmacol Exp Ther 306(3), 821-7.

Tham, C.S., Lin, F.F., Rao, T.S., Yu, N., Webb, M. 2003. Microglial activation state and lysophospholipid acid receptor expression. Int J Dev Neurosci 21(8), 431-43.

Thier, M., Marz, P., Otten, U., Weis, J., Rose-John, S. 1999. Interleukin-6 (IL-6) and its soluble receptor support survival of sensory neurons. J Neurosci Res 55(4), 411-22.

Tietze, F. 1969. Enzymic method for quantitative determination of nanogram amounts of total and oxidized glutathione: applications to mammalian blood and other tissues. Anal Biochem 27(3), 502-22.

Verret, L., Jankowsky, J.L., Xu, G.M., Borchelt, D.R., Rampon, C. 2007. Alzheimer's-type amyloidosis in transgenic mice impairs survival of newborn neurons derived from adult hippocampal neurogenesis. J Neurosci 27(25), 6771-80.

Walsh, D.M., Klyubin, I., Fadeeva, J.V., Cullen, W.K., Anwyl, R., Wolfe, M.S., Rowan, M.J., Selkoe, D.J. 2002. Naturally secreted oligomers of amyloid beta protein potently inhibit hippocampal long-term potentiation in vivo. Nature 416(6880), 535-9.

Walton, N.M., Sutter, B.M., Chen, H.X., Chang, L.J., Roper, S.N., Scheffler, B., Steindler, D.A. 2006a. Derivation and large-scale expansion of multipotent astroglial neural progenitors from adult human brain. Development 133(18), 3671-81.

Walton, N.M., Sutter, B.M., Laywell, E.D., Levkoff, L.H., Kearns, S.M., Marshall, G.P., 2nd, Scheffler, B., Steindler, D.A. 2006b. Microglia instruct subventricular zone neurogenesis. Glia 54(8), 815-25.

Wang, L., Zhang, Z.G., Zhang, R.L., Gregg, S.R., Hozeska-Solgot, A., LeTourneau, Y., Wang, Y., Chopp, M. 2006. Matrix metalloproteinase 2 (MMP2) and MMP9 secreted by erythropoietin-activated endothelial cells promote neural progenitor cell migration. J Neurosci 26(22), 5996-6003.

Wang, R., Dineley, K.T., Sweatt, J.D., Zheng, H. 2004. Presenilin 1 familial Alzheimer's disease mutation leads to defective associative learning and impaired adult neurogenesis. Neuroscience 126(2), 305-12.

Watson, D.J., Walton, R.M., Magnitsky, S.G., Bulte, J.W., Poptani, H., Wolfe, J.H. 2006. Structure-specific patterns of neural stem cell engraftment after transplantation in the adult mouse brain. Hum Gene Ther 17(7), 693-704.

Wegiel, J., Imaki, H., Wang, K.C., Wegiel, J., Rubenstein, R. 2004. Cells of monocyte/microglial lineage are involved in both microvessel amyloidosis and fibrillar plaque formation in APPsw tg mice. Brain Res 1022(1-2), 19-29.

Wei, J., Xu, H., Davies, J.L., Hemmings, G.P. 1992. Increase of plasma IL-6 concentration with age in healthy subjects. Life Sci 51(25), 1953-6.

Wei, L.H., Kuo, M.L., Chen, C.A., Chou, C.H., Cheng, W.F., Chang, M.C., Su, J.L., Hsieh, C.Y. 2001. The anti-apoptotic role of interleukin-6 in human cervical cancer is mediated by up-regulation of Mcl-1 through a PI 3-K/Akt pathway. Oncogene 20(41), 5799-809.

Westerman, M.A., Cooper-Blacketer, D., Mariash, A., Kotilinek, L., Kawarabayashi, T., Younkin, L.H., Carlson, G.A., Younkin, S.G., Ashe, K.H. 2002. The relationship between Abeta and memory in the Tg2576 mouse model of Alzheimer's disease. J Neurosci 22(5), 1858-67.

Wong, P.C., Cai, H., Borchelt, D.R., Price, D.L. 2002. Genetically engineered mouse models of neurodegenerative diseases. Nat Neurosci 5(7), 633-9.

Wyss-Coray, T., Lin, C., Yan, F., Yu, G.Q., Rohde, M., McConlogue, L., Masliah, E., Mucke, L. 2001. TGF-beta1 promotes microglial amyloid-beta clearance and reduces plaque burden in transgenic mice. Nat Med 7(5), 612-8.

Xu, G., Gonzales, V., Borchelt, D.R. 2002. Abeta deposition does not cause the aggregation of endogenous tau in transgenic mice. Alzheimer Dis Assoc Disord 16(3), 196-201.

Xu, Q., Li, Y., Cyras, C., Sanan, D.A., Cordell, B. 2000. Isolation and characterization of apolipoproteins from murine microglia. Identification of a low density lipoprotein-like apolipoprotein J-rich but E-poor spherical particle. J Biol Chem 275(41), 31770-7.

Yan, P., Hu, X., Song, H., Yin, K., Bateman, R.J., Cirrito, J.R., Xiao, Q., Hsu, F.F., Turk, J.W., Xu, J., Hsu, C.Y., Holtzman, D.M., Lee, J.M. 2006. Matrix metalloproteinase-9 degrades amyloid-beta fibrils in vitro and compact plaques in situ. J Biol Chem 281(34), 24566-74.

Yan, S.D., Chen, X., Fu, J., Chen, M., Zhu, H., Roher, A., Slattery, T., Zhao, L., Nagashima, M., Morser, J., Migheli, A., Nawroth, P., Stern, D., Schmidt, A.M. 1996. RAGE and amyloid-beta peptide neurotoxicity in Alzheimer's disease. Nature 382(6593), 685-91.

Yasojima, K., Akiyama, H., McGeer, E.G., McGeer, P.L. 2001. Reduced neprilysin in high plaque areas of Alzheimer brain: a possible relationship to deficient degradation of beta-amyloid peptide. Neurosci Lett 297(2), 97-100.

Ye, S.M., Johnson, R.W. 1999. Increased interleukin-6 expression by microglia from brain of aged mice. J Neuroimmunol 93(1-2), 139-48.

Yin, K.J., Cirrito, J.R., Yan, P., Hu, X., Xiao, Q., Pan, X., Bateman, R., Song, H., Hsu, F.F., Turk, J., Xu, J., Hsu, C.Y., Mills, J.C., Holtzman, D.M., Lee, J.M. 2006. Matrix metalloproteinases expressed by astrocytes mediate extracellular amyloid-beta peptide catabolism. J Neurosci 26(43), 10939-48.

Yoon, I.S., Chen, E., Busse, T., Repetto, E., Lakshmana, M.K., Koo, E.H., Kang, D.E. 2007. Low-density lipoprotein receptor-related protein promotes amyloid precursor protein trafficking to lipid rafts in the endocytic pathway. Faseb J.

Zandi, P.P., Anthony, J.C., Khachaturian, A.S., Stone, S.V., Gustafson, D., Tschanz, J.T., Norton, M.C., Welsh-Bohmer, K.A., Breitner, J.C. 2004. Reduced risk of Alzheimer disease in users of antioxidant vitamin supplements: the Cache County Study. Arch Neurol 61(1), 82-8.

Zheng, T., Marshall, G.P., 2nd, Laywell, E.D., Steindler, D.A. 2006. Neurogenic astrocytes transplanted into the adult mouse lateral ventricle contribute to olfactory neurogenesis, and reveal a novel intrinsic subependymal neuron. Neuroscience 142(1), 175-85.

Ziabreva, I., Perry, E., Perry, R., Minger, S.L., Ekonomou, A., Przyborski, S., Ballard, C. 2006. Altered neurogenesis in Alzheimer's disease. J Psychosom Res 61(3), 311-6.

BIOGRAPHICAL SKETCH

eMalick Njie is from The Gambia and has always dreamed of being a scientist.